# IN SHAPE

## A Novel Approach to White Matter Hyperintensity Analysis



Jasmin Annica Kuhn-Keller

# IN SHAPE:

## A Novel Approach to White Matter Hyperintensity Analysis

Jasmin Annica Kuhn

# IN SHAPE:

## A Novel Approach to White Matter Hyperintensity Analysis

**Proefschrift**

ter verkrijging van
de graad van doctor aan de Universiteit Leiden,
op gezag van rector magnificus prof.dr.ir. H. Bijl,
volgens besluit van het college voor promoties
te verdedigen op donderdag 21 november 2024
klokke 14:30 uur

door

**Jasmin Annica Kuhn**
geboren te Böblingen, Duitsland
in 1995

Studiere nur und raste nie,
Du kommst nicht weit mit deinen Schlüssen;
Das ist das Ende der Philosophie,
Zu wissen, daß wir glauben müssen.

*Emanuel Geibel*

# CONTENTS

CHAPTER

1

# GENERAL INTRODUCTION

## 1.1 AGEING AND DEMENTIA

With an ageing population age-related diseases such as dementia will continue to increase in the coming years.[1] This will create an increasing burden for society and health care systems.[1] There are several types of dementia, the most common ones being Alzheimer's disease, vascular dementia, frontotemporal dementia and Lewy body dementia.[2] Multiple co-existing diseases contribute to the dementia phenotype and cardiovascular risk factors are an important contributor. Cerebrovascular disease is an umbrella term for a range of conditions that result in pathological changes in or surrounding the cerebral blood vessels.[3] Large vessel disease, a type of cerebrovascular disease, is caused by atherosclerosis in the upstream arteries leading to the brain and is a major cause of ischemic stroke.[4,5] Cerebral small vessel disease (SVD) refers to a group of pathological changes affecting the cerebral small arteries, arterioles, capillaries and venules of the brain.[3] SVD is a major contributor to ischemic stroke, cognitive decline, and dementia.[6] SVD cannot be referred to as a single disease, but should be considered a combination of radiological features that can be caused by different genetic and non-genetic diseases.[3] Examples of genetic SVD forms are Dutch-type cerebral amyloid angiopathy (D-CAA) and cerebral autosomal dominant arteriopathy with subcortical infarcts and leukoencephalopathy (CADASIL). Genetic forms of SVD typically have a more early time of onset compared to the sporadic forms. The main types of cerebral SVD that occur in older adults are ischemic SVD (including e.g. arteriolosclerosis)[4] and sporadic cerebral amyloid angiopathy (CAA), where amyloid is deposited in the walls of the cerebral blood vessels increasing the risk for hemorrhage.[3] SVD often starts with asymptomatic changes in the vasculature and parenchyma, which can be captured best in population-based studies or in targeted studies in genetic cases. To date, treatment options are limited for vascular dementia. There are some preventive life-style changes and several new pharmaceutical options that make it important to select patients at an early stage. For example, a new pharmaceutical trial on CAA will start in 2024, also including patients with Dutch-type cerebral amyloid angiopathy[7] For patient selection and especially when aiming for the earlier disease stages, specific markers are currently lacking. This thesis aims to identify and characterize novel specific SVD markers.

## 1.2 NEUROIMAGING IN CEREBRAL SVD

Magnetic resonance imaging (MRI) has developed a lot since its introduction in the early 1980s. Today, MRI is a versatile technique that allows the investigation of brain changes in humans in a non-invasive manner both in clinical as well as in research settings. Changes in blood vessel properties caused by SVD, such as arteriolosclerosis, lipohyalinosis, and fibrinoid necrosis are difficult to image directly

with MRI, but they will eventually also lead to pathology of the brain parenchyma that can be made visible by MRI.[3,6] The most common SVD related brain changes are white matter hyperintensities (WMH), lacunes, microbleeds, enlarged perivascular spaces and also atrophy.[6] WMH appear as hyperintense lesions on fluid-attenuated inversion recovery (FLAIR) MRI.[6,8] WMH can be categorized into three types based on their location and extent: periventricular, confluent and deep WMH. Periventricular and confluent WMH surround the margins of the lateral ventricles, while deep WMH are punctual lesions located in the deep white matter. In clinical practice assessments of brain MRI scans are usually based on visual inspection and scoring. However, automated segmentation techniques can provide more objective results and are especially useful for research and even more when working with larger datasets. For example, WMH volumes or brain atrophy can be calculated based on automated segmentations.[9–12] Different MRI markers of parenchymal changes and their distribution over the brain can be used to discriminate different SVD types.[6,13]

SVD is a heterogeneous disease including many possible underlying pathologies. Some brain changes in SVD might be the result of impaired clearance of waste products, which has been associated with aging and dementia.[14] It is postulated that the brain clearance process is partly driven by the glymphatic system, where cerebrospinal fluid and interstitial fluid 'flush' brain tissue and transport metabolic waste out of the parenchyma via perivascular spaces. In cerebral amyloid angiopathy[15] and Alzheimer's dementia, glymphatic function might be impaired.[16] Currently, brain clearance related processes are mainly studied invasively in humans, for example by contrast-enhanced MRI following intrathecal injection.[17] In this thesis a study including non-invasive MR imaging techniques of the glymphatic system is proposed.

## 1.3 WMH SHAPE

Traditionally, WMH were investigated in research settings by visual rating scales or volume measurements.[18] While WMH volume is an objective measure that can be obtained automatically, it is also a rather crude measure. When inspecting MRI scans visually, WMHs can appear very different from each other in shape and location, even if their calculated volumes may be roughly the same. However, measures to objectively quantify such differences that may easily be caught by the eye of a neuroradiologist were lacking. For example, the borders of WMH can in some cases look smooth while in other cases they are irregular and complex. To automatically quantify shape differences of WMHs, several WMH shape markers were introduced previously.[19,20] For periventricular/confluent WMH solidity, convexity, concavity index, and fractal dimension specific measures were introduced using the formulas shown

in Figure 1.1.[20] High solidity and convexity, as well as low concavity index and fractal dimension reflect a more irregular shape. For deep WMH, the shape markers that were found appropriate are fractal dimension and eccentricity. Higher eccentricity suggests a more elongated shape. Periventricular/confluent WMH and deep WMH have very different shape appearances which is why different shape markers are used for each of them to most accurately capture their shape.

**WMH shape markers**



Solidity

$$\text{Solidity} = \frac{\text{Volume}}{\text{Convex Hull Volume}}$$

Convexity

$$\text{Convexity} = \frac{\text{Convex Hull Area}}{\text{Area}}$$

Concavity index

$$\text{Concavity index} = \sqrt{(2 - C)^2 + (1 - S)^2}$$

Fractal dimension

$$\text{Fractal Dimension} = \lim_{r \to 1} \frac{\log(n_r)}{\log\left(\frac{1}{r}\right)}$$

Eccentricity

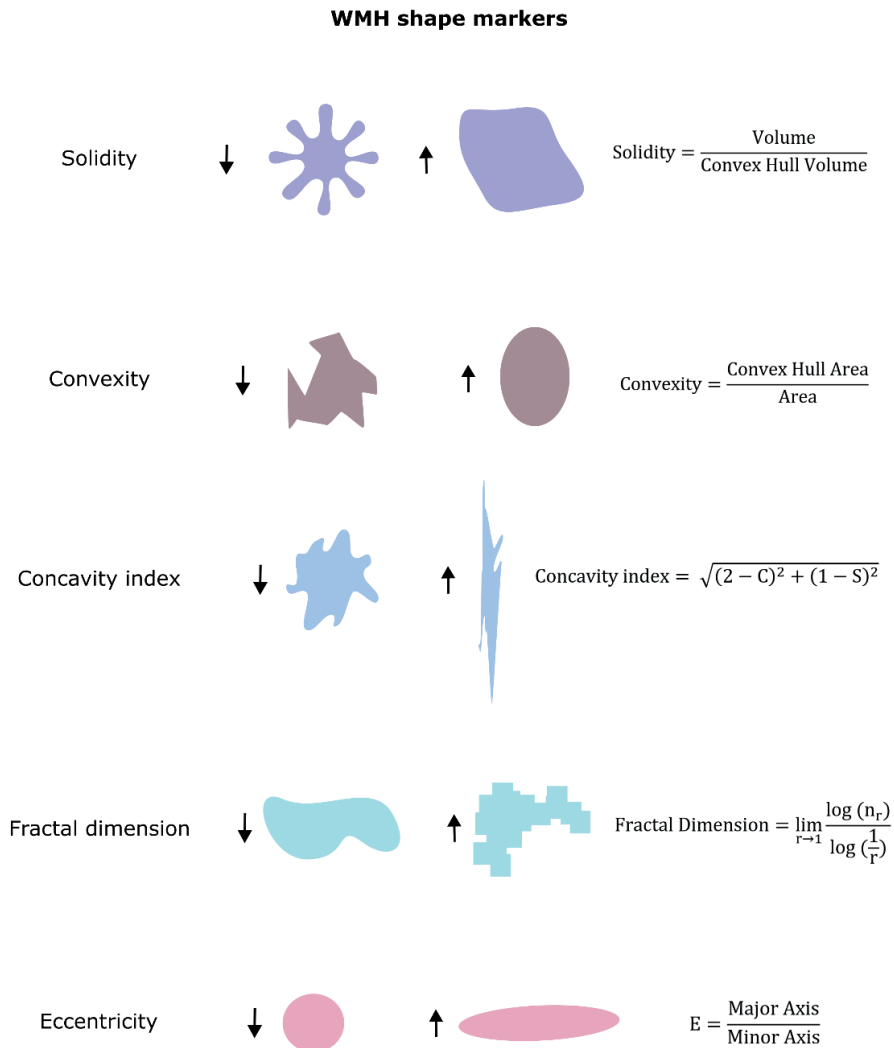$$E = \frac{\text{Major Axis}}{\text{Minor Axis}}$$

**Figure 1.1. Illustration of shapes and different shape markers**. Solidity, convexity, concavity index, and fractal dimension are calculated for periventricular/confluent WMH. Eccentricity and fractal dimension are calculated for deep WMH. This Figure is modified from figure 7.3 of **Chapter 7**.

1

Different WMH types (periventricular/confluent and deep) and also different WMH shape patterns seem to be associated with different underlying pathological changes. A more irregular shape of WMH go hand-in-hand with more severe parenchymal changes.[21–23] Furthermore, a previous study has shown that a more irregular WMH shape was associated with increased stroke risk and increased mortality in patients with manifest arterial disease.[24] I hypothesize that different underlying SVD pathologies result in a different WMH shape that can be quantified by MRI-based WMH shape markers. These shape markers may provide a more detailed characterization of WMH than volume alone.

## 1.4 AGES-REYKJAVIK STUDY

Large longitudinal population-based studies focused on ageing are rare since they are expensive and labor-intensive to carry out. This study type is, however, extremely valuable as it allows investigations with high statistical power. At the same time, they provide high external validity, since the participants of the study come from the general population with minimal inclusion bias.

A substantial part of this thesis is focused on data from the Age-Gene/Environment Susceptibility (AGES)-Reykjavik study, a large population-based study.[25] The AGES–Reykjavik study originates from the Reykjavik Study, a cohort established in 1967 to prospectively study cardiovascular disease in the general population of Iceland. Included participants were born between 1907 and 1935 and were living in Reykjavik in 1967. For the AGES-Reykjavik study, participants that were still alive were randomly selected for a follow-up between 2002 and 2006 when they underwent amongst other measures, a baseline brain MRI scan and cognitive assessment.[26] Another visit took place between 2007 and 2011, where the same brain MRI protocol and the same cognitive assessments were repeated.[27] Furthermore, the participants were followed for dementia outcome up to 13.4 years after the first MRI scan session through vital statistics and hospital records, and by the nursing home and home-based resident assessment instrument.[28] The AGES-Reykjavik study is an extensive multidisciplinary study and includes besides neuroimaging and neurocognitive data also genetic, cardiovascular and musculoskeletal data.[25] In the related chapters of this thesis, the focus will be on neuroimaging and neurocognitive data obtained as part of the AGES study.

## 1.5 AIM AND OUTLINE OF THIS THESIS

The overarching aim of this thesis is to exploit the shape of WMHs to better characterize WMH and thereby to improve the clinical interpretation of WMHs and to investigate whether it could predict clinical outcome. This thesis is mostly based on non-demented and community-dwelling older individuals. Moreover, a study set up focusing on a memory-clinic population will be discussed to get more pathology-focused insights into the formation of WMH.

In **Chapter 2**, the association of different cardiovascular risk factors with WMH shape was investigated in older adults as included in the Biomarker Development for Postoperative Cognitive Impairment in the Elderly (BIOCOG) study. The study included non-demented older adults scheduled for major elective surgery. Next, in **Chapter 3**, it was examined whether WMH shape is related to long-term progression of cerebrovascular disease in the AGES Reykjavik dataset. Besides WMH, different types of infarcts, microbleeds and enlarged perivascular spaces and their relationship with WMH shape were evaluated in this chapter. In **Chapter 4**, the focus was on investigating the association between baseline WMH shape and cognitive decline measured in three different domains (memory, executive function, and processing speed) over 5.2 years in the AGES Reykjavik dataset. In **Chapter 5**, the association of baseline WMH shape and long-term dementia risk after up to 13.4 years was assessed in the AGES Reykjavik study. In **Chapter 6**, brain MRI phenotypes were obtained using a hierarchical clustering method in the AGES Reykjavik dataset. In a second step, it was investigated whether these phenotypes are related to long-term risk (10 years) for dementia. In **Chapter 7**, a novel prospective cross-sectional study is presented applying WMH shape markers and other cutting-edge MRI techniques to further understand processes involved in SVD. This WHIte MAtter hyperintensity Shape and glymphatics (WHIMAS) study is focused on brain MRI determinants of cognitive impairment in geriatric clinic outpatients. Lastly, in **Chapter 8**, the main findings of this thesis and future directions of research are discussed.

## 1.6 REFERENCES

1.  World Health Organization. Dementia. Fact Sheet. 2023. https://www.who.int/news-room/fact-sheets/detail/dementia (accessed 23 Feb 2024).

2.  Livingston G, Sommerlad A, Orgeta V, Costafreda SG, Huntley J, Ames D et al. Dementia prevention, intervention, and care. The Lancet 2017; 390: 2673–2734.

3.  Wardlaw JM, Smith C, Dichgans M. Small vessel disease: mechanisms and clinical implications. Lancet Neurol 2019; 18: 684–696.

4.  Wardlaw JM, Smith C, Dichgans M. Mechanisms of sporadic cerebral small vessel disease: Insights from neuroimaging. Lancet Neurol 2013; 12: 483–497.

5.  Pantoni L. Cerebral small vessel disease: from pathogenesis and clinical characteristics to therapeutic challenges. Lancet Neurol 2010; 9: 689–701.

6.  Duering M, Biessels GJ, Brodtmann A, Chen C, Cordonnier C, de Leeuw FE et al. Neuroimaging standards for research into small vessel disease—advances since 2013. Lancet Neurol 2023; 22: 602–618.

7.  Voigt S, Koemans EA, Rasing I, van Etten ES, Terwindt GM, Baas F et al. Minocycline for sporadic and hereditary cerebral amyloid angiopathy (BATMAN): study protocol for a placebo-controlled randomized double-blind trial. Trials 2023; 24: 1–6.

8.  Hajnal J V., de Coene B, Lewis PD, Baudouin CJ, Cowan FM, Pennock JM et al. High signal regions in normal white matter shown by heavily T2-weighted CSF nulled IR sequences. J Comput Assist Tomogr 1992; 16: 506–513.

9.  de Bresser J, Portegies MP, Leemans A, Biessels GJ, Kappelle LJ, Viergever MA. A comparison of MR based segmentation methods for measuring brain atrophy progression. Neuroimage 2011; 54: 760–768.

10. Pini L, Pievani M, Bocchetta M, Altomare D, Bosco P, Cavedo E et al. Brain atrophy in Alzheimer's Disease and aging. Ageing Res Rev 2016; 30: 25–48.

11. Balakrishnan R, Valdés Hernández M del C, Farrall AJ. Automatic segmentation of white matter hyperintensities from brain magnetic resonance images in the era of deep learning and big data – A systematic review. Computerized Medical Imaging and Graphics 2021; 88: 101867.

12. Kuijf HJ, Casamitjana A, Collins DL, Dadar M, Georgiou A, Ghafoorian M et al. Standardized Assessment of Automatic Segmentation of White Matter Hyperintensities and Results of the WMH Segmentation Challenge. IEEE Trans Med Imaging 2019; 38: 2556–2568.

13. Charidimou A, Boulouis G, Frosch MP, Baron JC, Pasi M, Albucher JF et al. The Boston criteria version 2.0 for cerebral amyloid angiopathy: a multicentre, retrospective, MRI–neuropathology diagnostic accuracy study. Lancet Neurol 2022; 21: 714–725.

14. Benveniste H, Nedergaard M. Cerebral small vessel disease: A glymphopathy? Curr Opin Neurobiol 2022; 72: 15–21.

15. van Veluw SJ, Benveniste H, van Osch MJP, Clearance the LFTN of E on B, Bakker ENTP, Carare RO et al. A translational approach towards understanding brain waste clearance in cerebral amyloid angiopathy. Eur Heart J 2024.

16. Peng W, Achariyar TM, Li B, Liao Y, Mestre H, Hitomi E et al. Suppression of glymphatic fluid transport in a mouse model of Alzheimer's disease. Neurobiol Dis 2016; 93: 215–225.

17. Ringstad G, Valnes LM, Dale AM, Pripp AH, Vatnehol SAS, Emblem KE et al. Brain-wide glymphatic enhancement and clearance in humans assessed with MRI. JCI Insight 2018; 3.

18. Wardlaw JM, Valdés Hernández MC, Muñoz-Maniega S. What are white matter hyperintensities made of? Relevance to vascular cognitive impairment. J Am Heart Assoc 2015; 4: 001140.

19.  De Bresser J, Kuijf HJ, Zaanen K, Viergever MA, Hendrikse J, Biessels GJ et al. White matter hyperintensity shape and location feature analysis on brain MRI; Proof of principle study in patients with diabetes. Sci Rep 2018; 8: 1–10.

20.  Ghaznawi R, Geerlings MI, Jaarsma-Coes MG, Zwartbol MHT, Kuijf HJ, van der Graaf Y et al. The association between lacunes and white matter hyperintensity features on MRI: The SMART-MR study. Journal of Cerebral Blood Flow and Metabolism 2019; 39: 2486–2496.

21.  Alber J, Alladi S, Bae H, Barton DA, Beckett LA, Bell JM et al. White matter hyperintensities in vascular contributions to cognitive impairment and dementia (VCID): Knowledge gaps and opportunities. Alzheimer's & Dementia: Translational Research & Clinical Interventions 2019; 5: 107–117.

22.  Fazekas F, Kleinert R, Offenbacher H, Schmidt R, Kleinert G, Payer F et al. Pathologic correlates of incidental MRI white matter signal hyperintensities. Neurology 1993; 43: 1683–1689.

23.  Kim KW, MacFall JR, Payne ME. Classification of White Matter Lesions on Magnetic Resonance Imaging in Elderly Persons. Biol Psychiatry 2008; 64: 273–280.

24.  Ghaznawi R, Geerlings M, Jaarsma-Coes M, Hendrikse J, de Bresser J. Association of White Matter Hyperintensity Markers on MRI and Long-term Risk of Mortality and Ischemic Stroke. Neurology 2021.

25.  Harris TB, Launer LJ, Eiriksdottir G, Kjartansson O, Jonsson P V., Sigurdsson G et al. Age, gene/environment susceptibility-reykjavik study: Multidisciplinary applied phenomics. Am J Epidemiol 2007; 165: 1076–1087.

26.  Saczynski JS, Sigurdsson S, Jonsdottir MK, Eiriksdottir G, Jonsson P V., Garcia ME et al. Cerebral infarcts and cognitive performance: importance of location and number of infarcts. Stroke 2009; 40: 677–682.

27.  Sigurdsson S, Aspelund T, Kjartansson O, Gudmundsson EF, Jonsdottir MK, Eiriksdottir G et al. Incidence of Brain Infarcts, Cognitive Change, and Risk of Dementia in the General Population: The AGES-Reykjavik Study (Age Gene/Environment Susceptibility-Reykjavik Study). Stroke 2017; 48: 2353–2360.

28.  Morris JN, Hawes C, Fries BE, Phillips CD, Mor V, Katz S et al. Designing the National Resident Assessment Instrument for Nursing Homes. Gerontologist 1990; 30: 293–307.

CHAPTER

2

# DIFFERENT CARDIOVASCULAR RISK FACTORS ARE RELATED TO DISTINCT WHITE MATTER HYPERINTENSITY MRI PHENOTYPES IN OLDER ADULTS

Jasmin A. Keller, Ilse M.J. Kant, Arjen J.C. Slooter, Simone J.T. van Montfort, Mark A. van Buchem, Matthias J.P. van Osch, Jeroen Hendrikse, Jeroen de Bresser.

## 2.1 ABSTRACT

The underlying mechanisms of the association between cardiovascular risk factors and a higher white matter hyperintensity (WMH) burden are unknown. We investigated the association between cardiovascular risk factors and advanced WMH markers in 155 non-demented older adults (mean age: 71 ± 5 years). The association between cardiovascular risk factors and quantitative MRI-based WMH shape and volume markers were examined using linear regression analysis. Presence of hypertension was associated with a more irregular shape of periventricular/confluent WMH (convexity (B (95 % CI)): −0.12 (−0.22−−0.03); concavity index: 0.06 (0.02−0.11)), but not with total WMH volume (0.22 (−0.15−0.59)). Presence of diabetes was associated with deep WMH volume (0.89 (0.15−1.63)). Body mass index or hyperlipidemia showed no association with WMH markers. In conclusion, different cardiovascular risk factors seem to be related to a distinct pattern of WMH shape markers in non-demented older adults. These findings may suggest that different underlying cardiovascular pathological mechanisms lead to different WMH MRI phenotypes, which may be valuable for early detection of individuals at risk for stroke and dementia.

## 2.2 INTRODUCTION

Cerebral small vessel disease (SVD) is associated with the occurrence of dementia and stroke.[1] In SVD, different underlying pathological mechanisms (such as small or large vessel atheromas or embolisms) lead to the phenotype of MRI-visible brain changes, namely white matter hyperintensities (WMH), lacunes and microbleeds.[2,3] Individual cardiovascular risk factors play an important role in the etiology of SVD as they impact the small vessels via different pathological pathways and hence lead to distinct patterns of SVD related brain changes that may be differentiated.[4] An example of this principle is the association between hypertension and deep cerebral microbleeds versus cerebral amyloid angiopathy and lobar microbleeds.[5] Although WMH are the key MRI marker of idiopathic SVD, little is known about the association of individual cardiovascular risk factors and distinct patterns of WMH. WMH volume is typically used to study WMH, but this marker fails to fully quantify the complex brain changes related to underlying pathological changes of SVD.[4] Moreover, WMH volume alone is insufficient for differentiation of underlying disease mechanisms leading to WMH. Aiming to overcome the limitations of conventional WMH volume markers, in recent studies WMH type and shape were introduced as more advanced WMH markers.[6,7] For example, different WMH type (periventricular, deep and confluent) and also different WMH shape is associated with different underlying pathological changes.[4,8,9] Furthermore, previous studies on WMH shape show potential diagnostic and prognostic value related to an increased mortality and stroke risk.[6,7,10] The investigation of WMH type and shape markers may therefore help in the postulation of potential mechanisms of WMH development. Our hypothesis is that in older adults specific cardiovascular risk factors relate to distinct patterns of WMH, which can be quantified using advanced WMH MRI markers. Studying this hypothesis may aid in the understanding of WMH development and could in the future be used for earlier detection of individuals at risk for stroke or dementia. Therefore, we aimed to investigate the association between cardiovascular risk factors and advanced WMH markers (shape, type, and volume) in non-demented older adults.

## 2.3 METHODS

### 2.3.1 Participants

We included data from the BioCog consortium study, collected from the University Medical Center Utrecht site.[11] Inclusion criteria for the BioCog study were: minimal age of 65 years, a mini-mental state exam (MMSE) score of 24 or higher, and major surgery scheduled of at least 60 min (cardiothoracic (n = 35), gastroenterological (n = 22), gynecologic (n = 6), jaw (n = 11), ear nose throat (13), orthopedic (43), urological

(25)). The MMSE was used as a screening for dementia in order to exclude severely cognitively impaired participants. The study was approved by the medical ethics committee (Medical Ethical Committee Utrecht nr. 14/469). Written informed consent was obtained from all participants.

### 2.3.2 Procedure and demographics

All participants were invited to the hospital before surgery for questionnaires and MRI scanning. Demographic data and medical his- tory questionnaires, and MMSE scores were obtained prior to surgery. Symptoms of anxiety and depression were assessed using the hospital and depression scale (HADS). Scores equal to or above 8 on the depression subscale were considered indicative of depressive symptoms.[12] American Society of Anesthesiologists (ASA) classification scores were performed before surgery by anesthesiologists in training.

### 2.3.3 Cardiovascular risk factors

Demographic data and data concerning cardiovascular risk factors was collected using questionnaires and medical history records. Diabetes (type I&II), hypertension and hyperlipidemia were registered in the database if they were known by the subject, and treated. BMI in $kg/m^3$ was collected as an additional cardiovascular risk factor. Obesity was defined as a BMI equal to or above 30 $kg/m^3$.

### 2.3.4 MRI scans

The scans were performed before surgery on a Philips Achieva 3 Tesla MRI system. The standardized MRI scan protocol included a 3D T1-weighted sequence (voxel size = 1.0 × 1.0 × 1.0 $mm^3$; TR/TE = 7.9/4.5 ms) and a 3D fluid-attenuated inversion recovery (FLAIR) sequence (voxel size = 1.11 × 1.11 × 0.56 $mm^3$; TR/TE/TI = 4800/125/1650 ms).

### 2.3.5 WMH volume, type and shape

Two categories of WMH were automatically determined: 'deep' WMH, and 'periventricular/confluent' WMH. WMH volumes were calculated automatically using validated methods.[7] Based on the WMH segmentation data, the mean values per WMH shape marker (solidity, convexity, concavity index, fractal dimension for periventricular/confluent WMH; fractal dimension and eccentricity for deep WMH) were calculated for each participant with an in-house developed method.[7] The image processing pipeline is illustrated in Figure 2.1. Statistical parametric mapping (SPM version 12; Wellcome Institute of Neurology University College London, UK, http://www.fil.ion.ucl.ac. uk/spm/doc/) in MATLAB (The MathWorks, Inc., Natick, Massachusetts, United States) was used to register 3D FLAIR images to 3D T1-weighted images. Intracranial volume was calculated using the SPM12 with the option

'tissue volumes'. The lesion prediction algorithm of the lesion segmentation toolbox version 2.0.15[13] (https://www.sta tistical-modeling.de/lst.html) for SPM12 was used for WMH segmentation. The quality of the WMH segmentations was visually checked by a trained researcher (IK) under supervision of a neuroradiologist experienced in brain segmentation (JB). Cortical brain infarcts were manually delineated and removed from the WMH probability maps. The lateral ventricles were segmented on the T1-weighted images using the automated lateral ventricle delineation toolbox[14] (ALVIN; https://www.nitrc. org/projects/alvin_lv/ in SPM8. A threshold of 0.10 was applied on the probabilistic WMH segmentations. Periventricular WMH were defined as WMH contiguous with the lateral ventricles and extending ≤ 10 mm into the deep white matter. Confluent WMH were defined as WMH contiguous with the lateral ventricles and extending > 10 mm into the deep white matter. Deep WMH were defined as being located > 3 mm from the lateral ventricles and > 5 voxels (3.45 × $10^{-3}$ ml). Based on the binary WMH segmentation data, WMH shape markers were calculated.[7] For periventricular/confluent WMH, solidity was calculated by dividing lesion volume by the volume of its convex hull. Dividing the convex hull sur- face area by the lesion surface area provides the convexity of the WMH. A lower solidity and a lower convexity indicates a more complex shape.[7] The concavity index is a measure of roughness and was calculated from solidity and convexity.[7] A higher concavity index indicates a more irregular shape.[15] Eccentricity of deep WMH was calculated by dividing the minor axis of the WMH by its major axis. Fractal dimension was calculated as a measure for irregularity of deep, and periventricular/confluent WMH using the box-counting method. Higher fractal dimension and eccentricity values suggest a more complex WMH shape.[7] These WMH shape markers were selected because of their ability to capture the expected shape variations of different types of WMH accurately (see Supplementary Table S.2.8.1 for an overview).[7] Mean values per WMH shape marker were calculated per patient and used for further analyses. The accuracy of the WMH shape marker calculation is dependent on WMH size. Periventricular/confluent lesions vary in size and especially in earlier stages the lesions are not only smaller, but are in a different range of shape markers. The shape parameters used in our study are more accurate in capturing the WMH shape of bigger periventricular/confluent lesions. Therefore a minimum WMH volume of 4 ml was applied as a threshold for the analyses of periventricular/confluent WMH shape markers to assure our method is robust and accurate.

## 2.4 RESULTS

A total of 178 participants met the inclusion criteria and were included, of which 23 participants had to be excluded from the current study for the following reasons: WMH segmentation errors (n = 2), over- segmentation of WMH (n = 8), anatomic abnormalities (n = 2), missing scans (n = 3), a large cyst (n = 1), MRI motion artefacts (n = 4) or other artefacts (n = 3). Baseline characteristics of the remaining 155 participants are shown in Table 2.1. A total of 47 % of the participants had hypertension, 34 % had hyperlipidemia, 16 % had diabetes and the mean BMI was 27 ± 4 kg/m$^2$.

Presence of hypertension was associated with a more irregular shape of periventricular/confluent WMH (a lower convexity: B (95 % CI): −0.12 (−0.22−−0.03); p = 0.01; a higher concavity index: 0.06 (0.02−0.10); p = 0.01) (see Table 2.2), but not with total WMH volume (0.22 (−0.15−0.59); p = 0.24).

Presence of diabetes was associated with a higher deep WMH volume (B (95 % CI): 0.97 (0.25−1.70); p = 0.02) (see Table 2.3). Trends were found for an association between the presence of diabetes and a higher total WMH volume (0.45 (−0.05−0.95); p = 0.07) and a higher perivascular/confluent WMH volume (0.43 (−0.07−0.92); p = 0.09). No associations were found between presence of diabetes and WMH shape markers (see Table 2.2).

Neither BMI nor hyperlipidemia were associated with WMH volume (B (95 % CI): 0.97 (0.25−1.70); p = 0.02) (see Table 2.3). Trends were found for an association between the presence of diabetes and a higher total WMH volume (0.45 (−0.05−0.95); p = 0.07) and a higher perivascular/confluent WMH volume (0.43 (−0.07−0.92); p = 0.09). No associations were found between presence of diabetes and WMH shape markers (see Table 2.2).

Neither BMI nor hyperlipidemia were associated with WMH volume or shape markers. The mean WMH shape markers stratified for cardiovascular risk factor are shown in Table 2.4 and the mean WMH volumes values stratified for cardiovascular risk factor can be found in Table 2.5. In secondary analyses, we performed a stepwise linear regression to investigate which of the significantly associated cardiovascular risk factors accounts for most of the variation of the WMH marker. The results of these analyses were in line with our primary linear regression analyses (see the Supplementary results). In other secondary analyses, age was associated with periventricular/confluent WMH shape (convexity, concavity index and fractal dimension) and WMH volumes (see Supplementary Tables S.2.8.2 and S.2.8.3). Furthermore, sex was associated with periventricular/confluent WMH shape (solidity).

**Table 2.1.** Baseline characteristics of the patient population.

|  | Total (n=155) |
|---|---|
| **Age** | 71 ± 5 |
| **Female sex** | 50 (32%) |
| **MMSE** | 29 (27,30) |
| **ASA score** |  |
| 1 | 19 (12%) |
| 2 | 84 (54%) |
| 3 | 52 (34%) |
| **Depressive symptoms** | 7 (5%) |
| **Vascular risk factors** |  |
| Hypertension | 72 (47%) |
| Diabetes (type I & II) | 24 (16%) |
| BMI (kg/m$^2$) | 27 ± 4 |
| Hyperlipidemia | 55 (34%) |
| Obesity | 30 (19%) |
| Current smoker | 13 (8%) |
| Prior TIA or CVA | 8 (5%) |

Data represent n (percentage), mean ± SD or median (interquartile range). MMSE: mini mental state exam; ASA: classification of disease severity for the American Society of Anesthesiologists. BMI: body-mass index. TIA: transient ischemic attack. CVA: cerebrovascular accident.

**Table 2.2** The association between cardiovascular risk factors and WMH shape markers.

|  | Hypertension | Diabetes | BMI | Hyperlipidemia |
|---|---|---|---|---|
| **Periventricular/ Confluent WMH[†]** |  |  |  |  |
| Solidity[‡] | 0.84 (-0.10−0.27) | -0.02 (-0.24−0.20) | 0.00 (-0.02−0.02) | -0.01 (-0.18−0.19) |
| Convexity | -0.12 (-0.22−-0.03)* | -0.03 (-0.15−0.09) | 0.00 (-0.01−0.01) | 0.01 (-0.09−0.11) |
| Concavity index[‡] | 0.06 (0.02−0.11)* | 0.01 (-0.04−0.06) | -0.00 (-0.01-0.01) | -0.01 (-0.05-0.04) |
| Fractal dimension | 0.04 (-0.01−0.10) | 0.01 (-0.07−0.07) | -0.00 (-0.01−0.01) | -0.03 (-0.08−0.03) |
| **Deep WMH** |  |  |  |  |
| Eccentricity | 0.01 (-0.03−0.06) | 0.00 (-0.05−0.06) | -0.00 (-0.01−0.01) | 0.02 (-0.02−0.06) |
| Fractal dimension | 0.01 (-0.10−0.12) | -0.03 (-0.17−0.10) | -0.01 (-0.02−0.00) | -0.08 (-0.17−0.03) |

The values represent B values (95% confidence interval) of the linear regression analyses adjusted for age and sex. * p<0.05. [‡]Solidity and concavity index were multiplied by 100 and natural log transformed, due to non-normal distribution. [†] Periventricular/confluent WMH with a volume >4 ml. Periventricular/ confluent WMH: n=73; Deep WMH: n=122.

**Table 2.3.** The association between cardiovascular risk factors and WMH volume.

|  | Hypertension | Diabetes | BMI | Hyperlipidemia |
|---|---|---|---|---|
| **Total WMH volume** | 0.22 (-0.15−0.59) | 0.45 (-0.05−0.95) | 0.00 (-0.04−0.05) | 0.14 (-0.24−0.52) |
| **Periventricular/confluent WMH volume** | 0.21 (-0.16−0.57) | 0.43 (-0.07−0.92) | 0.00 (-0.04−0.05) | 0.15 (-0.23−0.53) |
| **Deep WMH volume** | 0.24 (-0.32−0.80) | 0.89 (0.15−1.63)* | 0.05 (-0.02−0.11) | -0.08 (-0.65−0.48) |

These values represent B values (95% confidence interval) of the linear regression analyses adjusted for age, sex and intracranial volume. WMH volumes were multiplied by 100 and natural log transformed, due to non-normal distribution. * $p<0.05$. WMH: white matter hyperintensities. BMI: body-mass index.

**Table 2.4** : Mean WMH shape values per cardiovascular risk factor

|  | Total | Hypertension | Diabetes | Obesity | Hyperlipidemia |
|---|---|---|---|---|---|
| **Periventricular/confluent WMH*** |  |  |  |  |  |
| Solidity | 0.19 ± 0.08 | 0.19 ± 0.07 | 0.19 ± 0.06 | 0.19 ± 0.07 | 0.19 ± 0.08 |
| Convexity | 1.15 ± 0.21 | 1.08 ± 0.18 | 1.15 ± 0.21 | 1.19 ± 0.12 | 1.16 ± 0.22 |
| Concavity index | 1.19 ± 0.13 | 1.23 ± 0.14 | 1.19 ± 0.16 | 1.15 ± 0.08 | 1.18 ± 0.13 |
| Fractal dimension | 1.83 ± 0.13 | 1.87 ± 0.14 | 1.82 ± 0.13 | 1.80 ± 0.12 | 1.82 ± 0.13 |
| **Deep WMH** |  |  |  |  |  |
| Eccentricity | 0.56 ± 0.12 | 0.57 ± 0.11 | 0.56 ± 0.10 | 0.56 ± 0.15 | 0.57 ± 0.14 |
| Fractal Dimension | 1.83 ± 0.28 | 1.84 ± 0.32 | 1.80 ± 0.17 | 1.76 ± 0.40 | 1.79 ± 0.34 |

Data are represented as means ± SD. Obesity was defined as a BMI >30 kg/m$^2$. WMH shape markers are given for the total number of individuals, individuals with diabetes (type I & II), individuals with hypertension, obesity or hyperlipidemia, respectively. *Periventricular/confluent WMH with a volume >4 ml. Periventricular/confluent WMH: total n=73;  hypertension: n=36; diabetes: n=16; obesity: n=16; hyperlipidemia: n=31. Deep WMH: total n=122; hypertension: n = 57; diabetes: n=22; obesity: n=25; hyperlipidemia: n=45.

**Table 2.5:** Mean WMH volumes per cardiovascular risk factor

|  | Total | Hypertension | Diabetes | Obesity | Hyperlipidemia |
|---|---|---|---|---|---|
| **Total WMH volume** | 7.84 ± 11.37 | 10.07 ± 13.29 | 10.14 ± 13.93 | 6.77 ± 6.74 | 7.92 ± 10.62 |
| **Periventricular/ confluent WMH volume** | 7.53 ± 11.18 | 9.67 ± 13.09 | 9.54 ± 13.56 | 6.34 ± 6.57 | 7.61 ± 10.38 |
| **Deep WMH volume** | 0.32 ± 0.59 | 0.40 ± 0.69 | 0.61 ± 0.93 | 0.44 ± 0.74 | 0.31 ± 0.63 |

Data are represented as mean volumes (ml) ± SD. WMH volumes are given for the total number of individuals, individuals with diabetes (type I & II), individuals with hypertension, obesity or hyperlipidemia, respectively. Obesity was defined as a BMI >30 kg/m$^2$. Total: n=155; hypertension: n=72; diabetes: n=24; obesity: n=30; hyperlipidemia: n=55. Missing values:  hypertension: n=3; BMI: n=5; hyperlipidemia: n=3.

## 2.5 DISCUSSION

The present study aimed to investigate the association of cardiovascular risk factors and novel advanced WMH markers in non-demented older adults. We showed that the presence of hypertension was associated with a more irregular shape of periventricular/confluent WMH, but not with WMH volume. Presence of diabetes was associated with deep WMH volume. BMI or hyperlipidemia showed no association with WMH markers in our study.

We found an association between hypertension and a more irregular WMH shape, but did not find an association with WMH volume. An association between hypertension and WMH volume has previously been shown in several large population-based studies focusing on older adults.[16,17] Accordingly, hyper- tension is seen as one of the strongest cardiovascular risk factors associated with WMH. In our study—with a smaller sample size than other population-based studies—we did not find such an association. No previous studies have focused on the association between hypertension and WMH shape. The findings of our study might indicate that WMH shape is a more sensitive marker of hypertension-induced brain changes than WMH volume, since WMH shape was associated with hypertension while WMH volume was not. Based on the results of our study, we postulate that hypertension leads to distinct pathological changes within the small vessels of the brain, which manifest as a distinct WMH MRI phenotype. Hypertension has a direct destructive effect on small arteries, arterioles, venules and capillaries in the brain. Progressive pathological changes to the small vessels of the brain, induced by atheromas and micro-embolisms[2,18], may manifest as distinct WMH phenotypes on MRI due to the anatomical macrostructure of the small vessels located around the ventricles in the white matter. This highlights the strong vascular component in WMH development already suggested in previous research.[3,4] In our study each WMH shape marker that was analyzed represents a different spectrum of shape variations. For example, presence of hypertension is related to the variation in shape of periventricular/confluent WMH represented by a low convexity and high concavity index, but not to variations in shape represented by solidity or fractal dimension. Important to acknowledge in this regard is that convexity and the concavity index are mathematically related to each other. It is difficult to directly translate our described associations on a group-level to an individual patient in a clinical setting. For future translation to clinical practice, artificial intelligence-based models including a combination of several MRI biomarkers are required for more accurate applications in the field of diagnosis or prognosis. At present, the association between diabetes and WMH volume is not entirely understood. Previous studies in community-dwelling older individuals have shown associations of type 2 diabetes mellitus and total WMH volume[19,20], while other cross-sectional studies in

similar study populations failed to show such an association.[21,22] A recent systematic review addressing a possible association between type 2 diabetes and total WMH volume shows an association.[23] The review did not only focus on cross-sectional or cohort studies, but also included case-control, and Mendelian randomization studies. Furthermore, a previous case-control study focused on patients with type 2 diabetes showed a higher eccentricity of deep WMH and a larger number of periventricular/confluent WMH in diabetic patients compared to controls, but no differences in WMH volume.[6] In our study in non-demented older adults, we did not find an association of diabetes with WMH shape markers, but found an association of diabetes with deep WMH volume. No previous studies have explored WMH shape in non-demented older adults, therefore our results cannot be directly compared to other studies. Based on these findings, WMH shape may be more sensitive than WMH volume for hypertension-induced brain changes, but not for diabetes-induced brain changes. The association between hyperlipidemia and WMH remains ambiguous. In a previous study, an association between high cholesterol levels and a larger WMH burden was found in the general population above 65 years of age.[24] Participants in this previous study are quite comparable to our study regarding age and cardiovascular risk factor profile. A previous case-control study focusing on stroke patients has shown a potential protective role of hyperlipidemia, as hyperlipidemia was associated with lower WMH volumes in two independent cohorts.[25] However, it is unclear if this protective effect is (partially) mediated through the pharmacological treatment of hyperlipidemia with statins.[25] This previous study has assessed a specific patient population (stroke patients) with a lower mean age in one of the cohorts compared to our study. No previous study has examined the association between hyper- lipidemia and WMH shape. In our study we did not find an association between hyperlipidemia and WMH volume, nor shape markers. Previous studies conducted using UK-biobank data, with a cross-sectional[26], as well as an observational cohort study design[27], showed an association of BMI with WMH volume. This effect may be mediated via low-grade systemic inflammation.[28] However, no previous study has examined the association between BMI and WMH shape markers. In our study, we found no associations between BMI and WMH volume or shape markers. It should be noted that mean BMI in the UK-biobank study was similar to our study, while mean age was lower compared to our study.[26] Little is known about the exact histopathological mechanisms underlying the formation of WMH, mainly due to the small number of pathology studies that have been conducted.[29] Interestingly, in a histopathological study, structural markers of vascular dysfunction were found to be associated with WMH.[30] More specifically, vascular integrity was shown to be reduced in areas where WMH were present compared to normal appearing white matter.[30] Periventricular, and deep WMH were associated with different underlying neuropathological findings in a study

including Alzheimer's patients, subjects at risk for cerebrovascular disease and healthy controls.[31] The study found periventricular WMH volume to be correlated with severity of arteriolosclerosis and breakdown of the ventricular lining.[31] Deep WMH volume, however, was correlated with cerebral hemorrhages and microinfarcts, as well as demyelination.[31] Depending on the affected cell type (e.g. vascular or parenchymal), the type of pathophysiology and the anatomical structure of the affected areas, WMH shape may be influenced. These differences in WMH etiology may become evident as different WMH shape patterns and locations (for example punctuate versus elongated deep WMH). Some previous studies have also shown a link between WMH shape and underlying histological findings.[8,9] Overall, pathological studies confirm the hypothesis that WMH have a heterogenous etiology[18]—with a strong vascular component. Vascular pathologies may lead to parenchymal changes, subsequently leading to distinct WMH phenotypes on MRI. How different WMH lesion and shape patterns develop related to a certain underlying pathology remains to be investigated in future studies, as in our study it is impossible to link WMH shape patterns to specific underlying mechanisms. Novel advanced MRI markers (such as WMH shape) that are more specific than WMH volume, may help in elucidating the link between histopathology and MRI findings. The strengths of our study are the relatively large sample size, and the application of novel advanced MRI image processing methods. A limitation of our study could be that participants were all scheduled for major elective surgery, and therefore this sample might not be an equivalent of a general population-based group. This could limit the generalizability of our findings to the general population, as this could have led to an underestimation of the associations. Another limitation of our study could be that the cardiovascular risk factors were based on medical records and self-reported rather than objective measurements (e.g. blood pressure, glucose levels and cholesterol/triglyceride levels). Although these risk factors were scored by qualified physicians (anesthesiologists (in training)), we cannot exclude the possibility that some patients may have undiagnosed hypertension, diabetes or hypercholesterolemia. This may partially account for the lack of significant associations between these cardiovascular risk factors and the WMH markers. An additional limitation could be that although most participants had a relatively high MMSE score (median: 29, (IQR: 27,30)), there may have been participants included in this study with mild cognitive impairment. A technical limitation of our method could be that when total WMH volume increases, usually the deep WMH count decreases, as bigger WMH lesions start to overlap with each other. For instance, deep WMH may become part of confluent WMH and only shape markers for periventricular/confluent WMH can be determined. This can partially explain why we found fewer associations with deep WMH shape markers.

In conclusion, we showed that different cardiovascular risk factors seem to be related to a distinct pattern of WMH shape markers in non-demented older adults. These findings may suggest that different underlying cardiovascular pathological mechanisms lead to different WMH MRI phenotypes, which may be valuable for early detection of individuals at risk for stroke and dementia.

2

## 2.6 ACKNOWLEDGEMENTS

## 2.7 REFERENCES

1.  Jellinger KA, Attems J. Challenges of multimorbidity of the aging brain: a critical update. J Neural Transm 2015; 122: 505–521.

2.  Wardlaw JM, Smith C, Dichgans M. Mechanisms of sporadic cerebral small vessel disease: Insights from neuroimaging. Lancet Neurol 2013; 12: 483–497.

3.  Wardlaw JM, Smith EE, Biessels GJ, Cordonnier C, Fazekas F, Frayne R et al. Neuroimaging standards for research into small vessel disease and its contribution to ageing and neurodegeneration. Lancet Neurol. 2013; 12: 822–838.

4.  Alber J, Alladi S, Bae H, Barton DA, Beckett LA, Bell JM et al. White matter hyperintensities in vascular contributions to cognitive impairment and dementia (VCID): Knowledge gaps and opportunities. Alzheimer's & Dementia: Translational Research & Clinical Interventions 2019; 5: 107–117.

5.  Gao Z, Zhai Y, Zhao X, Wang W, Wu W, Wang Z et al. Deep cerebral microbleeds are associated with the severity of lacunar infarcts and hypertension. Medicine 2018; 97: e11031.

6.  De Bresser J, Kuijf HJ, Zaanen K, Viergever MA, Hendrikse J, Biessels GJ et al. White matter hyperintensity shape and location feature analysis on brain MRI; Proof of principle study in patients with diabetes. Sci Rep 2018; 8: 1–10.

7.  Ghaznawi R, Geerlings MI, Jaarsma-Coes MG, Zwartbol MHT, Kuijf HJ, van der Graaf Y et al. The association between lacunes and white matter hyperintensity features on MRI: The SMART-MR study. Journal of Cerebral Blood Flow and Metabolism 2019; 39: 2486–2496.

8.  Fazekas F, Kleinert R, Offenbacher H, Schmidt R, Kleinert G, Payer F et al. Pathologic correlates of incidental MRI white matter signal hyperintensities. Neurology 1993; 43: 1683–1689.

9.  Kim KW, MacFall JR, Payne ME. Classification of White Matter Lesions on Magnetic Resonance Imaging in Elderly Persons. Biol Psychiatry 2008; 64: 273–280.

10. Ghaznawi R, Geerlings MI, Jaarsma-Coes M, Hendrikse J, Bresser J de, Group on behalf of the U-SS. Association of White Matter Hyperintensity Markers on MRI and Long-term Risk of Mortality and Ischemic Stroke. Neurology 2021; 96: e2172–e2183.

11. Winterer G, Androsova G, Bender O, Boraschi D, Borchers F, Dschietzig TB et al. Personalized risk prediction of postoperative cognitive impairment – rationale for the EU-funded BioCog project. European Psychiatry 2018; 50: 34–39.

12. Zigmond AS, Snaith RP. The Hospital Anxiety and Depression Scale. Acta Psychiatr Scand 1983; 67: 361–370.

13. Schmidt, P. Bayesian inference for structured additive regression models for large-scale problems with applications to medical imaging. (Maximilians-Universität München, 2017).

14. Kempton MJ, Underwood TSA, Brunton S, Stylios F, Schmechtig A, Ettinger U et al. A comprehensive testing protocol for MRI neuroanatomical segmentation techniques: Evaluation of a novel lateral ventricle segmentation method. Neuroimage 2011; 58: 1051–1059.

15. Liu EJ, Cashman K V., Rust AC. Optimising shape analysis to quantify volcanic ash morphology. GeoResJ 2015; 8: 14–30.

16. Marcus J, Gardener H, Rundek T, Elkind MSV, Sacco RL, Decarli C et al. Baseline and longitudinal increases in diastolic blood pressure are associated with greater white matter hyperintensity volume: The northern manhattan study. Stroke 2011; 42: 2639–2641.

17. Muller M, Sigurdsson S, Kjartansson O, Aspelund T, Lopez OL, Jonnson P V. et al. Joint effect of mid- and late-life blood pressure on the brain: The AGES-Reykjavik Study. Neurology 2014; 82: 2187–2195.

18. Gouw AA, Seewann A, Van Der Flier WM, Barkhof F, Rozemuller AM, Scheltens P et al. Heterogeneity of small vessel disease: A systematic review of MRI and histopathology correlations. J Neurol Neurosurg Psychiatry. 2011; 82: 126–135.

19. Murray AD, Staff RT, Shenkin SD, Deary IJ, Starr JM, Whalley LJ. Brain white matter hyperintensities: Relative importance of vascular risk factors in nondemented elderly people. Radiology 2005; 237: 251–257.

20. Saczynski JS, Siggurdsson S, Jonsson P V, Eiriksdottir G, Olafsdottir E, Kjartansson O et al. Glycemic Status and Brain Injury in Older Individuals The Age Gene/Environment Susceptibility-Reykjavik Study. 2009. doi:10.2337/dc08-2300.

21. Den Heijer T, Vermeer SE, Van Dijk EJ, Prins ND, Koudstaal PJ, Hofman A et al. Type 2 diabetes and atrophy of medial temporal lobe structures on brain MRI. Diabetologia 2003; 46: 1604–1610.

22. Schmidt R, Launer LJ, Nilsson LG, Pajak A, Sans S, Berger K et al. Magnetic Resonance Imaging of the Brain in Diabetes: The Cardiovascular Determinants of Dementia (CASCADE) Study. Diabetes 2004; 53: 687–692.

23. Wang D-Q, Wang L, Wei M-M, Xia X-S, Tian X-L, Cui X-H et al. Relationship Between Type 2 Diabetes and White Matter Hyperintensity: A Systematic Review. Front Endocrinol (Lausanne) 2020; 0: 998.

24. Breteler MMB, van Swieten JC, Bots ML, Grobbee DE, Claus JJ, van den Hout JHW et al. Cerebral white matter lesions, vascular risk factors, and cognitive function in a population-based study: The Rotterdam study. Neurology 1994; 44: 1246–1252.

25. Jimenez-Conde J, Biffi A, Rahman R, Kanakis A, Butler C, Sonni S et al. Hyperlipidemia and Reduced White Matter Hyperintensity Volume in Patients with Ischemic Stroke. Stroke 2010; 41: 437–442.

26. Ferguson AC, Tank R, Lyall LM, Ward J, Welsh P, Celis-Morales C et al. Association of SBP and BMI with cognitive and structural brain phenotypes in UK Biobank. J Hypertens 2020; 38: 2482–2489.

27. Morys F, Dadar M, Dagher A. Association between mid-life obesity, its metabolic consequences, cerebrovascular disease and cognitive decline. J Clin Endocrinol Metab 2021. doi:10.1210/clinem/dgab135.

28. Lampe L, Zhang R, Beyer F, Huhn S, Kharabian Masouleh S, Preusser S et al. Visceral obesity relates to deep white matter hyperintensities via inflammation. Ann Neurol 2019; 85: 194–203.

29. Wardlaw JM, Valdés Hernández MC, Muñoz-Maniega S. What are white matter hyperintensities made of? Relevance to vascular cognitive impairment. J Am Heart Assoc 2015; 4: 001140.

30. Young VG, Halliday GM, Kril JJ. Neuropathologic correlates of white matter hyperintensities. Neurology 2008; 71: 804–811.

31. Shim YS, Yang D-W, Roe CM, Coats MA, Benzinger TL, Xiong C et al. Pathological Correlates of White Matter Hyperintensities on MRI. Dement Geriatr Cogn Disord 2015; 39: 92.

2

# 2.8 SUPPLEMENTARY MATERIAL

**S.2.8.1.** Definition of shape descriptors.

| Shape marker | Formula | WMH type | Comment |
|---|---|---|---|
| Convexity (C) | $C = \dfrac{\text{Convex Hull Area}}{\text{Area}}$ | Periventricular/ Confluent WMH | Convexity and Solidity describe how concave or convex the shape is. A maximally convex shape has a convexity and solidity value of 1. The values decrease with a more concave, complex shape. |
| Solidity (S) | $S = \dfrac{\text{Volume}}{\text{Convex Hull Volume}}$ | Periventricular/ Confluent WMH | |
| Concavity Index (CI) | $CI = \sqrt{(2-C)^2 + (1-S)^2}$ | Periventricular/ Confluent WMH | As a measure of roughness, concavity index describes how dense, irregular or elongated and curved a lesion is. Higher CI values suggest a more complex WMH shape. |
| Fractal Dimension (FD) | $FD = \lim_{r \to 1} \dfrac{\log(n_r)}{\log\left(\frac{1}{r}\right)}$ <br> n = number of boxes <br> r = box size | Periventricular/ Confluent WMH Deep WMH | Textural roughness is measured using the Minkowski-Bouligand dimension (box counting dimension). Higher FD values suggest a more complex WMH shape. |
| Eccentricity (E) | $E = \dfrac{\text{Minor Axis}}{\text{Major Axis}}$ <br> Major axis: largest diameter in 3D space. Minor axis: smallest diameter orthogonal to the major axis. | Deep WMH | Eccentricity assesses the deviation from a circle. The eccentricity of a circle is 1 and the eccentricity of a line is 0. |

**S.2.8.2.** The association between age, sex, and WMH shape markers.

| | Age | Sex |
|---|---|---|
| **Periventricular/Confluent WMH[†]** | | |
| Solidity[‡] | 0.02 (-0.04−0.00) | -0.21 (-0.41−-0.01)* |
| Convexity | -0.01 (-0.02−-0.00)* | -0.00 (-0.11−0.11) |
| Concavity index[‡] | 0.01 (0.00−0.01)** | 0.02 (-0.03−0.08) |
| Fractal dimension | 0.01 (0.0−0.02)*** | 0.01 (-0.06−0.08) |
| **Deep WMH** | | |
| Eccentricity | 0.00 (-0.00−0.00) | 0.04 (-0.01−0.08) |
| Fractal dimension | -0.00 (-0.01−0.00) | 0.00 (-0.11−0.11) |

The values represent B values (95% confidence interval) of the linear regression. * $p<0.05$. ** $p<0.01$. *** $p<0.001$. [‡] Solidity and concavity index were multiplied by 100 and natural log transformed, due to non-normal distribution. [†] Periventricular/confluent WMH with a volume >4 ml. Periventricular/confluent WMH: n=73; Deep WMH: n=122.

**S.2.8.3.** The association between age, sex, and WMH volume.

|  | Age | Sex |
| --- | --- | --- |
| **Total WMH volume** | 0.11 (0.08−0.15)** | 0.20 (-0.34−0.78) |
| **Periventricular/confluent WMH volume** | 0.12 (0.08−0.15)** | 0.22 (-0.36−0.80) |
| **Deep WMH volume** | 0.07 (-0.01−0.12)* | -0.08 (-0.88−0.71) |

These values represent B values (95% confidence interval) of the linear regression analyses controlled for intracranial volume. WMH volumes were multiplied by 100 and natural log transformed, due to non-normal distribution. * p<0.05. ** p<0.001. WMH: white matter hyperintensities.

2

CHAPTER

3

# WHITE MATTER HYPERINTENSITY SHAPE IS RELATED TO LONG-TERM PROGRESSION OF CEREBROVASCULAR DISEASE IN COMMUNITY-DWELLING OLDER ADULTS

Jasmin Annica Kuhn-Keller, Sigurdur Sigurdsson, Lenore J. Launer, Mark A. van Buchem, Matthias J.P. van Osch, Vilmundur Gudnason, Jeroen de Bresser.

## 3.1 ABSTRACT

White matter hyperintensity (WMH) shape is associated with long-term dementia risk in community-dwelling older adults, but the underlying structural correlates of this association are unknown. We therefore aimed to investigate the association between baseline WMH shape and cerebrovascular disease progression over time in community-dwelling older adults.

The association of WMH shape and cerebrovascular disease markers was investigated using linear and logistic regression models in the Age, Gene/Environment Susceptibility-Reykjavik (AGES) study (n = 2297; average time to follow-up: 5.2 years).

A more irregular shape of periventricular/confluent WMH at baseline was associated with a larger increase in WMH volume, and with occurrence of new subcortical infarcts, new microbleeds, new enlarged perivascular spaces, and new cerebellar infarcts at the 5.2-year follow-up (all p<0.05). Furthermore, less elongated and more irregularly shaped deep WMHs were associated with a larger increase in WMH volume, and new cortical infarcts at follow-up (p<0.05). A less elongated shape of deep WMH was associated with new microbleeds at follow-up (p<0.05).

Our findings show that WMH shape may be indicative of the type of cerebrovascular disease marker progression. This underlines the significance of WMH shape to aid in the assessment of cerebrovascular disease progression.

## 3.2 INTRODUCTION

Most healthy older adults have changes on brain MRI scans related to cerebrovascular disease. The most common cerebrovascular changes are white matter hyperintensities (WMHs). These WMHs are associated with long term dementia occurrence and cognitive decline.[1,2] However, the structural correlates of these associations remain unknown.

Different quantitative MRI markers exist to study WMH, such as the commonly used WMH volume. However, this marker can be considered rather crude and is disease-unspecific. This hinders more in-depth investigations related to disease mechanisms. In recent studies, WMH shape was introduced as a novel marker that may provide a more detailed and more disease specific characterization of WMH compared to WMH volume. Previous studies have shown that a more irregular shape of periventricular/confluent WMH is associated with the occurrence of future stroke and increased mortality in patients with an increased vascular burden.[3] Moreover, a more irregular shape of periventricular/confluent WMHs was associated with an increased long-term risk for dementia.[4] These studies indicate that different WMH shape patterns are probably related to different underlying pathologies (e.g. gliosis, fiber loss, and demyelination).[5] This could provide crucial information about potential disease progression.

We hypothesized that different WMH shape patterns are related to different types of underlying pathologies and that some shape patterns may be related to progression of specific cerebrovascular markers. We therefore aimed to investigate the association between baseline WMH shape and progression of cerebrovascular disease markers over 5.2 years in community-dwelling older adults.

## 3.3 METHODS

### 3.3.1 Participants & study design

Data from the AGES Reykjavik study was used in the current study.[6] The study was approved by the Icelandic National Bioethics Committee, VSN:00-063, and the institutional review board responsible for the National Institute on Aging (NIA) research; all participants signed informed consent. Brain MRI scans were acquired at baseline from 2002 to 2006 and approximately five years later at follow-up from 2007 to 2011. A flow-chart describing the inclusion and exclusion of participants in the current study is shown in figure 3.1. Of the 4614 included participants, a total of 654 participants were excluded after MRI quality control (WMH oversegmentation: n = 124;

WMH segmentation outside of the brain: n = 6; ventricle segmentation failed: n = 4); artefacts: n = 30; infarcts > 1.5 cm: n = 460; tumor: n = 12; technical error: n = 7; traumatic brain injury: n = 2). WMH oversegmentation outside of the brain was automatically corrected using brain masks. Another 1672 participants were excluded because of missing follow-up data (death: n = 505 (30%), disability or refused: n = 859 (51%), lost to follow-up: n = 104 (6%), claustrophobia: n = 86 (5%), MRI contradictions: n = 116 (7%), technical issues: n = 2 (0.1%)). A total of 2297 participants were included in the current study.
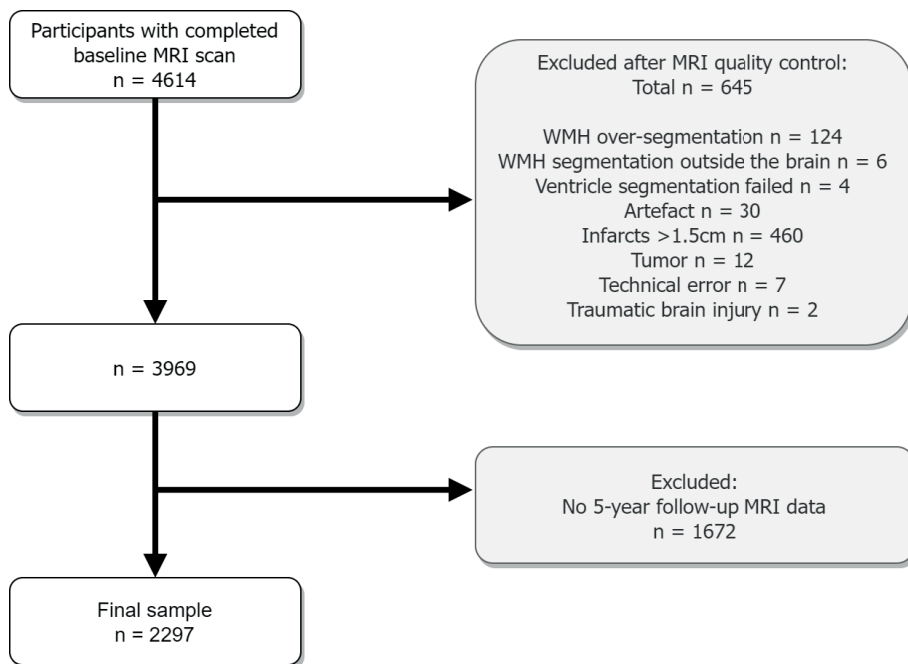
Figure 3.1 Flowchart illustrating the exclusions of the study. Participants with infarcts bigger than 1.5 cm were excluded to avoid false positive WMH segmentation. WMH oversegmentation outside the brain was automatically corrected using brain masks.

## 3.3.2 MRI acquisition protocol

The same MRI scanning protocol was used at baseline and follow-up on a 1.5 Tesla Signa Twinspeed system (General Electric Medical Systems, Waukesha, Wisconsin). Sequences included in the protocol: a 3D T1-weighted, spoiled-gradient echo (repetition time = 21 ms; time to echo = 8 ms; field of view = 240 mm; slice thickness = 1.5 mm; voxel size = 0.94 × 0.94 × 1.50 mm³); a fluid attenuated inversion recovery (FLAIR) (repetition time = 8000 ms; time to echo = 100 ms; field of view = 220 mm; voxel size = 0.86 × 0.86 × 3.00 mm³); a 2D T2*-weighted gradient-echo-type echo planar

imaging (GRE-EPI) (repetition time = 3050 ms; time to echo = 50 ms; field of view: 220 mm; matrix = 256 x 256); a proton density/T2-weighted fast spin-echo (repetition time = 3220 ms; time to first echo = 22 ms; time to second echo = 90 ms; echo train length =  8; field of view = 220 mm; matrix = 256 × 256). The FLAIR, T2*, and proton density/T2 scans were acquired with 3 mm thick interleaved slices with voxel sizes of 0.86 mm x 0.86 mm x 3.00 mm.

### 3.3.3 WMH shape

WMH shape markers were calculated using an in-house developed pipeline, as described in detail previously.[4] In short, WMH were segmented automatically on the registered FLAIR images using the LST toolbox[7] in SPM12. Lateral ventricles were segmented from the T1 scans and the ventricle masks were inflated with 3 and 10 mm. The inflated ventricle masks aided WMH classification into periventricular/confluent, and deep WMH (figure 3.2). Periventricular and confluent WMH were merged into one category, because of spatial overlap in these lesion types preventing separated shape analyses. WMH need to be at least 3 mm distant from the ventricular wall to be classified as deep WMH. WMH shape markers were calculated based on the WMH segmentations. Convexity, solidity, concavity index, and fractal dimensions were determined for periventricular/confluent WMHs.[8] A lower convexity and solidity, and higher concavity index and fractal dimension indicate more irregularly shaped periventricular/confluent WMH. Fractal dimensions and eccentricity were calculated for deep WMH.[8] A higher eccentricity indicates a more elongated shape, while a higher fractal dimensions indicates a more irregular shape of deep WMH. The formulas used to calculate the WMH shape markers are shown in figure 3.2. Average shape markers were calculated per participant. Each WMH shape marker captures a slightly different variation of WMH shape. In supplementary figure S.3.9.1 examples of shapes with high or low values of different shape markers are shown.

### 3.3.4 Other cerebrovascular markers

Gray matter, white matter, cerebrospinal fluid and WMH volume were segmented automatically with a modified algorithm based on the Montreal Neurological Institute pipeline.[9] Intracranial volume resulted from the addition of the volumes of gray matter, white matter, cerebrospinal fluid and WMH.[10] The same processing-pipeline was used at baseline and follow-up. The WMH volume change was calculated by substracting the baseline WMH volumes from the follow-up WMH volumes.
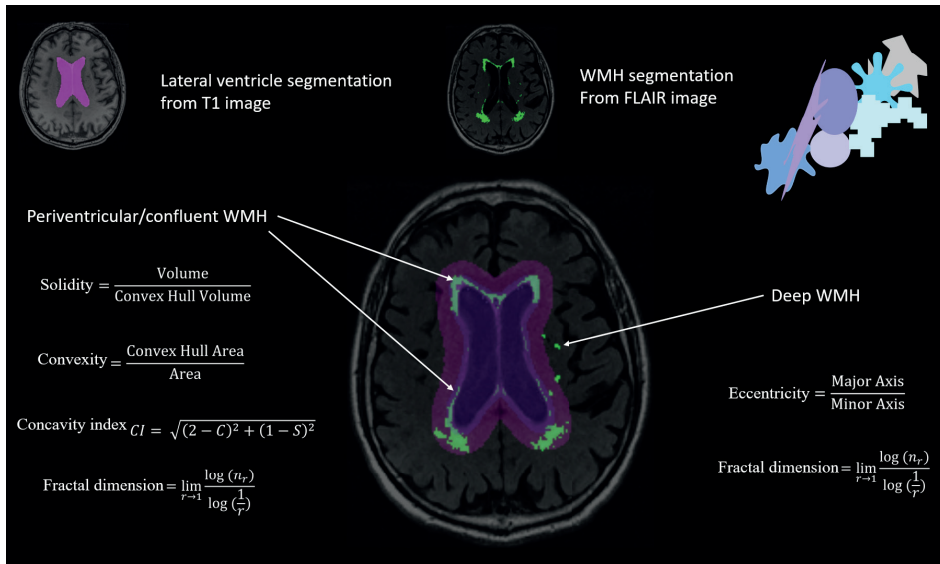
**Figure 3.2. Illustration of the WMH shape image processing pipeline.** Lateral ventricles were segmented using T1-weighted MRI images. WMH segmentation was performed on the registered FLAIR images. Using two different inflated ventricle masks (3 mm and 10 mm), WMH were classified into three types (deep, periventricular and confluent). Based on the resulting WMH type, different WMH shape markers were calculated using the shown formulas.

Occurrence of new subcortical brain infarcts, microbleeds, enlarged perivascular spaces, cerebellar infarcts, and cortical infarcts at follow-up were rated by trained radiographers by comparing the baseline and follow-up MRI scans.[11] Follow-up MRI scans were examined and if a lesion was detected, the baseline scan was checked to see if the lesion was new.

Microbleeds were scored if they were visible on the T2*-weighted scans.[12] Infarcts were scored if they were visible on the FLAIR, T2-weighted and the proton-density scan.[13] Cortical infarcts were labelled as such if they involved or were limited to the cerebral cortex and were surrounded by an area of high signal intensity on FLAIR images. Cerebellar infarcts had no size criteria. Subcortical infarcts were scored if they did not extend into the cortex and were surrounded by an area of high signal intensity on FLAIR images with a minimal diameter of 4 mm.[13] Enlarged perivascular spaces were defined as round or tubular defects with a short axis >3 mm in the subcortical area, without a surrounding area with high signal intensity on FLAIR images.[14]

### 3.3.5 Baseline characteristics and cardiovascular risk factors

Baseline information, such as age, sex, education level, and smoking status, were collected via questionnaires. The highest completed education level (primary school, secondary school, college, or university) was noted. Non-smokers were participants

who never smoked, former smokers were regular smokers of at least 100 cigarettes or 20 cigars in a lifetime, and the third category was current smokers. Participant's height (cm) and weight (kg) were measured and used to calculate body mass index (BMI). Systolic and diastolic blood pressure were measured using a standard mercury sphygmomanometer; the mean of 2 measurements was calculated. Hypertension was registered in the database based on self-report and/or use of antihypertensive medication, and/or measured systolic blood pressure >140 mm Hg and/or diastolic blood pressure >90 mm Hg. Diabetes mellitus was registered based on self-report of diabetes, or use of anti-diabetic medication, or fasting blood glucose level >7.0 mmol/L. Coronary artery disease was registered upon self-report and the use of nitrates, a coronary bypass, and/or evidence of myocardial infarction on an electrocardiogram.

## 3.3.5 Statistical analysis

Solidity, convexity, and eccentricity were inverted for the logistic regression analyses to aid comparability of the results. Solidity and baseline WMH volumes were multiplied by 100 and natural log transformed due to non-normal distribution. Z-scores of WMH shape markers and baseline WMH volumes were calculated to aid comparability. The average intracranial volume of baseline and follow-up was calculated to improve precision. To study the association between periventricular/confluent and deep WMH shape markers and change in WMH volume, linear regression analyses controlled for age, sex, and intracranial volume were performed. To study the association between periventricular/confluent and deep WMH shape markers and occurrence of new subcortical brain infarcts, microbleeds, enlarged perivascular spaces, cerebellar infarcts, and cortical infarcts, logistic regression analyses were performed controlled for age and sex.

As a frame of reference, the association between baseline WMH volume and change in WMH volume was tested with linear regression analyses controlled for age, sex, and intracranial volume. Furthermore, the association between baseline WMH volume and occurrence of new subcortical brain infarcts, microbleeds, enlarged perivascular spaces, cerebellar infarcts, and cortical infarcts was tested with logistic regression analyses controlled for age, and sex. A p value <0.05 was considered statistically significant.

## 3.4 RESULTS

A total of 2297 participants were included in the current study. A flowchart showing the inclusions/exclusions of the study is shown in figure 3.1. Supplementary table S.3.9.1 contains a comparison of the baseline characteristics of the participants included (n=2297) and excluded (n=2317) from our study. As to be expected, cardiovascular risk factors, such as diabetes, coronary artery disease, and hypertension were significantly more prevalent in the excluded group. Moreover, the excluded group is older and has a lower BMI.

The mean age at baseline of the included community-dwelling older adults was 74.5±4.7 years and the mean time to follow-up was 5.2 ± 0.2 years. The characteristics of the study sample, including cardiovascular risk factors, are shown in Table 3.1. At baseline 153 participants (7%) had subcortical infarcts, 381 participants (17%) had microbleeds, 358 participants (16%) had enlarged perivascular spaces, 428 participants (19%) had cerebellar infarcts, and 176 participants (8%) had cortical infarcts (table 3.2). The average WMH volume at baseline was 16.6 ± 17.2 ml. At follow-up, 68 participants (3%) had new subcortical infarcts, 299 participants (13%) had new microbleeds, 39 participants (2%) had new enlarged perivascular spaces, 168 participants (7%) had new cerebellar infarcts and 123 participants (5%) had new cortical infarcts (table 3.2). The average WMH volume at follow-up was 22.3 ± 22.2 ml. A detailed description of the cerebrovascular changes on MRI of the participants can be found in supplementary table S.3.9.2.

### 3.4.1 Periventricular/confluent WMH shape and progression of cerebrovascular changes

A more irregular shape of periventricular/confluent WMH (lower solidity (B: 0.91 (95% CI: 0.59–1.23); $p<0.001$), lower convexity (B: 1.94 (1.62–2.26); $p<0.001$), higher concavity index (B: 2.28 (1.95–2.61); $p<0.001$), higher fractal dimension (B: 2.62 (2.31–2.93); $p<0.001$)) at baseline was significantly associated with a larger increase in WMH volume over 5.2 years (Table 3.3 and supplementary figure S.3.9.2). Furthermore, a more irregular shape of periventricular/confluent WMH at baseline was associated with new subcortical infarcts (lower solidity (OR: 1.75 (95% CI: 1.16–2.62); $p<0.001$); lower convexity (OR: 1.44 (1.17–1.76); $p<0.001$); higher concavity index (OR: 1.58 (1.29–1.94); $p<0.001$); higher fractal dimension (OR: 1.91 (1.49–2.44); $p<0.001$)), new microbleeds (lower solidity (OR: 1.24 (1.07–1.44); $p=0.004$); lower convexity (OR: 1.16 (1.04–1.30); $p=0.009$); higher concavity index (OR: 1.24 (1.11–1.39); $p<0.001$); higher fractal dimension (OR: 1.47 (1.30–1.65); $p<0.001$)), new enlarged perivascular spaces (lower convexity (OR: 1.34 (1.05–1.71); $p<0.017$); higher concavity index (OR: 1.34 (1.05–1.71); $p<0.020$)), and new cerebellar infarcts at follow-up (lower convexity (OR:

1.16 (1.02–1.33); p<0.022); higher concavity index (OR: 1.16 (1.02–1.33); p<0.027)). Periventricular/confluent WMH shape at baseline was not significantly associated with new cortical infarcts at follow-up (solidity (OR: 1.27 (0.97–1.65); p=0.078), convexity (OR: 1.04 (0.88–1.22); p=0.652), concavity index (OR: 1.09 (0.92–1.29); p=0.345), fractal dimension (OR: 1.20 (1.00–1.44); p=0.051).

### 3.4.2 Deep WMH shape and progression of cerebrovascular changes

A less elongated and irregular shape of deep WMH at baseline was significantly associated with a larger increase in WMH volume (lower eccentricity (B: 2.02 (1.72–2.33); p<0.001); higher fractal dimension (B: 2.09 (1.78–2.41); p<0.001)), and with new cortical infarcts at follow-up (lower eccentricity (OR: 1.30 (1.10–1.55); p<0.003); higher fractal dimension (OR: 1.31 (1.11–1.55); p=0.001)) (Table 3 and supplementary figure S.3.9.2 and S.3.9.7). Furthermore, a less elongated shape of deep WMH was associated with new microbleeds at follow-up (lower eccentricity: OR:1.14 (1.01–1.27); p=0.027). Baseline deep WMH shape markers were not significantly associated with new subcortical infarcts, new enlarged perivascular spaces, or new cerebellar infarcts at follow-up. WMH shape markers in participants with or without cerebrovascular changes can be found in supplementary figure S.3.9.3 to S.3.9.7.

### 3.4.3 WMH volume and progression of cerebrovascular changes

A higher baseline WMH volume was significantly associated with a larger increase in WMH volume over 5.2 years (B: 4.05 (3.77–4.33); p<0.001); Table 3.3). Moreover, a higher baseline WMH volume was associated with new subcortical infarcts (OR: 2.26 (1.75–2.92); p<0.001), new microbleeds (OR: 1.52 (1.35–1.70); p<0.001), new cerebellar infarcts (OR: 1.25 (1.09–1.42); p<0.001), and new cortical infarcts at follow-up (OR: 1.44 (1.21–1.72); p<0.001), but not with new enlarged perivascular spaces at follow-up (OR: 1.28 (0.99–1.64); p=0.058).

**3**

**Table 3.1.** Characteristics of the participants.

|  | Older adult participants (n= 2297) |
| --- | --- |
| **Age at baseline** (years) | 74.5 ± 4.7 |
| **Females** | 1399 (61%) |
| **Hypertension** | 1763 (77%) |
| **Type 2 diabetes mellitus** | 192 (8%) |
| **BMI at baseline** (kg/m³) | 27.2 ± 4.1 |
| **Cholesterol** (mmol/L) | 5.70 ± 1.13 |
| **Smoking status** |  |
| Never | 1017 (44%) |
| Former | 1030 (45%) |
| Current | 250 (11%) |
| **Coronary artery disease** | 361 (16%) |
| **Time to follow-up (years)** | 5.2 ± 0.2 |

Data are shown as mean ± SD or frequency (%). Baseline characteristics were collected via questionnaires.

**Table 3.2.** Cerebrovascular MRI markers of the participants.

|  | Baseline | Follow-up | Change over time |
| --- | --- | --- | --- |
| **Periventricular/confluent WMH** |  |  |  |
| Solidity | 0.19 ± 0.12 | - | - |
| Convexity | 1.03 ± 0.18 | - | - |
| Concavity index | 1.27 ± 0.15 | - | - |
| Fractal dimension | 1.71 ± 0.15 | - | - |
| **Deep WMH** |  |  |  |
| Eccentricity | 0.61 ± 0.07 | - | - |
| Fractal dimension | 1.70 ± 0.14 | - | - |
| **WMH volume (ml)** | 16.56 ± 17.21 | 22.32 ± 22.18 | 5.76 ± 7.74 |
| **Participants with subcortical infarcts** | 153 (7%) | 221 (10%) | 68 (3%) |
| **Participants with microbleeds** | 381 (17%) | 680 (30%) | 299 (13%) |
| **Participants with enlarged perivascular spaces** | 358 (16%) | 397 (17%) | 39 (2%) |
| **Participants with cerebellar infarcts** | 434 (19%) | 596 (26%) | 162 (7%) |
| **Participants with cortical infarcts** | 176 (8%) | 299 (13%) | 123 (5%) |

Data are indicated as mean ± SD, or frequency (%).

**Table 3.3.** Linear and logistic regression analyses of baseline WMH shape and volume markers and cerebrovascular changes over 5.2 years.

| | Change in WMH volume B (95% CI) | New subcortical infarcts OR (95% CI) | New microbleeds OR (95% CI) | New enlarged perivascular spaces OR (95% CI) | New cerebellar infarcts OR (95% CI) | New cortical infarcts OR (95% CI) |
|---|---|---|---|---|---|---|
| **Periventricular/ confluent WMH (n=2297)** | | | | | | |
| Solidity | 0.91 (0.59–1.23)*** | 1.75 (1.16–2.62)** | 1.24 (1.07–1.44)** | 1.07 (0.79–1.47) | 0.99 (0.86–1.15) | 1.27 (0.97–1.65) |
| Convexity | 1.94 (1.62–2.26)*** | 1.44 (1.17–1.76)*** | 1.16 (1.04–1.30)** | 1.34 (1.05–1.71)* | 1.16 (1.02–1.33)* | 1.04 (0.88–1.22) |
| Concavity index | 2.28 (1.95–2.61)*** | 1.58 (1.29–1.94)*** | 1.24 (1.11–1.39)*** | 1.34 (1.05–1.71) * | 1.16 (1.02–1.33) * | 1.09 (0.92–1.29) |
| Fractal dimension | 2.62 (2.32–2.93) *** | 1.91 (1.49–2.44)*** | 1.47 (1.30–1.65)*** | 1.28 (0.97–1.68) | 1.14 (0.99–1.31) | 1.20 (1.00–1.44) |
| **Deep WMH (n=2293)** | | | | | | |
| Eccentricity | 2.02 (1.72–2.33)*** | 1.04 (0.84–1.28) | 1.14 (1.01–1.27)* | 0.97 (0.75–1.26) | 1.02 (0.89–1.17) | 1.30 (1.10–1.55)** |
| Fractal dimension | 2.09 (1.78–2.41)*** | 1.09 (0.88–1.35) | 1.03 (0.92–1.15) | 1.04 (0.81–1.34) | 1.06 (0.93–1.21) | 1.31 (1.11–1.55)** |
| **WMH volume (n=2297)** | 4.05 (3.77–4.33)*** | 2.26 (1.75–2.92)*** | 1.52 (1.35–1.70)*** | 1.28 (0.99–1.64) | 1.25 (1.09–1.42)** | 1.44 (1.21–1.72)*** |

Lower solidity and convexity, as well as a higher concavity index and fractal dimension indicate a more irregular WMH shape. Higher eccentricity indicates a rounder shape and a lower eccentricity indicates a more elongated shape. Solidity, convexity, and eccentricity were inverted to aid comparability in direction of effect. The association of baseline WMH shape with WMH volume change was investigated using linear regression models, controlled for age, sex, and intracranial volume. The association of baseline WMH shape with new subcortical brain infarcts, microbleeds, enlarged perivascular spaces, cerebellar infarcts, and cortical infarcts at follow-up was investigated with logistic regression models, controlled for age and sex. Data is shown as B values (95% CI) or odds ratio (OR) (95% CI). Positive B values indicate that WMH progression increases with every unit increase of the WMH shape marker. Negative B values show that WMH progression decreases with every unit increase of the WMH shape marker. OR above 1 show that with increase of the WMH shape marker, the risk is OR-times higher to have e.g. an infarct. OR below 1 show that with increase of the WMH shape marker, the risk is OR-times lower to have e.g. infarcts. * p<0.05 ** p<0.01 *** p<0.001.

3

## 3.5 DISCUSSION

We found that a more irregular shape of periventricular/confluent WMH at baseline was associated with a larger increase in WMH volume, and with occurrence of new subcortical infarcts, new microbleeds, new enlarged perivascular spaces, and new cerebellar infarcts at the 5.2 year follow-up. Furthermore, less elongated and more irregularly shaped deep WMHs were associated with a larger increase in WMH volume, and new cortical infarcts at follow-up. A rounder shape of deep WMH was associated with new microbleeds at follow-up.

It has been previously shown that a more irregular WMH shape is associated with an increased long-term risk for dementia in community-dwelling older adults,[4] but how this effect is mediated remained unclear. The current study showed that specific WMH shape patterns are indicative of specific markers of cerebrovascular disease progression.

The aetiology of WMH of presumed vascular origin in older adults is heterogenous and the exact pathophysiology remains poorly understood. Based upon our findings, we can speculate that a more irregular shape of WMH may reflect a more severe underlying aetiology of cerebrovascular disease, and as such is subsequently followed by increased progression of cerebrovascular disease-related brain changes. Histopathological studies have previously suggested that a more irregular WMH shape is associated with more severe parenchymal damage.[5,15] Areas of smooth periventricular WMH showed demyelination and tortuous venules, as well as damage to the ventricular lining.[5] On the other hand, previous histopathological investigations showed that irregular periventricular/confluent WMH showed gliosis, fiber loss, and reduced myelin.[5] Moreover, the vessel walls in the areas of irregular WMH were thickened due to fibrohyalinosis and lipohyalinosis.[5] A more complex and irregular shape of WMH may, therefore, be related to underlying pathologies that accelerate cerebrovascular disease progression.

WMH are a hallmark imaging marker of cerebral small vessel disease (SVD). In SVD changes in the normal functioning of especially the arterioles, and capillaries (such as small or large vessel atheromas or emboli) subsequently lead to WMH through hypoperfusion. MRI markers that are typically associated with SVD are WMHs, microbleeds, enlarged perivascular spaces and subcortical infarcts.[16] Large vessel disease (LVD), on the other hand, is mostly caused by atherosclerosis and atheroma depositions in the wall of larger upstream arteries, such as the carotid arteries. A typical brain MRI marker of LVD is a cortical infarct.[16] LVD can also lead to lacune-like infarcts via atheromas in the larger parent arteries,[16,17] which is also where SVD and LVD pathology may be linked.[16]

There are several possible mechanisms to explain the association of WMH shape and progression of different SVD and LVD markers. For example, subcortical infarcts and WMHs may share (part of) the same SVD-related pathological pathways.[18,19] WMHs might be related to subcortical infarcts via secondary hypoperfusion and the resulting ischemia in the parenchyma surrounding the WMHs.[20] We found that a more irregular shape of periventricular/confluent WMHs was related to, among others, new subcortical infarcts, new microbleeds, and new enlarged perivascular spaces. In a previous population-based study, pre-existing and incident microbleeds were associated with incident lacunes and progression of WMH volume.[21] The authors propose that this association can be explained by shared pathways of haemorrhagic and ischemic pathologies in the preclinical phase of cerebrovascular disease.[21] While some previous studies report an association between WMH burden and enlarged perivascular spaces, a previous meta-analysis has concluded that there is no clear association.[22] In the current study, baseline periventricular/confluent WMH shape was associated with new enlarged perivascular spaces at follow-up, but we did not find an association between baseline WMH volume and new enlarged perivascular spaces at follow-up. This result was found despite the relatively limited progression of enlarged perivascular spaces at follow-up. This suggests that WMH shape might contain additionally relevant information regarding SVD compared to WMH volume alone. Furthermore, enlarged perivascular spaces are a relatively new marker of SVD[23] and the current findings strengthen their presumed connection to SVD pathology. Combined, these findings illustrate that WMH shape may help to differentiate between different further subtypes of SVD, which is reflected in the association of different WMH shape patterns to different cerebrovascular markers. For example previous research has already shown that different more rare subtypes of SVD lead to different patterns of MRI changes (e.g. in cerebral amyloid angiopathy (CAA) or cerebral autosomal dominant arteriopathy with subcortical infarcts and leukoencephalopathy (CADASIL)[24,25]), but much is still unknown in this heterogenous disease. WMH shape may help to further differentiate subtypes of SVD by providing a more detailed characterization of WMHs on MRI.

In the current study, less elongated and more irregularly shaped deep WMHs were associated, among others, with new cortical infarcts at follow-up. Since cortical infarcts are a marker of LVD, the related WMH shape patterns of deep WMH may be indicative of a pathophysiological involvement of LVD. Periventricular/confluent WMH shape, on the other hand, was not related to new cortical infarcts at follow-up. Cerebellar infarcts can represent both SVD and LVD and are presumed to be of embolic origin. In the current study, cerebellar infarcts were associated with periventricular/confluent WMH shape, but not with deep WMH shape markers.

The difference of the results depending on WMH type might support the notion that deep and periventricular/confluent WMH are resulting from different underlying pathologies.[26,27] Different baseline WMH shape patterns were associated with progression of different cerebrovascular disease markers at the 5-year follow-up, which shows that WMH shape might be indicative of the type of cerebrovascular disease progression at an early stage.

The strengths of the current study are the automatic assessment of WMH shape and volume, and the longitudinal study design with a relatively long follow-up. Significant external validity is added to the study by the large sample size from the general population. A limitation of the current study is the use of a 1.5T MRI system, which was a common field strength for clinical MRI scanners at the time of data collection. MRI images with a lower signal-to-noise ratio or spatial resolution could have resulted in a less accurate WMH shape estimation. However, we have reported on significant associations with cerebrovascular disease markers despite this limitation. Another limitation of our study is that lacunes were not scored separately, but were scored in the category of subcortical infarcts. However, we expect the possible effect of this to be small as the prevalence of large subcortical infarct is very low. Another limitation of our study could be that the strength of the associations found in the current study may have been influenced and weakened by selective loss to follow-up. It is likely that participants who had died, refused or were not eligible for a follow-up MRI were less healthy than the participants who did undergo the follow-up. This could have resulted in an underestimation of the associations shown in our study.

In conclusion, our findings show that WMH shape may be indicative of the type of cerebrovascular disease marker progression. This underlines the significance of WMH shape to aid in the assessment of cerebrovascular disease progression.

## 3.6 ACKNOWLEDGEMENTS

## 3.7 DISCLOSURE

M.J.P. van Osch reports to be an unpaid member of a clinical trial steering committee of Alnylam.

## 3.8 REFERENCES

1.  Alber J, Alladi S, Bae H, Barton DA, Beckett LA, Bell JM et al. White matter hyperintensities in vascular contributions to cognitive impairment and dementia (VCID): Knowledge gaps and opportunities. Alzheimer's & Dementia: Translational Research & Clinical Interventions 2019; 5: 107–117.

2.  Prins ND, Scheltens P. White matter hyperintensities, cognitive impairment and dementia: An update. Nat Rev Neurol 2015; 11: 157–165.

3.  Ghaznawi R, Geerlings MI, Jaarsma-Coes M, Hendrikse J, Bresser J de, Group on behalf of the U-SS. Association of White Matter Hyperintensity Markers on MRI and Long-term Risk of Mortality and Ischemic Stroke. Neurology 2021; 96: e2172–e2183.

4.  Keller JA, Sigurdsson S, Klaassen K, Hirschler L, van Buchem MA, Launer LJ et al. White matter hyperintensity shape is associated with long-term dementia risk. Alzheimer's and Dementia 2023; 19: 5632-5641.

5.  Fazekas F, Kleinert R, Offenbacher H, Schmidt R, Kleinert G, Payer F et al. Pathologic correlates of incidental MRI white matter signal hyperintensities. Neurology 1993; 43: 1683–1689.

6.  Harris TB, Launer LJ, Eiriksdottir G, Kjartansson O, Jonsson P V., Sigurdsson G et al. Age, gene/environment susceptibility-reykjavik study: Multidisciplinary applied phenomics. Am J Epidemiol 2007; 165: 1076–1087.

7.  Schmidt P. Bayesian inference for structured additive regression models for large-scale problems with applications to medical imaging. (Maximilians-Universität München, 2017).

8.  Ghaznawi R, Geerlings MI, Jaarsma-Coes MG, Zwartbol MHT, Kuijf HJ, van der Graaf Y et al. The association between lacunes and white matter hyperintensity features on MRI: The SMART-MR study. Journal of Cerebral Blood Flow and Metabolism 2019; 39: 2486–2496.

9.  Zijdenbos AP, Forghani R, Evans AC. Automatic 'pipeline' analysis of 3-D MRI data for clinical trials: Application to multiple sclerosis. IEEE Trans Med Imaging 2002; 21: 1280–1291.

10. Sigurdsson S, Aspelund T, Forsberg L, Fredriksson J, Kjartansson O, Oskarsdottir B et al. Brain tissue volumes in the general population of the elderly The AGES-Reykjavik Study. Neuroimage 2012; 59: 3862–3870.

11. Sigurdsson S, Aspelund T, Kjartansson O, Gudmundsson E, Jonsson P V., Van Buchem MA et al. Cerebrovascular Risk-Factors of Prevalent and Incident Brain Infarcts in the General Population: The AGES-Reykjavik Study. Stroke 2022; 53: 1199–1206.

12. Ding J, Sigurosson S, Jónsson P V., Eiriksdottir G, Meirelles O, Kjartansson O et al. Space and location of cerebral microbleeds, cognitive decline, and dementia in the community. Neurology 2017; 88: 2089–2097.

13. Saczynski JS, Sigurdsson S, Jonsdottir MK, Eiriksdottir G, Jonsson P V., Garcia ME et al. Cerebral infarcts and cognitive performance: importance of location and number of infarcts. Stroke 2009; 40: 677–682.

14. Ding J, Sigurðsson S, Jónsson P V., Eiriksdottir G, Charidimou A, Lopez OL et al. Large MRI-visible perivascular spaces, cerebral small vessel disease progression and risk of dementia: the AGES-Reykjavik Study. JAMA Neurol 2017; 74: 1105.

15. Kim KW, MacFall JR, Payne ME. Classification of White Matter Lesions on Magnetic Resonance Imaging in Elderly Persons. Biol Psychiatry 2008; 64: 273–280.

16. Wardlaw JM, Smith C, Dichgans M. Mechanisms of sporadic cerebral small vessel disease: Insights from neuroimaging. Lancet Neurol 2013; 12: 483–497.

17. Adachi T, Kobayashi S, Yamaguchi S, Okada K. MRI findings of small subcortical 'lacunar-like' infarction resulting from large vessel disease. J Neurol 2000; 247: 280–285.

18. Wardlaw JM, Smith EE, Biessels GJ, Cordonnier C, Fazekas F, Frayne R et al. Neuroimaging standards for research into small vessel disease and its contribution to ageing and neurodegeneration. Lancet Neurol. 2013; 12: 822–838.

19. Pantoni L. Cerebral small vessel disease: from pathogenesis and clinical characteristics to therapeutic challenges. Lancet Neurol 2010; 9: 689–701.

20. Gouw AA, Van Der Flier WM, Pantoni L, Inzitari D, Erkinjuntti T, Wahlund LO et al. On the etiology of incident brain lacunes: longitudinal observations from the LADIS study. Stroke 2008; 39: 3083–3085.

21. Akoudad S, Ikram MA, Koudstaal PJ, Hofman A, Niessen WJ, Greenberg SM et al. Cerebral Microbleeds Are Associated with the Progression of Ischemic Vascular Lesions. Cerebrovascular Diseases 2014; 37: 382–388.

22. Francis F, Ballerini L, Wardlaw JM. Perivascular spaces and their associations with risk factors, clinical disorders and neuroimaging features: A systematic review and meta-analysis. International Journal of Stroke 2019; 14: 359–371.

23. Mestre H, Kostrikov S, Mehta RI, Nedergaard M. Perivascular spaces, glymphatic dysfunction, and small vessel disease. Clin Sci 2017; 131: 2257–2274.

24. Di Donato I, Bianchi S, De Stefano N, Dichgans M, Dotti MT, Duering M et al. Cerebral Autosomal Dominant Arteriopathy with Subcortical Infarcts and Leukoencephalopathy (CADASIL) as a model of small vessel disease: update on clinical, diagnostic, and management aspects. BMC Medicine 2017 15:1 2017; 15: 1–12.

25. Charidimou A, Boulouis G, Frosch MP, Baron JC, Pasi M, Albucher JF et al. The Boston criteria version 2.0 for cerebral amyloid angiopathy: a multicentre, retrospective, MRI–neuropathology diagnostic accuracy study. Lancet Neurol 2022; 21: 714–725.

26. Gao Z, Wang W, Wang Z, Zhao X, Shang Y, Guo Y et al. Cerebral Microbleeds Are Associated with Deep White Matter Hyperintensities, but Only in Hypertensive Patients. PLoS One 2014; 9: e91637.

27. Gouw AA, Seewann A, Van Der Flier WM, Barkhof F, Rozemuller AM, Scheltens P et al. Heterogeneity of small vessel disease: A systematic review of MRI and histopathology correlations. J Neurol Neurosurg Psychiatry. 2011; 82: 126–135.

## 3.9 SUPPLEMENTARY MATERIAL

**Table S.3.9.1.** Baseline characteristics of the participants included and excluded from our study.

|  | Included participants (n= 2297) | Excluded participants (n= 2317) | p-values |
|---|---|---|---|
| **Age at baseline** (years) | 74.5 ± 4.7 | 78.3 ± 5.6 | <0.001 |
| **Females** | 1399 (61%) | 1281 (55%) | <0.001 |
| **Hypertension** | 1763 (77%) | 2226 (96%) | <0.001 |
| **Type 2 diabetes mellitus** | 192 (8%) | 324 (14%) | <0.001 |
| **BMI at baseline** (kg/m³) | 27.2 ± 4.1 | 26.8 ± 4.6 | <0.001 |
| **Cholesterol** (mmol/L) | 5.70 ± 1.13 | 5.58 ± 1.18 | <0.001 |
| **Smoking status** |  |  |  |
| Never | 1017 (44%) | 979 (42%) | 0.166 |
| Former | 1030 (45%) | 1031 (45%) | 0.178 |
| Current | 250 (11%) | 304 (13%) | 0.019 |
| **Coronary artery disease** | 361 (16%) | 760 (33%) | <0.001 |

Data are shown as mean ± SD or frequency (%). Baseline characteristics were collected via questionnaires. One-way ANOVA's were performed for continuous variables, and Chi-square tests for categorical variables.

3

**Table S.3.9.2.** In depth cerebrovascular MRI markers of the participants (n=2297).

| | Baseline | Follow-up | Change over time |
|---|---|---|---|
| **WMH volume (ml)** | 16.56 ± 17.21 | 22.32 ± 22.18 | 5.76 ± 7.74 |
| **Participants with subcortical infarcts** | 153 (7%) | 221 (10%) | 68 (3%) |
| with 1 subcortical infarct | 118 [77%] | 157 [71%] | 39 [57%] |
| with 2 subcortical infarcts | 21 [14%] | 33 [15%] | 12 [18%] |
| with 3 subcortical infarcts | 5 [3%] | 17 [8%] | 12 [18%] |
| with 4 subcortical infarcts | 5 [3%] | 7 [3%] | 2 [3%] |
| with ≥5 subcortical infarcts | 4 [3%] | 7 [3%] | 3 [4%] |
| **Participants with microbleeds** | 381 (17%) | 680 (30%) | 299 (13%) |
| with 1 microbleed | 268 [70%] | 434 [64%] | 166 [56%] |
| with 2 microbleeds | 62 [16%] | 119 [18%] | 57 [19%] |
| with 3 microbleeds | 22 [6%] | 46 [7%] | 24 [8%] |
| with 4 microbleeds | 14 [4%] | 27 [4%] | 13 [4%] |
| with ≥5 microbleeds | 15 [4%] | 54 [8%] | 39 [13%] |
| **Participants with enlarged PVS** | 358 (16%) | 397 (17%) | 39 (2%) |
| with 1 enlarged PVS | 273 [76%] | 296 [75%] | 23 [59%] |
| with 2 enlarged PVS | 54 [15%] | 62 [16%] | 8 [21%] |
| with 3 enlarged PVS | 13 [4%] | 20 [5%] | 7 [18%] |
| with 4 enlarged PVS | 10 [3%] | 7 [18%] | -3 [8%] |
| with ≥5 enlarged PVS | 8 [2%] | 12 [3%] | 4 [10%] |
| **Participants with cerebellar infarcts** | 434 (19%) | 596 (26%) | 162 (7%) |
| with 1 cerebellar infarct | 279 [64%] | 336 [56%] | 57 [35%] |
| with 2 cerebellar infarcts | 91 [22%] | 140 [23%] | 43 [27%] |
| with 3 cerebellar infarcts | 19 [4%] | 50 [8%] | 31 [19%] |
| with 4 cerebellar infarcts | 14 [3%] | 22 [4%] | 8 [5%] |
| with ≥5 cerebellar infarcts | 25 [6%] | 48 [8%] | 23 [14%] |
| **Participants with of cortical infarcts** | 176 (8%) | 299 (13%) | 123 (5%) |
| with 1 cortical infarct | 134 [76%] | 189 [63%] | 55 [45%] |
| with 2 cortical infarcts | 28 [16%] | 66 [22%] | 38 [31%] |
| with 3 cortical infarcts | 10 [6%] | 22 [7%] | 12 [10%] |
| with 4 cortical infarcts | 1 [1%] | 7 [2%] | 6 [5%] |
| with ≥5 cortical infarcts | 3 [2%] | 15 [5%] | 12 [10%] |

Data are shown as mean ± SD, or frequency (%). The table shows number of participants with cerebrovascular disease markers and a specification in markers. Number of participants with cerebrovascular disease marker as percentage of the total sample size (in brackets: ( )). Number of participants with a specific cerebrovascular disease markers as percentage of the total number of participants with this cerebrovascular disease marker (in square brackets: [ ]). PVS: perivascular spaces.
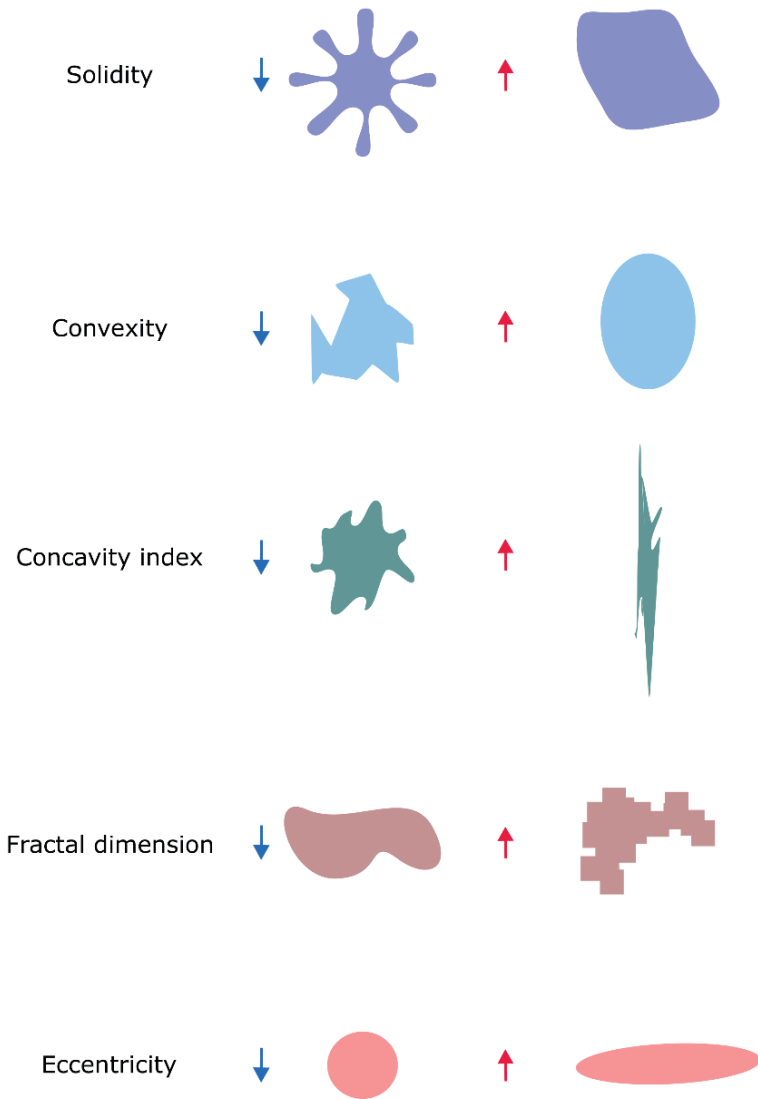
**Figure S.3.9.1. WMH shape markers and examples of shapes with high or low values of different shape markers.** For periventricular/confluent WMHs solidity, convexity, concavity index, and fractal dimension were calculated. For deep WMHs eccentricity and fractal dimension were the calculated shape markers.
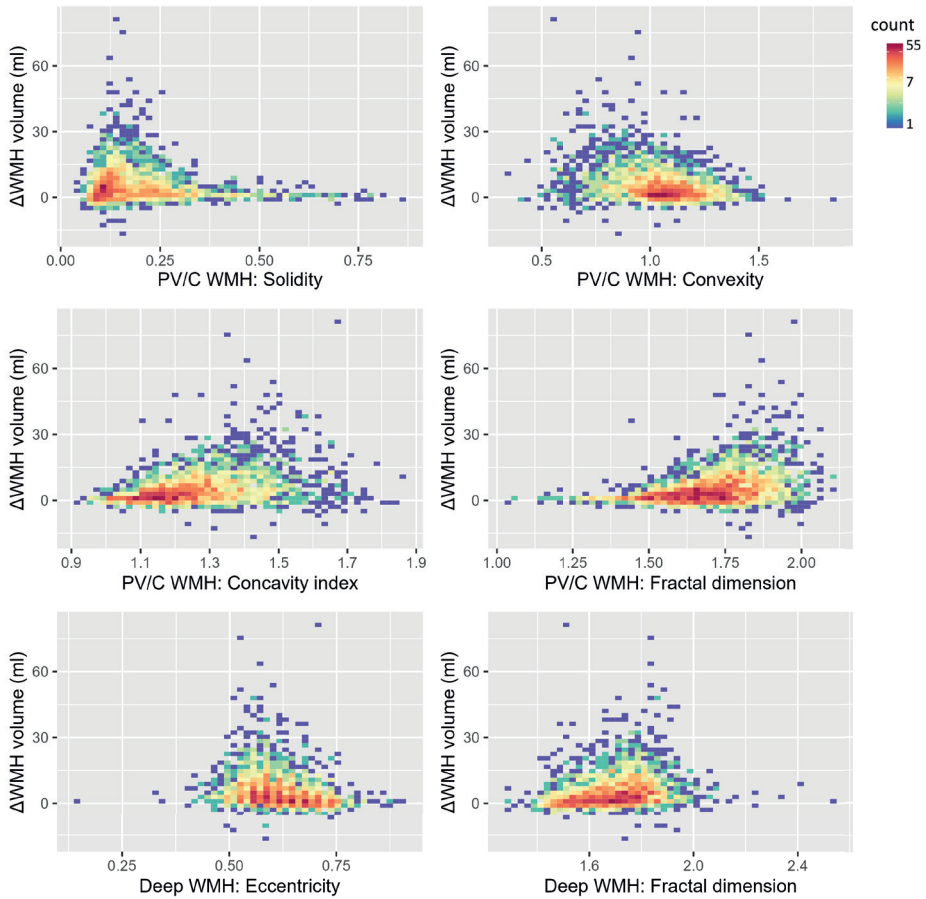
**Figure S.3.9.2. Density plots showing baseline WMH shape markers in relation to change in WMH volume over time determined at the 5-year follow-up.** The color scale represents the number of participants per datapoint.
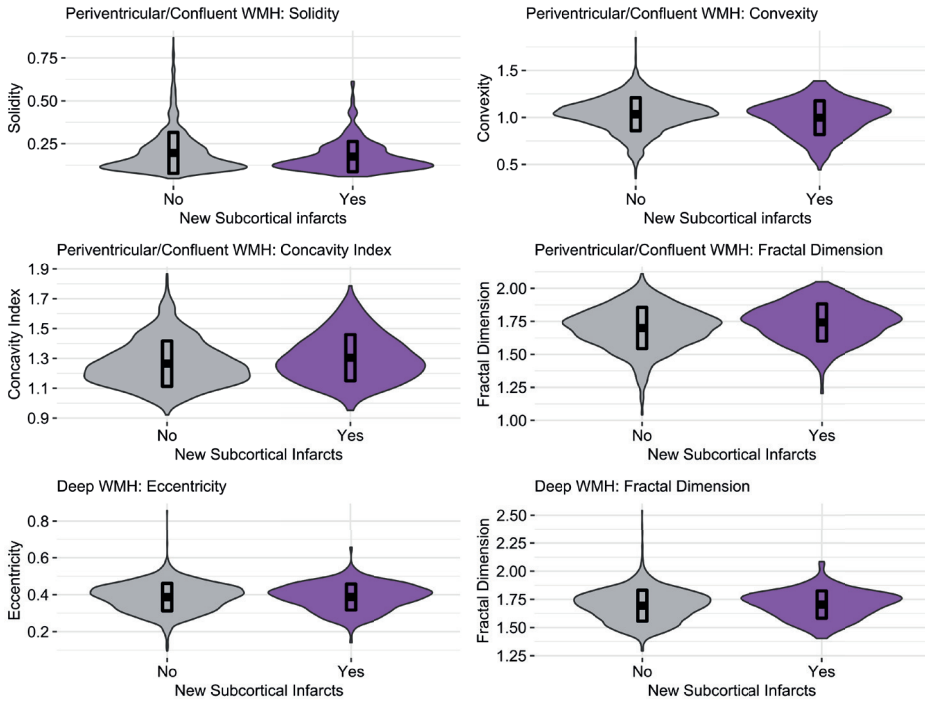
**Figure S.3.9.3. WMH shape markers at baseline in participants with new subcortical infarcts versus participants without new subcortical infarcts at follow-up.**
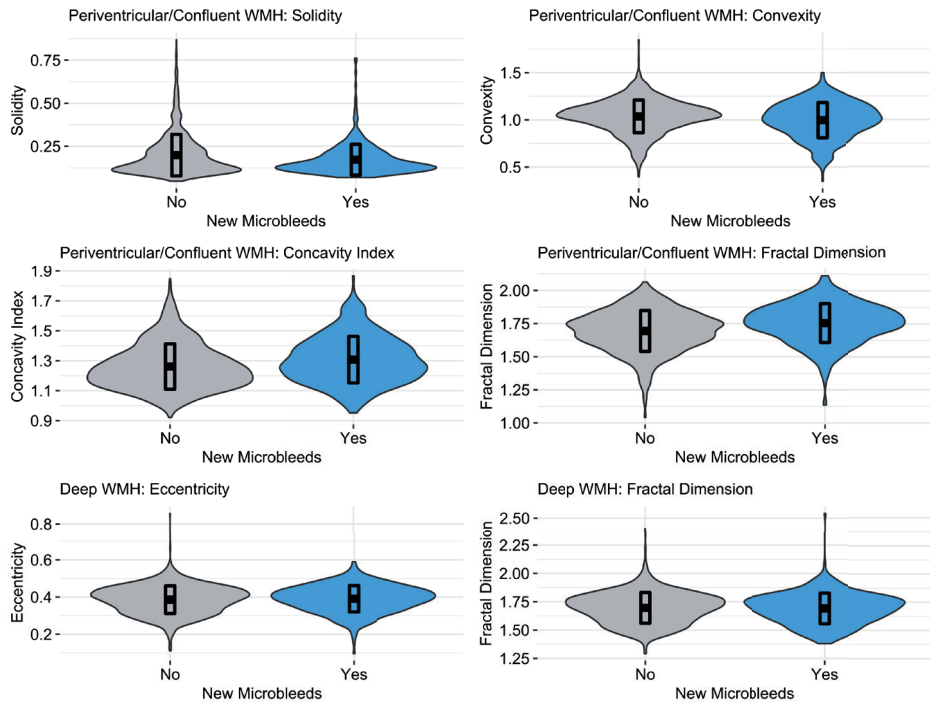
**Figure S.3.9.4. WMH shape markers at baseline in participants with new microbleeds versus participants without new microbleeds at follow-up.**
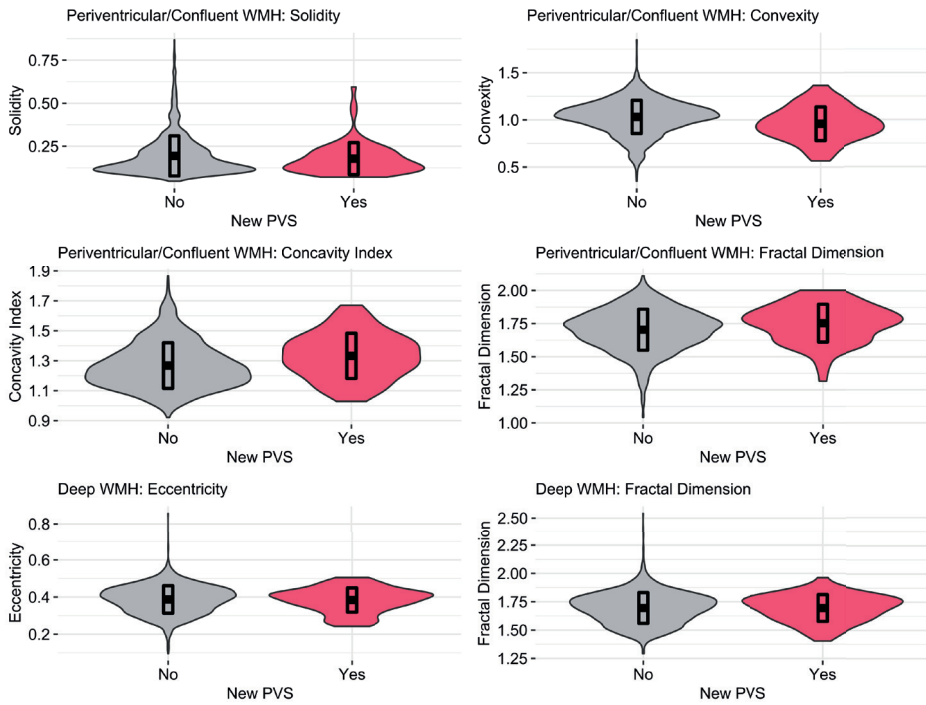
**Figure S.3.9.5. WMH shape markers at baseline in participants with new enlarged perivascular spaces versus participants without new enlarged perivascular spaces at follow-up.**
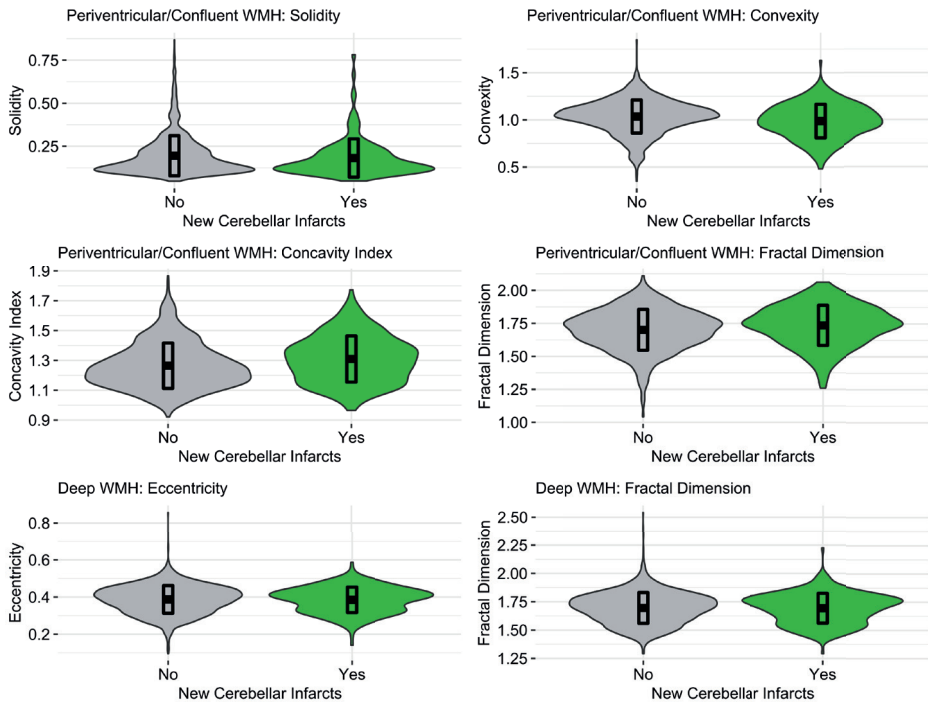
**Figure S.3.9.6. WMH shape markers at baseline in participants with new cerebellar infarcts versus participants without new cerebellar infarcts at follow-up.**
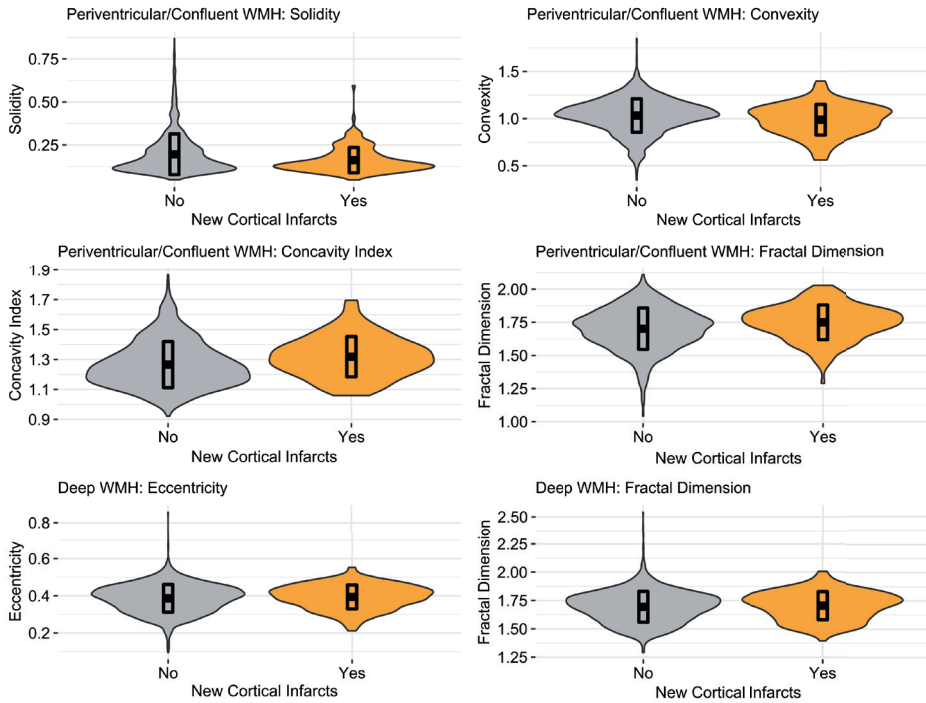
**Figure S.3.9.7. WMH shape markers at baseline in participants with new cortical infarcts versus participants without new cortical infarcts at follow-up.**

CHAPTER

4

# A MORE IRREGULAR SHAPE OF WHITE MATTER HYPERINTENSITIES IS ASSOCIATED WITH COGNITIVE DECLINE OVER 5 YEARS IN COMMUNITY-DWELLING OLDER ADULTS

Jasmin Annica Kuhn-Keller, Sigurdur Sigurdsson, Lenore J. Launer, Mark A. van Buchem, Matthias J.P. van Osch, Vilmundur Gudnason, Jeroen de Bresser.

# 4.1 ABSTRACT

A previous study has shown that WMH shape is associated with long-term risk for dementia after 10 years in community-dwelling older adults. However, the exact association with decline in different cognitive domains remains unknown. The current study aimed to investigate the association of WMH shape and decline in three cognitive domains over 5 years' time in community-dwelling older adults.

The association of baseline WMH shape (solidity, convexity, concavity index, fractal dimension, and eccentricity) and cognitive decline over 5.2 ± 0.3 years (domains: memory, executive function, and processing speed) were investigated using linear regression models in the Age, Gene/Environment Susceptibility-Reykjavik (AGES) study (n = 2560).

A more irregular shape of periventricular/confluent WMH was related to cognitive decline in the memory domain (lower solidity (B: -0.04 (95% CI: -0.07─-0.01); p=0.005), lower convexity (-0.07 (-0.10─-0.04); p<0.001), a higher concavity index (-0.09 (-0.12─-0.06); p<0.001), and a higher fractal dimension (-0.07 (-0.10─-0.04); p<0.001)), the executive function domain (lower convexity ((-0.04 (-0.07─-0.01); p=0.009), a higher concavity index (-0.04 (-0.07─-0.01); p=0.003), and a higher fractal dimension (-0.04 (-0.07─-0.01); p=0.009)), and the processing speed domain (lower solidity (-0.04 (-0.07─-0.02); p<0.001), lower convexity (-0.06 (-0.08─-0.03); p<0.001), a higher concavity index (-0.08 (-0.10─-0.05); p<0.001), and higher fractal dimension (-0.06 (-0.09─-0.04); p<0.001)) over 5.2 years. No associations were found between deep WMH shape and cognitive decline in any of the cognitive domains.

These findings show that WMH shape patterns may be indicative of relatively short-term cognitive decline in community-dwelling older adults. This supports the evidence of WMH shape being a valuable marker that may be used to assess and predict cognitive outcome related to cerebrovascular disease progression.

## 4.2 INTRODUCTION

Cerebral small vessel disease (SVD) is associated with cognitive decline and is an important contributor to occurrence of dementia in older adults.[1,2] A key MRI marker of SVD is white matter hyperintensities (WMH), which become evident as hyperintense lesions on T2-weighted MRI scans. Total WMH volume is a commonly used MRI marker and is related to cognitive decline.[3,4] However, WMH volume is a relatively crude marker that only shows a moderate association with cognitive decline and is also not specific for underlying pathophysiological changes. In recent studies, WMH shape has been introduced as a more descriptive measure related to severity and progression of WMH compared to WMH volume alone.[5–7] For example, a more irregular shape of periventricular/confluent WMH has been associated with an increased long-term risk for ischemic stroke and mortality.[5] Furthermore, our previous study showed that a more irregular shape of periventricular/confluent WMHs was associated with an increased long-term dementia risk in community-dwelling older adults over 10 years.[6] However, the association between WMH shape and decline in different cognitive domains remains unknown. We hypothesized that a more irregular WMH shape is associated with increased cognitive decline over 5.2 years, especially in the memory domain. The current study therefore aimed to investigate the association of WMH shape and decline in three cognitive domains over 5 years' time in community-dwelling older adults.

## 4.3 METHODS

### 4.3.1 Participants & study design

The study is based on the AGES-Reykjavik study cohort.[8] This study was approved by the Icelandic National Bioethics Committee, VSN:00-063, and the institutional review board responsible for the National Institute on Aging (NIA) research. All participants signed informed consent prior to any experiments. Baseline brain MRI scans were acquired from 2002 to 2006. Five years later the follow-up visit took place from 2007 to 2011. The participants underwent cognitive testing at baseline and follow-up. A total of 2560 participants were included in the current study. A flow-chart describing the exclusion of participants for the current study is shown in supplementary figure S.4.9.1.

### 4.3.2 Baseline characteristics and cardiovascular risk factors

Education level and smoking status were collected via questionnaires. The highest completed education level (primary school, secondary school, college or university) was entered. Non-smokers were defined as persons who never smoked, former regular smokers of at least 100 cigarettes or 20 cigars in a lifetime were categorized

as former smokers, and the last category were current smokers. Body mass index (BMI) was calculated based on the measured participant's height (cm) and weight (kg). Systolic and diastolic blood pressure were measured with a standard mercury sphygmomanometer, and the mean of two measurements was calculated. Hypertension was defined based on self-report and/or use of antihypertensive medication, and/or measured systolic blood pressure >140 mm Hg and/or diastolic blood pressure >90 mm Hg. Diabetes mellitus was defined based on self-report, use of anti-diabetic medication, or fasting blood glucose level >7.0 mmol/L. Coronary artery disease was defined based on self-report plus the use of nitrates, a history of a bypass operation, and/or evidence of myocardial infarction on electrocardiogram.

## 4.3.3 MRI acquisition protocol

MRI scans were performed on a 1.5 Tesla Signa Twinspeed system (General Electric Medical Systems, Waukesha, Wisconsin). Sequences included in the protocol: a 3D T1-weighted, spoiled-gradient echo sequence (repetition time = 21 ms; time to echo = 8 ms; field of view = 240 mm; slice thickness = 1.5 mm; voxel size = 0.94 × 0.94 × 1.50 mm$^3$) and a fluid attenuated inversion recovery (FLAIR) sequence (repetition time = 8000 ms; time to echo = 100 ms; field of view = 220 mm; 3 mm interleaved slices; voxel size = 0.86 × 0.86 × 3.00 mm$^3$).

## 4.3.4 WMH markers

An in-house developed pipeline was used to calculate WMH shape markers, as described previously.[6] In brief, WMH were segmented automatically from FLAIR MRI scans using the LST toolbox[9] in SPM12. Lateral ventricles were segmented from T1 scans and these ventricle masks were inflated with 3 and 10 mm. The inflated ventricle masks were used to classify WMHs into periventricular, confluent, or deep WMH (figure 4.1, supplementary figure S.4.9.2). Convexity, solidity, concavity index, and fractal dimensions were determined based on the segmentations of the periventricular/confluent WMHs.[6] A lower convexity and solidity, and higher concavity index and fractal dimension indicate more irregular shapes. For deep WMH fractal dimensions and eccentricity were calculated.[6] Higher eccentricity indicates a rounder shape, and a higher fractal dimension indicates a more irregular shape of deep WMH. The formulas of the WMH shape markers are shown in figure 4.1. Moreover, total WMH volume, as well as the volumes of periventricular/confluent and deep WMH were calculated.
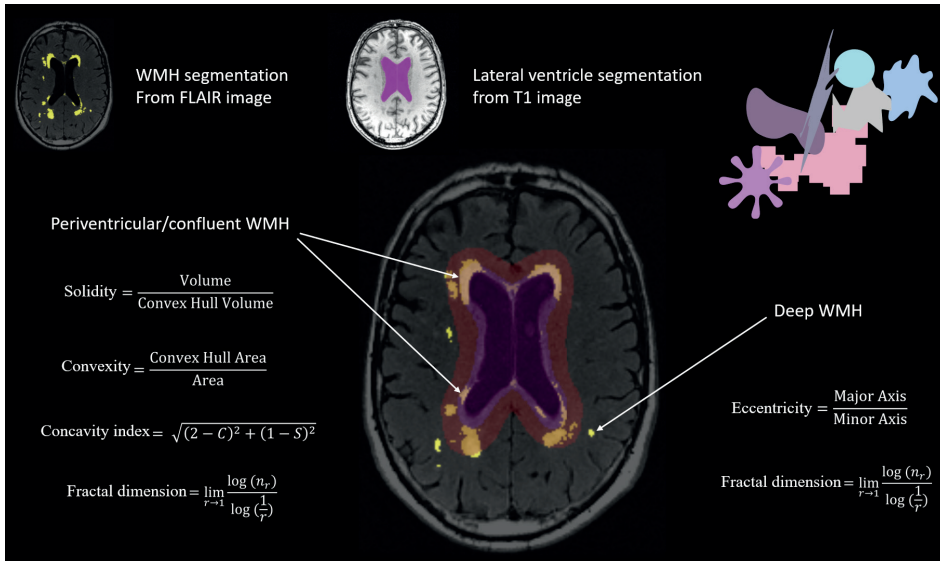
**Figure 4.1. Illustration of the calculation of WMH shape markers from brain MRI scans.** WMHs are automatically segmented from FLAIR images. The lateral ventricles are automatically segmented from T1 images and inflated in order to aid delineation of periventricular/confluent WMHs. Based on the segmentations, the shape markers (for periventricular/confluent WMH: solidity, convexity, concavity index, and fractal dimension; for deep WMH: eccentricity and fractal dimension) are calculated using the formula's shown in the figure.

## 4.3.5 Neuropsychological testing

Based on a cognitive test battery the composite scores were calculated for three cognitive domains: memory, executive function, and processing speed.[10–12] Immediate- and delayed-recall portions of the California Verbal Learning Test[13] were included in the memory composite score. The executive domain score included the Digits Backward Test[14], the Spatial Working Memory Test of the Cambridge Neuropsychological Test Automated Battery[15], and the Stroop Test, Part III (word-color interference). The processing speed domain score included the Digit Symbol Substitution Test[14], the Figure Comparison Test[16] and the Stroop Test[17] Part I (word naming) and Part II (color naming). Domain scores were calculated by converting raw scores on each test to standardized z-scores and averaging the z-scores across the tests in each composite score per participant. Change in cognitive function was determined per domain by subtracting the baseline scores from the follow-up scores.

## 4.3.6 Statistical analysis

To aid comparability of the results, solidity and convexity were inverted for the linear regression analyses. Solidity and WMH volumes were multiplied by 100 and natural log transformed due to non-normal distribution. Z-scores of WMH shape

markers and WMH volumes were calculated to aid comparability. Linear regression analyses were run to study the association of WMH shape and cognitive change per domain, corrected for age, sex, education, time to follow-up, and baseline cognitive domain scores. In secondary analysis to test for WMH volume independency of the associations between WMH shape and cognitive decline, WMH volume as a percentage of intracranial volume was added as an additional covariate to the linear regression models used in the main analysis. As a frame of reference linear regression analyses for WMH volumes were performed as secondary analyses, additionally corrected for intracranial volume. A p value <0.05 was considered statistically significant.

### 4.3.7 Sensitivity analysis

Different methods to analyze cognitive change over time were used in previous studies. To test the robustness of the linear regression models we therefore performed sensitivity analyses. To this end, linear regression analyses were run with the follow-up domain scores as dependent variable, WMH shape as independent variable and corrected for age, sex, education, time to follow-up, and baseline domain scores.

## 4.4 RESULTS

Baseline characteristics of the participants (n=2560) can be found in table 4.1. Mean age at baseline was 74.7 ± 4.8 years of age, and 61% of the participants were females. The cognitive decline (in z-scores) over 5.2 ± 0.3 years was -0.28 ± 0.98 in the memory domain, -0.25 ± 0.69 for executive function, and -0.32 ± 0.60 for processing speed. The z-scores per cognitive domain at baseline and follow-up for all participants per cognitive domain can be found in figure 4.2.

### 4.4.1 WMH Shape and cognitive decline
#### *4.4.1.1 Memory domain*
A more irregular shape of periventricular/confluent WMH expressed as a lower solidity (B: -0.04 (95% CI: -0.07—-0.01); p=0.005), lower convexity (-0.07 (-0.10—-0.04); p<0.01), a higher concavity index (-0.09 (-0.12—-0.06); p<0.001), and a higher fractal dimension (-0.07 (-0.10—-0.04); p<0.001) was related to cognitive decline in the memory domain over 5.2 years (table 4.2). No associations were found for deep WMH shape.

#### *4.4.1.2 Executive function domain*
A more irregular shape of periventricular/confluent WMH expressed as a lower convexity (-0.04 (-0.07—-0.01); p=0.009), a higher concavity index; (-0.04 (-0.07—-0.01); p=0.003), and a higher fractal dimension (-0.04 (-0.07—-0.01); p=0.009)

was related to cognitive decline in the executive function domain over 5.2 years (table 4.2). No associations were found for deep WMH shape.

### 4.4.1.3 Processing speed domain

A more irregular shape of periventricular/confluent WMH expressed as a lower solidity (-0.04 (-0.07―-0.02); p<0.001), a lower convexity (-0.06 (-0.08―-0.03); p<0.001), a higher concavity index (-0.08 (-0.10―-0.05); p<0.001), and a higher fractal dimension (-0.06 (-0.09―-0.04); p<0.001) was significantly associated with cognitive decline over 5.2 years in the processing speed domain (table 4.2). No associations were found for deep WMH shape.

**Table 4.1.** Baseline characteristics of the study sample.

| Baseline characteristics | Total n = 2560 |
|---|---|
| Age (years) | 74.7 ± 4.8 |
| Females | 1562 (61%) |
| BMI (kg/m³) | 27.2 ± 4.1 |
| Hypertension | 1978 (77%) |
| Diabetes type 2 diabetes | 228 (9%) |
| Cholesterol (mmol/L) | 5.69 ± 1.13 |
| Smoking status | |
| Never | 1141 (44%) |
| Former | 1145 (45%) |
| Current | 274 (11%) |
| Coronary artery disease | 402 (16%) |
| Time to follow-up (years) | 5.2 ± 0.3 |
| Total WMH volume (ml) | 17.44 ± 15.94 |
| Periventricular/confluent WMH volume (ml) | 15.93 ± 15.54 |
| Deep WMH volume (ml) | 1.51 ± 1.37 |
| Periventricular/confluent WMH | |
| Solidity | 0.19 ± 0.12 |
| Convexity | 1.03 ± 1.18 |
| Concavity index | 1.27 ± 1.15 |
| Fractal dimension | 1.71 ± 1.54 |
| Deep WMH | |
| Eccentricity | 0.61 ± 0.07 |
| Fractal dimension | 1.69 ± 0.13 |

Data are indicated as mean ± SD or frequency (%). WMH: white matter hyperintensities.

**4**
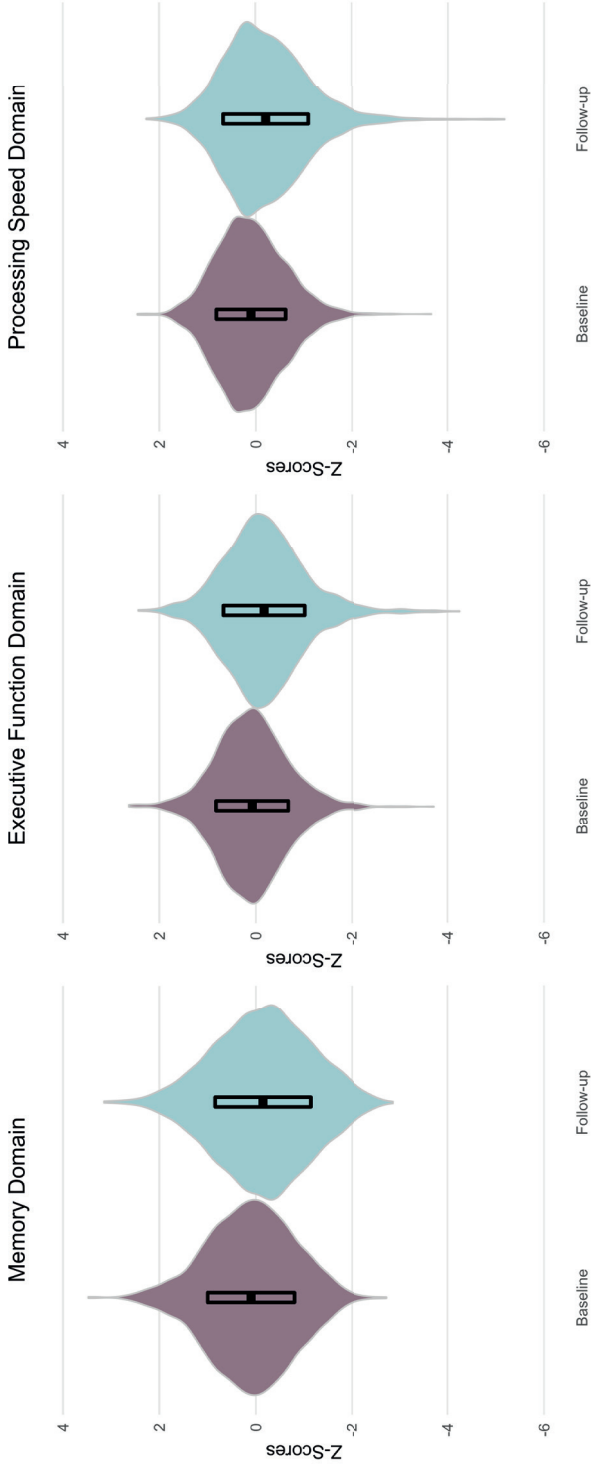
**Figure 4.2. Violin plots including z-scores and standard deviation per cognitive domain (memory, executive function and processing speed) at baseline and follow-up.**

#### *4.4.1.4 Secondary analysis*

In secondary analysis to test for WMH volume independency of the found associations of WMH shape and cognitive decline, we showed that these associations were for a small part WMH volume dependent. The results slightly attenuated, but stayed statistically significant in the memory domain (except for solidity) and the processing speed domain (supplementary table S.4.9.1). In the executive function domain all statistical significance was lost. Deep WMH eccentricity was found to be associated with cognitive decline in the memory domain, a finding that did not appear in the main results.

### 4.4.2 WMH volumes and cognitive decline

In secondary analyses, total WMH volume (memory domain: -0.10 (-0.13—-0.07); p < 0.001; executive function domain: -0.05 (-0.08—-0.02); p < 0.001; processing speed domain: -0.08 (0.10—-0.05); p < 0.001), the volume of periventricular/confluent WMH (memory domain: -0.10 (-0.13—-0.07); p < 0.001; executive function domain: -0.05 (-0.07—-0.02); p < 0.003; processing speed domain: -0.08 (0.10—-0.05); p < 0.001), and the volume of deep WMH (memory domain: -0.04 (-0.07—-0.02); p = 0.002; executive function domain: -0.04 (-0.06—-0.01); p = 0.007; processing speed domain: -0.04 (-0.06—-0.01); p = 0.002) were significantly associated with cognitive decline in the memory, executive function and processing speed domain (table 4.3).

### 4.4.3 Sensitivity analysis

To test the robustness of our results for a different method to analyse cognitive change, sensitivity analyses were performed. These results were quite comparable to our main results (supplementary table 4.9.2).

**4**

**Table 4.2.** Linear regression results for baseline WMH shape and decline in cognitive domain scores over 5.2 years.

| | Memory (n=2340) | Executive function (n=2356) | Processing speed (n=2443) |
|---|---|---|---|
| **Periventricular/confluent WMH** | | | |
| Solidity | -0.04 (-0.07–-0.01) ** | -0.01 (-0.04–0.02) | -0.04 (-0.07–-0.02)*** |
| Convexity | -0.07 (-0.10–-0.04) *** | -0.04 (-0.07–-0.01)** | -0.06 (-0.08–-0.03)*** |
| Concavity index | -0.09 (-0.12–-0.06) *** | -0.04 (-0.07–-0.01) ** | -0.08 (-0.10–-0.05)*** |
| Fractal dimension | -0.07 (-0.10–-0.04) *** | -0.04 (-0.07–-0.01)** | -0.06 (-0.09–-0.04)*** |
| **Deep WMH** | | | |
| Eccentricity | -0.01 (-0.04–0.02) | -0.01 (-0.04–0.02) | -0.01 (-0.04–-0.01) |
| Fractal dimension | 0.01 (-0.02–0.04) | 0.02 (-0.01–0.05) | 0.02 (-0.01–0.04) |

Linear regression models for the association between WMH shape and cognitive change over 5.2 years in each cognitive domain, controlled for age, sex, education, time to follow-up, and cognitive domain scores at baseline. The sample size varies per domain due to missing data in the cognitive domain scores. Solidity and convexity were inverted to aid in the comparability of the direction of effect. *<0.05; **<0.01; ***<0.001.

**Table 4.3.** Linear regression results for baseline WMH volume and decline in cognitive domain scores over 5.2 years.

| WMH volume | Memory (n=2340) | Executive function (n=2356) | Processing speed (n=2443) |
|---|---|---|---|
| Total WMH volume | -0.10 (-0.13–-0.07)*** | -0.05 (-0.08–-0.02)*** | -0.08 (-0.10–-0.05)*** |
| Periventricular/confluent WMH volume | -0.10 (-0.13–0.07)*** | -0.05 (-0.07–-0.02)** | -0.08 (-0.10–-0.05)*** |
| Deep WMH volume | -0.04 (-0.07–-0.02) ** | -0.04 (-0.06–-0.01)** | -0.04 (-0.06–-0.01)** |

Linear regression models for the association between WMH volume and cognitive change over 5.2 years in each cognitive domain, controlled for age, sex, education, time to follow-up, cognitive domain scores at baseline, and intracranial volume. The sample size varies per domain due to missing data in the cognitive domain scores. *<0.05; **<0.01; ***<0.001

# 4.5 DISCUSSION

We showed that a more irregular shape of periventricular/confluent WMH was related to cognitive decline in the memory domain, the executive function domain, and the processing speed domain over 5.2 years in community-dwelling older adults. No associations were found between deep WMH shape and cognitive decline in any of the cognitive domains. Our secondary analyses showed that a higher total, periventricular/confluent, and deep WMH volume was associated with cognitive decline in the memory domain, the executive function domain, and the processing speed domain over 5.2 years.

Previously, we found that a more irregular shape of periventricular/confluent WMHs was associated with an increased long-term dementia risk over 10 years in the same dataset.[6] However, which cognitive functions mediate this association at a more short-term (5 years) remained unclear. A recent cross-sectional study in patients with manifest arterial disease using the same WMH shape markers showed that a more irregular shape of periventricular/confluent WMH was related to decreased executive functioning and memory performance.[18] Moreover, another cross-sectional study in cognitively impaired individuals showed that mental speed and fluid abilities showed a stronger association to a more irregular shape of WMH (based on a confluency sum score) than WMH volume.[19] To the best of our knowledge, our study is the first to investigate WMH shape and cognitive decline over time in domain scores in community-dwelling older adults. Our study showed that WMH shape markers are associated with decline in individual cognitive domains over time. As these associations were largely independent of WMH volume, this suggests that WMH shape conveys additional information about WMHs, which is not captured by WMH volume alone.

In previous studies periventricular/confluent WMH burden or volume showed a stronger association with cognitive functioning and cognitive decline compared to deep WMH burden or volume.[20,21] In a longitudinal study in the general population (n=563), with a similar age and comparable population to our study, periventricular WMH burden was associated with cognitive decline over nearly 10 years, but deep WMH burden was not.[20] While deep WMH are often found in regions of short-looped U-fibers connecting different cortical regions, periventricular WMH largely involve regions of long associating fibers with subcortical nuclei and other more distant brain regions.[22,23] Therefore, changes in a long fiber region may have more severe consequences, and also cognitive reserve mechanisms may suffer more from changes in periventricular regions compared to deep white matter regions. Another explanation could be that periventricular/confluent WMH are typically larger in volume compared to deep WMH and therefore involve a larger area of the brain. In our study, we found that both periventricular/confluent WMH volume and deep WMH volume are related to cognitive decline in all three domains (memory, executive function, and processing speed), most pronounced in the memory and processing speed domains. In a previous meta-analysis in relatively healthy older adults without cognitive impairment from 60 years of age, WMH volume and burden were also related to cognitive decline in three cognitive domains (memory, attention and executive function), slightly more pronounced for the domain attention and executive function.[3]

**4**

In the present study, the effect sizes of the associations between WMH shape and cognitive decline showed differences between cognitive domains. The effect sizes for the associations of WMH shape with memory and processing speed were roughly similar, while the effect sizes for executive function were relatively smaller. An explanation could be that different WMH shape patterns are related to different underlying pathology resulting in different effects on the brain, and possibly on different cognitive domains. SVD is a whole-brain disease and with MRI we are only able to capture the tip of the iceberg of the disease process. WMH shape could therefore convey additional information on why some cognitive domains are affected earlier or to a greater extent than others.

In our study the effect sizes of the association between WMH markers and cognitive decline per domain are quite similar for WMH shape compared to WMH volume, especially for the WMH shape marker concavity index. As these associations were largely independent of WMH volume, this shows that WMH shape is an important and relevant additional marker besides WMH volume alone. Furthermore, in otherwise healthy older adults WMHs are commonly seen and at the moment the exact prognostic meaning for an individual is unclear. Since not all individuals with WMH will eventually develop cognitive decline or dementia, it is challenging to successfully identify individuals who are at a higher risk. Specific WMH patterns—defined by type and shape—may improve this early identification within risk-MR-phenotypes.

A important strength of our study is the large cohort from the general population, which gives the study a large external validity and aids generalizability. Moreover, automated image processing techniques, in combination with extensive visual quality checks are other strengths of our study. Furthermore, the study contains a full neuropsychological assessment at two time points (baseline and follow-up). The use of a 1.5T MRI system could be considered a limitation of our study. While these systems were standard at the time of data collection, most 1.5T research MRI scanners have now been replaced with 3T MRI systems. Another limitation of our study could be selective loss to follow-up as participants who develop the most cognitive decline over time are most likely to be lost-to-follow-up. Nevertheless, despite these limitations significant associations between WMH shape markers and cognitive decline in different domains were found in our study.

In conclusion, our findings show that WMH shape patterns may be indicative of relatively short-term cognitive decline in community-dwelling older adults. This supports the evidence of WMH shape being a valuable marker that may be used to assess and predict cognitive outcome related to cerebrovascular disease progression.

## 4.6 ACKNOWLEDGEMENTS

## 4.7 DISCLOSURES

M.J.P. van Osch reports to be an unpaid member of a clinical trial steering committee of Alnylam.

4

## 4.8 REFERENCES

1. Wardlaw JM, Smith C, Dichgans M. Small vessel disease: mechanisms and clinical implications. Lancet Neurol; 2019;18:684–696. https://doi.org/10.1016/S1474-4422(19)30079-1

2. Snyder HM, Corriveau RA, Craft S, et al. Vascular contributions to cognitive impairment and dementia including Alzheimer's disease. Alzheimers Dement; 2015;11:710–717. https://doi.org/10.1016/j.jalz.2014.10.008

3. Jansma A, Bresser J de, Schoones JW, Heemst D van, Akintola AA. Sporadic cerebral small vessel disease and cognitive decline in healthy older adults: A systematic review and meta-analysis. Journal of Cerebral Blood Flow & Metabolism. 2024;0:1-20. doi:10.1177/0271678X241235494

4. Alber J, Alladi S, Bae H, et al. White matter hyperintensities in vascular contributions to cognitive impairment and dementia (VCID): Knowledge gaps and opportunities. Alzheimer's & Dementia: Translational Research & Clinical Interventions; 2019;5:107–117. https://doi.org/10.1016/j.trci.2019.02.001

5. Ghaznawi R, Geerlings M, Jaarsma-Coes M, Hendrikse J, de Bresser J. Association of White Matter Hyperintensity Markers on MRI and Long-term Risk of Mortality and Ischemic Stroke. Neurology; 2017;96:e2172-2183. https://doi.org/10.1212/WNL.0000000000011827

6. Keller JA, Sigurdsson S, Klaassen K, et al. White matter hyperintensity shape is associated with long-term dementia risk. Alzheimers Dement. 2023;19(12):5632-5641. https://doi.org/10.1002/alz.13345

7. De Bresser J, Kuijf HJ, Zaanen K, et al. White matter hyperintensity shape and location feature analysis on brain MRI; Proof of principle study in patients with diabetes. Sci Rep. 2018;8:8:1893. https://doi.org/10.1038/s41598-018-20084-y

8. Harris TB, Launer LJ, Eiriksdottir G, et al. Age, gene/environment susceptibility-reykjavik study: Multidisciplinary applied phenomics. Am J Epidemiol. Am J Epidemiol; 2007;165:1076–1087. https://doi.org/10.1093/aje/kwk115

9. Schmidt P. Bayesian inference for structured additive regression models for large-scale problems with applications to medical imaging. Maximilians-Universität München; 2017.

10. Saczynski JS, Jónsdóttir MK, Garcia ME, et al. Cognitive Impairment: An Increasingly Important Complication of Type 2 DiabetesThe Age, Gene/Environment Susceptibility–Reykjavik Study. Am J Epidemiol. 2008;168:1132–1139. https://dx.doi.org/10.1093/aje/kwn228.

11. Ding J, Sigurðsson S, Jónsson P V., et al. Space and location of cerebral microbleeds, cognitive decline, and dementia in the community. Neurology. 2017;88:2089–2097. https://doi.org/10.1212/WNL.0000000000003983

12. Valsdóttir V, Magnúsdóttir BB, Chang M, et al. Cognition and brain health among older adults in Iceland: the AGES-Reykjavik study. Geroscience. 2022;44:2785–2800. https://doi.org/10.1007/s11357-022-00642-z

13. Delis D, Kramer J, Kaplan E, et al. California Verbal Learning Test Manual—Adult Version. New York, NY: Psychological Corporation; 1987.

14. Wechsler D. Wechsler Adult Intelligence Scale. New York, NY: Psychological Corporation; 1955.

15. Robbins TW, James M, Owen AM, Sahakian BJ, McInnes L, Rabbitt P. Cambridge Neuropsychological Test Automated Battery (CANTAB): a factor analytic study of a large sample of normal elderly volunteers. Dementia. 1994;5:266–281. https://doi.org/10.1159/000106735

16. Salthouse TA, Babcock RL. Decomposing Adult Age Differences in Working Memory. Dev Psychol. 1991;27:763–776. https://psycnet.apa.org/doi/10.1037/0012-1649.27.5.76318

17.  Stroop JR. Studies of interference in serial verbal reactions. J Exp Psychol. 935;18:643–662. https://psycnet.apa.org/doi/10.1037/h0054651

18.  Zwartbol MHT, Ghaznawi R, Jaarsma-Coes M, et al. White matter hyperintensity shape is associated with cognitive functioning – the SMART-MR study. Neurobiol Aging. 2022;120:81–87. https://doi.org/10.1016/j.neurobiolaging.2022.08.009

19.  Lange C, Suppa P, Mäurer A, et al. Mental speed is associated with the shape irregularity of white matter MRI hyperintensity load. Brain Imaging Behav. 2017;11:1720–1730. https://doi.org/10.1007/s11682-016-9647-x

20.  De Groot JC, De Leeuw FE, Oudkerk M, et al. Periventricular cerebral white matter lesions predict rate of cognitive decline. Ann Neurol. 2002;52:335–341. https://doi.org/10.1002/ana.10294

21.  Bolandzadeh N, Davis JC, Tam R, Handy TC, Liu-Ambrose T. The association between cognitive function and white matter lesion location in older adults: a systematic review. BMC Neurol. 2012;12:126. https://doi.org/10.1186/1471-2377-12-126

22.  Brodal Per. The central nervous system: structure and function. Oxford University Oxford University Press, USA, 2004.

23.  Filley CM. The behavioral neurology of cerebral white matter. Neurology. Neurology; 1998;50:1535–1540. https://doi.org/10.1212/WNL.50.6.1535

4

## 4.9 SUPPLEMENTARY MATERIAL
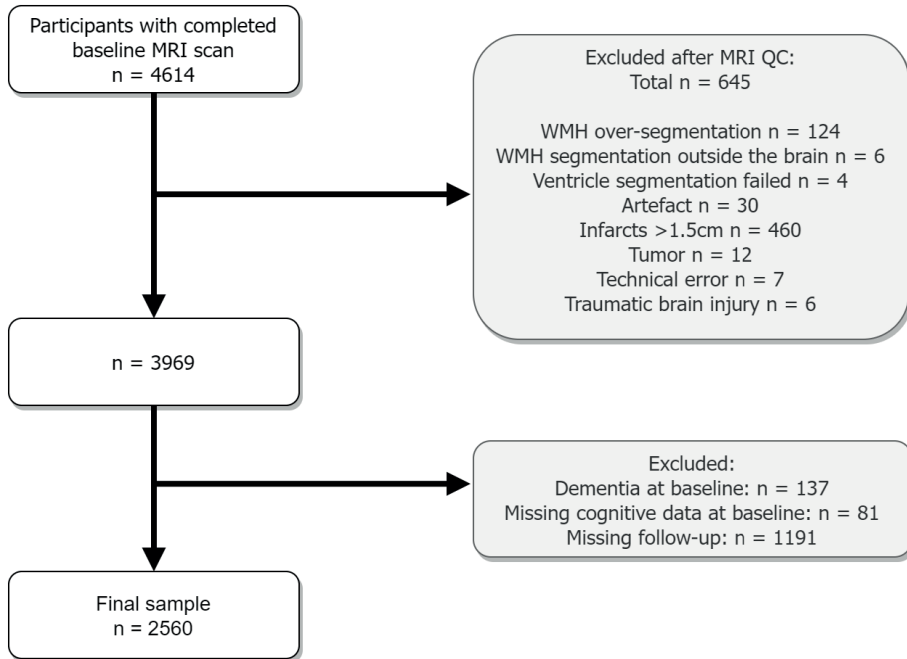


**Figure S.4.9.1. Flow-chart showing the inclusion and exclusion of participants in the current study.**
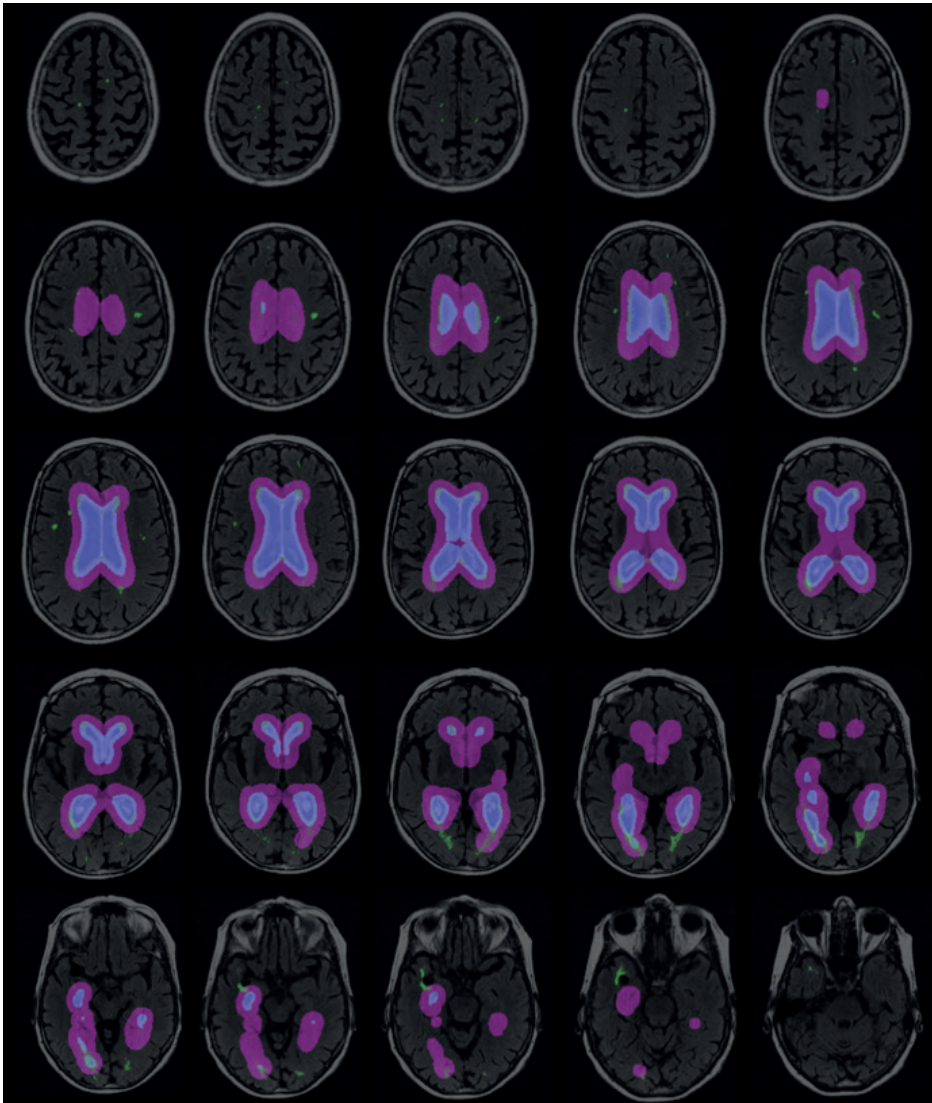
**Figure S.4.9.2. Illustration of the results of the WMH shape image processing pipeline showing different brain slices with automatic segmentations.** Green: white matter hyperintensities. Blue: 3 mm inflated lateral ventricle segmentation. Purple: 10 mm inflated lateral ventricle segmentation.

4

**Table S.4.9.1.** Secondary analysis to test WMH volume-dependency of the associations with the WMH shape markers.

| | Memory (n=2340) | Executive function (n=2356) | Processing speed (n=2443) |
|---|---|---|---|
| **Periventricular/confluent WMH** | | | |
| Solidity | -0.03 (-0.06—0.00) | -0.00 (-0.03—0.03) | -0.03 (-0.06—-0.01)** |
| Convexity | -0.05 (-0.08—-0.01)* | -0.03 (-0.06—-0.01) | -0.05 (-0.07—-0.02)** |
| Concavity index | -0.07 (-0.11—-0.03)*** | -0.03 (-0.07—0.01) | -0.07 (-0.10—-0.04)*** |
| Fractal dimension | -0.05 (-0.08—-0.01)* | -0.02 (-0.06—-0.01) | -0.05 (-0.08—-0.02)** |
| **Deep WMH** | | | |
| Eccentricity | -0.04 (-0.07—-0.01)* | -0.02 (-0.05—-0.01) | -0.02 (-0.05-0.00) |
| Fractal dimension | 0.03 (0.00—0.06) | 0.02 (-0.01—0.05) | -0.04 (0.00—0.05) |

Sensitivity analyses were performed to test the WMH volume-dependency of WMH shape markers. Linear regression models for the association between WMH shape and cognitive change were performed for each cognitive domain with follow-up domain score as dependent variable and WMH shape as independent variable, controlled for age, sex, education, time to follow-up, baseline domain score, and baseline WMH volume as percentage of intracranial volume. The sample size varies per domain due to missing data in the cognitive domain scores. Solidity and convexity were inverted to aid in the comparability of the direction of effect. *<0.05; **<0.01; ***<0.001.

**Table S.4.9.2.** Sensitivity analyses for baseline WMH shape markers and decline in cognitive domain scores after 5.2 years.

| | Memory (n=2340) | Executive function (n=2356) | Processing speed (n=2443) |
|---|---|---|---|
| **Periventricular/confluent WMH** | | | |
| Solidity | -0.04 (-0.07—-0.01) ** | -0.01 (-0.04—0.02) | -0.04 (-0.07—-0.02)*** |
| Convexity | -0.07 (-0.10—-0.04)*** | -0.04 (-0.07—-0.01)** | -0.06 (-0.08—-0.03)*** |
| Concavity index | -0.09 (-0.12—-0.06)*** | -0.04 (-0.07—-0.01)** | -0.08 (-0.10—-0.05)*** |
| Fractal dimension | -0.07 (-0.10—-0.04)*** | -0.04 (-0.07—-0.01)** | -0.06 (-0.09—-0.04)*** |
| **Deep WMH** | | | |
| Eccentricity | -0.01 (-0.04—0.02) | -0.01 (-0.04—0.02) | -0.01 (-0.04—0.01) |
| Fractal dimension | 0.01 (-0.02—0.04) | 0.02 (-0.01—0.05) | 0.02 (-0.01—0.04) |

Sensitivity analyses were performed to test the robustness of our results for a different method to analyse cognitive change. Linear regression models for the association between WMH shape and cognitive change were performed for each cognitive domain with follow-up domain score as dependent variable and WMH shape as independent variable, controlled for age, sex, education, time to follow-up, and baseline domain score. The sample size varies per domain due to missing data in the cognitive domain scores. Solidity and convexity were inverted to aid in the comparability of the direction of effect. In the executive function domain, however, there was a slight attenuation in the results and significance was lost for the association between periventricular/confluent WMH and change in executive function. *<0.05; **<0.01; ***<0.001.

4

CHAPTER

5

# WHITE MATTER HYPERINTENSITY SHAPE IS ASSOCIATED WITH LONG-TERM DEMENTIA RISK

Jasmin Annica Keller, Sigurdur Sigurdsson, Kelly Klaassen, Lydiane Hirschler, Mark A. van Buchem, Lenore J. Launer, Matthias J.P. van Osch, Vilmundur Gudnason, Jeroen de Bresser.

## 5.1 ABSTRACT

We aimed to investigate the association between white matter hyperintensity (WMH) shape and volume and the long-term dementia risk in community-dwelling older adults.

Three thousand seventy-seven participants (mean age: 75.6 ± 5.2 years) of the Age Gene/Environment Susceptibility (AGES)-Reykjavik study underwent baseline 1.5T brain magnetic resonance imaging and were followed up for dementia (mean follow-up: 9.9 ± 2.6 years).

More irregular shape of periventricular/confluent WMH (lower solidity (hazard ratio (95% confidence interval) 1.34 (1.17 to 1.52), p <0.001) and convexity 1.38 (1.28 to 1.49), p <0.001); higher concavity index 1.43 (1.32 to 1.54), p <0.001 and fractal dimension 1.45 (1.32 to 1.58), p <0.001)), higher total WMH volume (1.68 (1.54 to 1.87), p <0.001), higher periventricular/confluent WMH volume (1.71 (1.55 to 1.89), p <0.001), and higher deep WMH volume (1.17 (1.08 to 1.27), p <0.001) were associated with an increased long-term dementia risk.

WMH shape markers may in the future be useful in determining patient prognosis and may aid in patient selection for future preventive treatments in community-dwelling older adults.

## 5.2 BACKGROUND

Cerebral small vessel disease (SVD) contributes to the development of dementia and cognitive decline.[1, 2] SVD usually starts with only minor brain abnormalities that show slow progression over many decades. At an early stage individuals with SVD may benefit from available lifestyle interventions and future drug trials aimed at prevention of dementia, as previous studies showed that early lifestyle interventions in populations at risk could slow the pathophysiological processes in cerebral SVD.[3-5] However, it is currently impossible to accurately identify those individuals with SVD who have an increased risk of dementia at an early stage. Novel, more sensitive, and specific biomarkers are therefore needed.

WMHs are a common finding in older adults and may be caused by acquired diseases over the lifecourse.[6] A major cause of WMHs is cerebral SVD. Although WMHs are associated with the occurrence of dementia and cognitive decline,[7, 8] not everyone with WMHs will develop cognitive decline or dementia.[7] The challenge is to identify individuals with specific WMH patterns who are at risk to develop cognitive decline or dementia. WMH volume is a much used, but crude, marker that does not allow such a distinction. Other WMH markers, such as WMH type and shape, have therefore been introduced in recent studies as promising novel markers that may offer a more detailed characterization of WMHs than volume alone. Neuroimaging studies in community-dwelling older adults previously analyzed the burden or volumes of periventricular and deep WMH, suggesting that periventricular WMHs have a stronger association with cognitive decline than deep WMHs.[9] These findings are probably mostly driven by the usually larger volume of periventricular WMH compared to deep WMH. To date, WMH shape has received little attention. Some previous *post mortem* histopathological studies showed that WMH shape was associated with a difference in underlying pathologies.[7, 10] In these studies, a more irregular shape of confluent WMH was associated with more severe parenchymal changes than mild and smooth periventricular WMH.[11, 12]

We hypothesized that different underlying SVD pathologies result in a different WMH shape that can be quantified by MRI-based WMH shape markers. Indeed, our previous study showed that WMH shape was associated with long-term risk for stroke and increased mortality in patients with an increased vascular risk.[13] However, the association of WMH shape markers and long-term dementia risk remains unknown. We therefore aimed to investigate the association between WMH shape and volume and long-term dementia risk in community-dwelling older adults.

## 5.3 METHODS

### 5.3.1 Participants and study design

This study is based on data acquired within the Age Gene/Environment Susceptibility (AGES)-Reykjavik study, a population-based study.[14] The study was approved by the Icelandic National Bioethics Committee, VSN:00-063, and the institutional review board responsible for the National Institute on Aging (NIA) research. All participants signed informed consent. Participants of the AGES-Reykjavik study ($n$ = 4614) were born between 1907 and 1935 and underwent brain MRI scans between 2002 and 2006.[14]

Diagnosis of dementia at baseline was assessed in a three-step process, as described previously.[15] Briefly, all participants underwent the Mini-Mental State Examination and the Digit Symbol Substitution Test. Based on positive results of the tests, participants were administered a second battery of diagnostic tests and possibly a third step, which included neurological tests and a proxy interview.[15] Possible outcomes were dementia, mild cognitive impairment, or normal cognition.

Age, sex, education level, and smoking status were assessed via questionnaires at baseline. Education levels are primary school, secondary school, college, and university. The highest level of education completed was entered. Smoking status was categorized as non-smoker, former smoker, and current smoker. Participants who never smoked were classified as non-smokers, participants who smoked regularly and at least 100 cigarettes or 20 cigars in a lifetime were classified as former smokers, and participants who currently smoke were classified as current smokers. Body mass index (BMI) was calculated using height (cm) and weight (kg). Hypertension was defined as self-reported or use of antihypertensive medication or measured systolic blood pressure > 140 mm Hg and/or diastolic blood pressure > 90 mm Hg. Systolic and diastolic blood pressure were measured with a standard mercury sphygmomanometer, and the mean of two measurements was calculated. Diabetes mellitus was defined as self-reported history of diabetes, use of anti-diabetic medication, or fasting blood glucose level > 7.0 mmol/L. Coronary artery disease was defined as a self-report of angina plus the use of nitrates or evidence of myocardial infarction (on ECG). Brain infarcts were defined as the presence of subcortical, cerebellar, or cortical brain infarcts.

Results from individual examinations in the study, including MRI findings, were sent to the general practitioner of the study participant in a doctor´s report. The general practitioner then acted according to clinical guidelines. In case of major incidental

finding, for example, brain tumor detected on MRI, an additional follow-up was made with a phone call to the general practitioner or the emergency center at the hospital.

The participants were tracked for dementia diagnosis through vital statistics and hospital records and by the nursing home and home-based resident assessment instrument.[16] The average time to follow-up for dementia outcome (yes/no) was 9.9 ± 2.6 years (interquartile range 3.1 years). Participants were followed from the date of the baseline MRI scan until occurrence of dementia, loss to follow-up, or end of follow-up. Loss to follow-up means that the participants died or could not be contacted. The dementia follow-up was concluded in 2015.

### 5.3.2 MRI imaging protocol

The participants underwent a baseline brain MRI scan acquired on a 1.5 Tesla Signa Twinspeed system (General Electric Medical Systems, Waukesha, Wisconsin, USA). The imaging protocol included a FLAIR sequence (repetition time = 8000 ms; time to echo = 100 ms; field of view = 220 mm; voxel size = $0.86 \times 0.86 \times 3.00$ mm$^3$) with 3-mm-thick interleaved slices and a T1-weighted sequence (repetition time = 21 ms; time to echo = 8 ms; field of view = 240 mm; slice thickness = 1.5 mm; voxel size = $0.94 \times 0.94 \times 1.50$ mm$^3$).[17]

### 5.3.3 MRI analysis pipeline

Mean values per WMH shape marker (solidity, convexity, concavity index, fractal dimension for periventricular/confluent WMH; fractal dimension and eccentricity for deep WMH), as well as WMH volumes, were calculated per participant with a method developed in-house.[18] An overview of the image processing pipeline is given in Figure 5.1.

The FLAIR and T1 images were registered using Elastix[19] in Python (version 3.8; Phyton Software Foundation, Wilmington, DE, USA). WMHs were segmented automatically using the registered FLAIR images in the LST toolbox[20] in SPM 12 (Wellcome Trust Centre for Neuroimaging, London, UK) for MATLAB (version 9.9; MathWorks, Natick, MA, USA). A modified, SPM12-based version of the ALVIN script[21] was used to segment the lateral ventricles from the T1-weighted images.
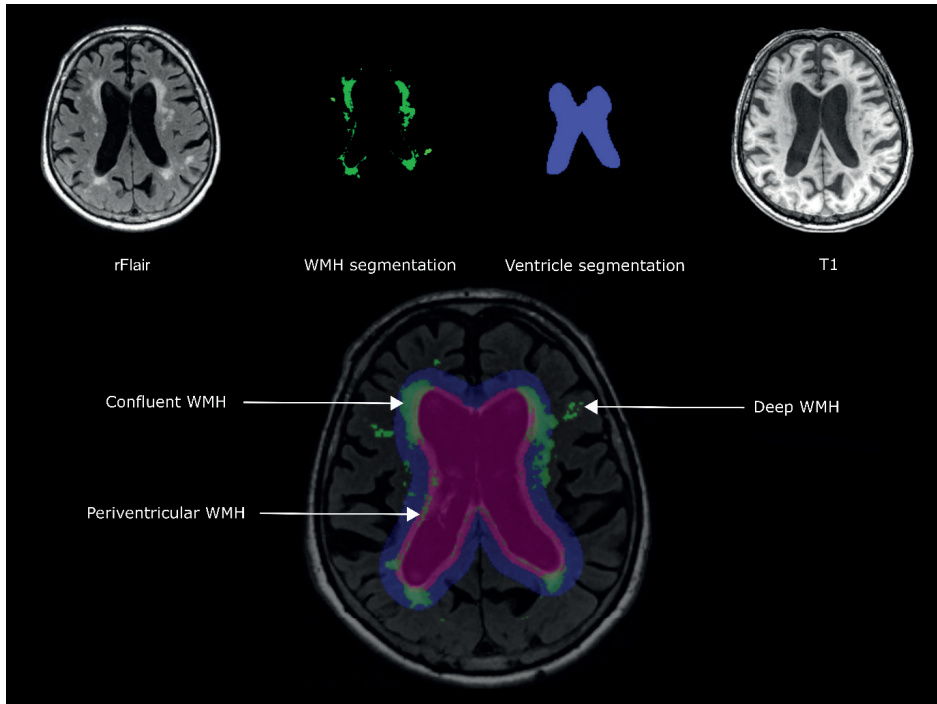
**Figure 5.1. Schematic overview of the MRI analysis pipeline.**

The lateral ventricle masks were inflated both 3 and 10 mm in order to classify WMH into periventricular/confluent and deep WMH. Periventricular WMHs were defined as lesions located within 3 mm from the lateral ventricular wall and extending up to 10 mm from the lateral ventricle into the white matter. Confluent WMHs were defined as lesions within 3 mm of the lateral ventricular wall and extending more than 10 mm from the lateral ventricles into the white matter. Deep WMHs were defined as lesions separated from the margins of the lateral ventricles; the distance between deep WMHs and the ventricular wall was at least 3 mm. Periventricular and confluent WMHs were further analyzed as one group because differentiation between these two subtypes would affect the WMH shape calculations. WMH lesions of less than five voxels were excluded, since WMH shape markers cannot be calculated accurately on small-volume WMHs.[22]

The WMH shape markers were defined based on previous studies.[18] For periventricular/confluent WMHs, solidity, convexity, concavity index, and fractal dimension were determined. Solidity was calculated by dividing the lesion volume by the volume of its convex hull. Convexity was obtained by dividing the convex hull surface area by the lesions' surface area. As a measure of roughness, the concavity index was calculated based on solidity and convexity. The fractal dimension was

calculated using the box counting technique for both periventricular/confluent and deep WMHs. Lower convexity and solidity and a higher concavity index and fractal dimension indicate a more irregularly shaped WMH.[18] In addition to fractal dimension, eccentricity was calculated for deep WMHs. Eccentricity was calculated by dividing the minor axis of a lesion by the major axis of the lesion and describes the deviation from a sphere. A lower eccentricity corresponds to a more elongated lesion, while a higher eccentricity corresponds to a rounder lesion.[18] A more complex shape of a deep WMH is described by a higher fractal dimension.[18] Table S.5.8.1 contains an overview of the shape markers. Mean shape values across all WMHs per participant were determined for periventricular/confluent WMHs, and for deep WMHs, shape values were calculated per WMH and then averages were calculated per participant.[18] Volumes of periventricular/confluent, deep, and total WMHs were calculated within the shape pipeline.

Intracranial volume was calculated by adding the volumes of gray matter, white matter, cerebrospinal fluid, and WMH.[23] Gray matter, white matter, cerebrospinal fluid, and WMH were segmented automatically with a modified algorithm based on the Montreal Neurological Institute pipeline.[24]

The researchers were blinded for participant characteristics, including dementia outcome at follow-up. Visual quality checks were performed on original and processed MRI images. Exclusions were performed in a consensus meeting between involved researchers, including a neuroradiologist.

## 5.3.4 Analytical sample

The inclusion and exclusion of participants from the AGES-Reykjavik study for the current study are illustrated in Figure S1. Participants were excluded for further analysis if their MRI images contained WMH oversegmentation (n = 124), incorrect ventricle segmentation (n = 4), artifacts (n = 30), brain infarcts > 15 mm (n = 460), tumors (n = 12), technical errors (n = 7), incorrect segmentations (n = 6), or traumatic brain injury (n = 2). A small group of participants (n = 62) had partial oversegmentation of WMHs besides (multiple) correct WMH segmentations. These participants were not excluded from further analysis. In addition, participants who were diagnosed with dementia at baseline (n = 137) were excluded for further analysis, because the present study focused on studying markers for developing dementia in the future. Participants with missing cognitive data at baseline (n = 81) or missing data at follow-up (n = 674) were also excluded for further analysis in this study. A final sample of n = 3077 was included in the final analysis (mean age: 75.6 ± 5.2 years).

## 5.3.5 Statistical analysis

T-tests, Mann-Whitney U tests, or chi-squared tests were performed for baseline characteristics in order to compare the group of participants who developed dementia at follow-up and the group of participants who did not develop dementia at follow-up.

Cox proportional hazard models were used to estimate hazard ratios (HRs) for dementia risk associated with WMH shape markers and WMH volumes. Values of solidity, convexity, and eccentricity were inverted to aid comparability of HRs. Solidity was multiplied by 100 and natural log-transformed due to non-normal distribution. Z-scores with total mean (whole group) as reference were calculated for WMH shape markers to enable comparability. Cox regression was performed on Z-scores of WMH shape markers, controlled for age, sex, and cognitive status at baseline (mild cognitive impairment or normal cognition). WMH volumes were multiplied by 100 and natural log-transformed due to non-normal distribution before a Z-score was calculated. Cox proportional hazard models for WMH volumes were controlled for age, sex, cognitive status at baseline, and intracranial volume. Additionally, the area under the ROC curve was estimated per WMH marker. Moreover, a second Cox regression model was run for both WMH shape markers and WMH volumes, where the regression analyses were additionally adjusted for cardiovascular risk factors (BMI, hypertension, diabetes mellitus, cholesterol level, and smoking status). Additionally, a third Cox regression model controlled for cardiovascular risk factors, the occurrence of coronary artery disease, and brain infarcts was run. In secondary analyses, we examined whether there were regional differences in the brain in relation to the discovered associations with dementia outcome by repeating Model 1 per brain lobe for WMH volumes. In additional secondary analyses to test for WMH volume dependency of the discovered associations with WMH shape markers, Model 1 was repeated for the WMH shape markers additionally corrected for total WMH volume (as a percentage of intracranial volume).

## 5.3.6 Sensitivity analyses

To confirm the robustness of our shape analysis method, all models were repeated with WMH shape markers recalculated by applying a volume-weighted approach, where each lesion shape marker was scaled according to lesion size before calculating an average per participant. To test whether the Cox regression outcome was affected by oversegmentation, 62 participants with partial oversegmentation in addition to multiple correct WMH segmentations were excluded and the analyses were rerun. To test whether the Cox regression outcome was affected by subcortical infarcts, 266 participants with subcortical infarcts were excluded and the analyses were rerun. To test whether non-linear age-related effects in dementia occurrence influenced our results, we repeated the Cox regression models in an age- and sex-matched subset of

our cohort (n = 1338). Lastly, to test the influence of neurodegenerative brain changes on the found associations, we repeated the models while adding hippocampal volume as an atrophy-sensitive variable.

All analyses were performed in SPSS version 25. A p value of <0.05 was considered statistically significant.

## 5.4 RESULTS

Baseline characteristics and cardiovascular risk factors of the study population are shown in Table 1. Of the 3077 participants, at follow-up 705 participants developed dementia (23%) and 2372 (77%) did not. The average age at baseline of participants who developed dementia at follow-up was significantly higher (p <0.001) compared to the age of participants who did not develop dementia at follow-up. Sixty-two percent of female participants were included in the total study population, with no differences between the two study groups. The average time to follow-up was significantly shorter for the dementia group (7.2 ± 2.5, p <0.001) compared to the follow-up time of participants without dementia (10.7 ± 1.9). The average BMI was significantly lower (p <0.001) compared to the BMI of participants without dementia. The percentage of participants who had hypertension or brain infarcts at baseline was significantly higher for the study group who developed dementia. No significant differences were found for diabetes mellitus, smoking status, cholesterol level, or occurrence of coronary artery disease (p >0.05).

### 5.4.1 WMH shape and long-term occurrence of dementia

Examples of WMHs and values of their respective shape markers are shown in Figure 5.2. Mean values (± standard deviation (SD)) for WMH shape markers are shown in Figure 5.3A and Table 5.2. Results of the Cox proportional hazard models for WMH shape markers at baseline are shown in Table 5.2 (see Table S.5.8.2 for area under the curve characteristics). The Cox proportional hazard Model 1 was adjusted for age, sex, and cognitive status at baseline. A more irregular shape of periventricular/confluent WMHs was associated with an increased long-term dementia risk (lower values for solidity (HR 1.34, 95% CI 1.17 to 1.52; p <0.001) and convexity (HR 1.38, 95% CI 1.28 to 1.49; p <0.001) and higher values for concavity index (HR 1.43, 95% CI 1.32 to 1.54; p <0.001) and fractal dimension (HR 1.45, 95% CI 1.32 to 1.58; p <0.001)). Additional adjustments for cardiovascular risk factors, infarcts, and coronary artery disease (Models 2 and 3) did not affect the association of periventricular/confluent WMH shape markers and long-term dementia risk. Therefore, the associations were independent of cardiovascular risk factors, the occurrence of coronary artery disease, or having brain infarcts at baseline.

**Table 5.1.** Baseline characteristics and cardiovascular risk factors of study sample (n = 3077).

| Baseline Characteristics | No dementia at follow-up n = 2372 | Dementia at follow-up n = 705 | P value |
|---|---|---|---|
| Age (years) | 74.7 ± 4.9 (66−93) | 78.7 ± 5.1 (67−94) | <0.001 |
| Time to follow-up (years) | 10.7 ± 1.9 (0.8−13.4) | 7.2 ± 2.5 (0.6−12.2) | <0.001 |
| Female sex | 1451 (61%) | 449 (64%) | 0.227 |
| BMI (kg/m2) | 27.1 ± 4.1 (14.8−47.5) | 26.4 ± 4.3 (13.6−45.0) | <0.001 |
| Hypertension | 1819 (77%) | 578 (82%) | 0.015 |
| Type 2 diabetes | 206 (9%) | 74 (10%) | 0.142 |
| Cholesterol (mmol/L) | 5.7 ± 1.1 (2.3−10.9) | 5.7 ± 1.1 (2.5−9.3) | 0.803 |
| Smoking status | | | |
| Never | 1061 (45%) | 346 (49%) | 0.046 |
| Former | 1058 (45%) | 284 (40%) | 0.048 |
| Current | 253 (11%) | 75 (11%) | 0.999 |
| Coronary artery disease | 169 (7%) | 52 (7%) | 0.821 |
| Infarcts[a] | 485 (20%) | 195 (28%) | <0.001 |
| Education level[b] | 2.2 ± 0.9 | 2.1 ± 0.9 | 0.099 |

Abbreviation: BMI, body mass index.
[a] Subcortical, cortical, and cerebellar infarcts.
[b] 1 = primary school; 2 = secondary school; 3 = college; 4 = university.
Values are given as mean ± SD (interquartile range) or n (%). Independent sample t tests were performed for age, BMI, cholesterol level, and time to follow-up. Pearson's chi-squared tests were executed for sex, education level, smoking status, hypertension, diabetes mellitus, coronary artery disease, and brain infarcts.
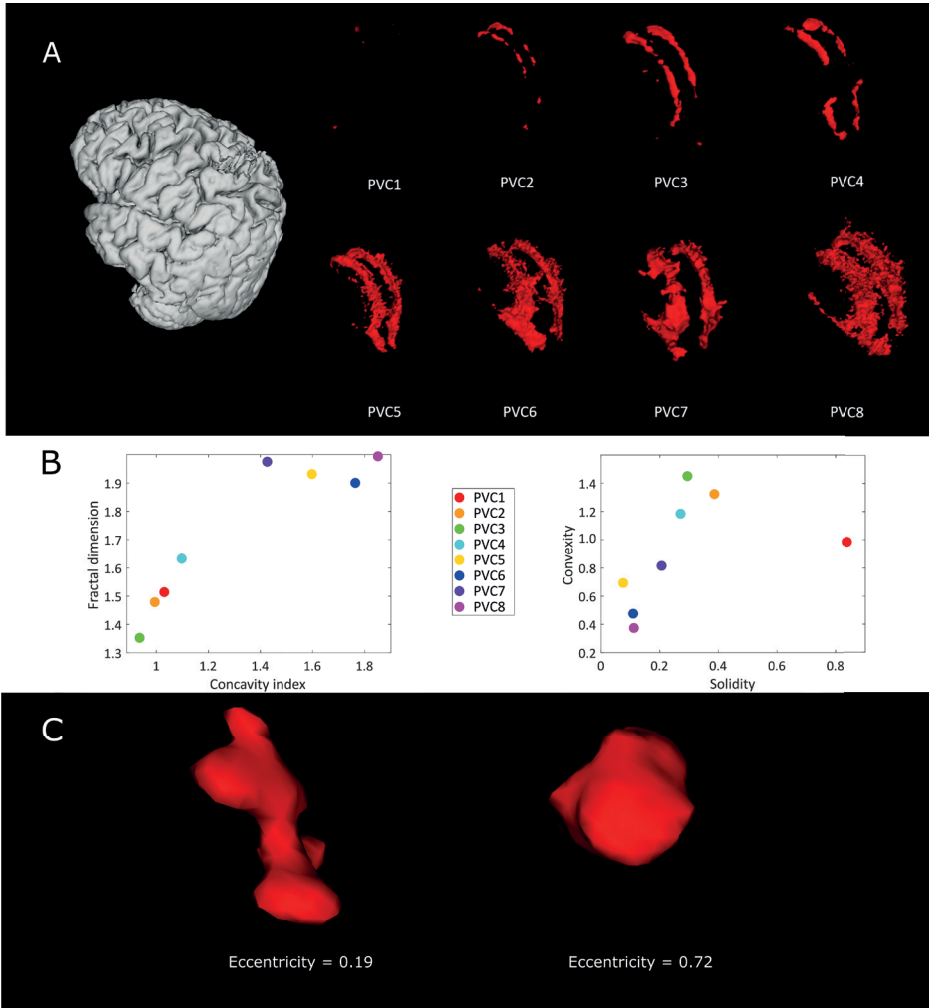
**Figure 5.2.** Examples of periventricular/confluent WMHs (A) and their corresponding WMH shape values in plots (B) to provide more insight into structural correlates of WMH shape marker values. A lower solidity and convexity, as well as a higher fractal dimension and concavity index, indicate a more irregular WMH shape. Examples of deep WMH and their corresponding WMH shape marker eccentricity (C). A lower eccentricity corresponds to a more elongated lesion, while a higher eccentricity corresponds to a more spherical lesion.

A
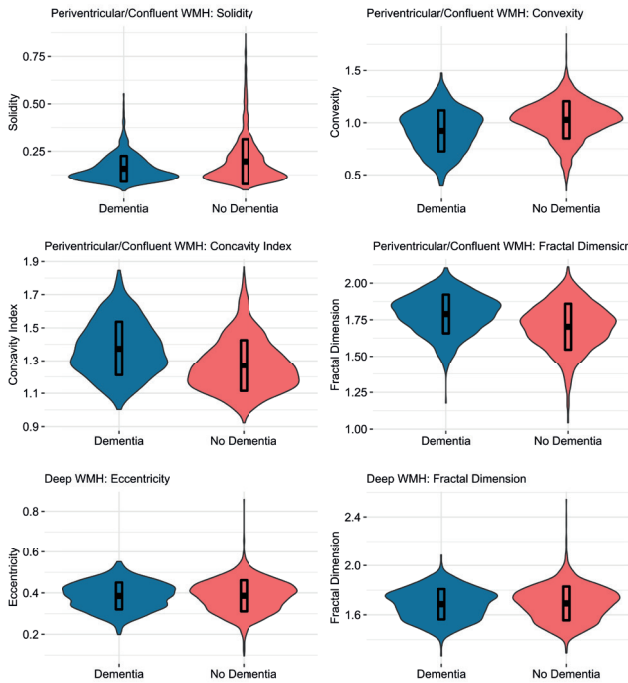


B
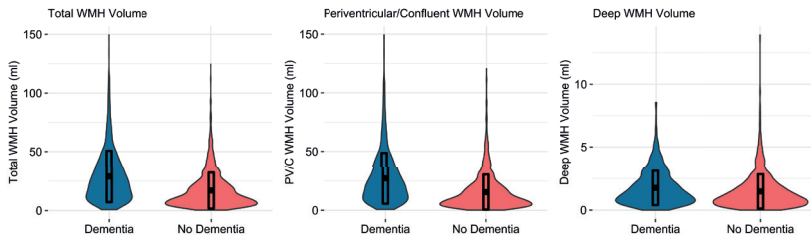


**Figure 5.3** (A) Violin plots including raw means ± SD of shape markers of periventricular/confluent, and deep WMH in group with dementia and group without dementia at follow-up. (B) Violin plots including raw means ± SD of WMH volumes for group with dementia and group without dementia at follow-up. WMH: white matter hyperintensity; SD: standard deviation.

**Table 5.2.** Cox regression models on association between WMH shape, WMH volumes, and long-term dementia risk.

| | No dementia at follow-up (mean ± SD) | Dementia at follow-up (mean ± SD) | Model 1 HR (95% CI) | Model 2 HR (95% CI) | Model 2 HR (95% CI) |
|---|---|---|---|---|---|
| **Periventricular/ confluent WMH** | | | | | |
| Solidity | 0.20 ± 0.12 | 0.16 ± 0.07 | 1.34 (1.17–1.52)*** | 1.32 (1.16–1.51)*** | 1.32 (1.17–1.51)*** |
| Convexity | 1.03 ± 0.18 | 0.92 ± 0.20 | 1.38 (1.28–1.49)*** | 1.39 (1.29–1.50)*** | 1.38 (1.28–1.49)*** |
| Concavity Index | 1.27 ± 0.16 | 1.37 ± 0.16 | 1.43 (1.32–1.54)*** | 1.44 (1.33–1.56)*** | 1.44 (1.33–1.55)*** |
| Fractal Dimension | 1.70 ± 0.16 | 1.79 ± 0.13 | 1.45 (1.32–1.58)*** | 1.45 (1.33–1.59)*** | 1.44 (1.32–1.58)*** |
| **Deep WMH** | | | | | |
| Eccentricity | 0.39 ± 0.08 | 0.39 ± 0.06 | 1.01 (0.93–1.10) | 1.00 (0.92–1.09) | 1.00 (0.92–1.08) |
| Fractal dimension | 1.69 ± 0.14 | 1.69 ± 0.12 | 1.03 (0.95–1.12) | 1.03 (0.95–1.11) | 1.02 (0.94–1.11) |
| **WMH Volume** | | | | | |
| Total WMH Volume | 16.97 ± 15.31 | 28.91 ± 21.80 | 1.68 (1.54–1.87)*** | 1.70 (1.54–1.87)*** | 1.70 (1.54–1.87)*** |
| Periventricular/ confluent WMH Volume | 15.50 ± 14.92 | 27.16 ± 21.55 | 1.71 (1.55–1.89)*** | 1.73 (1.56–1.91)*** | 1.72 (1.56–1.91)*** |
| Deep WMH Volume | 1.48 ± 1.36 | 1.75 ± 1.36 | 1.17 (1.08–1.27)*** | 1.17 (1.08–1.28)*** | 1.71 (1.08–1.28)*** |

A hazard ratio below 1 means that higher values decrease the risk of developing dementia. A hazard ratio above 1 means that higher values increase the risk of developing dementia. Model 1: controlled for age, sex, cognitive status at baseline. Model 2: controlled for age, sex, cognitive status at baseline, BMI, diabetes, hypertension, cholesterol level, smoking status. Model 3: controlled for age, sex, cognitive status at baseline, BMI, diabetes, hypertension, cholesterol level, smoking status, infarcts, coronary artery disease. WMH volumes are additionally controlled for total intracranial volume. HR: hazard ratio; CI: confidence interval; WMH: white matter hyperintensities; BMI: body mass index. ***p<0.001

5

For deep WMH, no significant associations were found for WMH shape markers and long-term dementia risk.

In secondary analysis to test for WMH volume dependency of the found associations of WMH shape and dementia occurrence, we showed that this association was partly WMH volume dependent (the results of the solidity and concavity index of periventricular/confluent WMHs attenuated slightly but remained statistically significant, while the results of the convexity and fractal dimension of periventricular/confluent WMHs showed attenuation and lost statistical significance; Table S.5.8.3).

## 5.4.2 WMH volumes and long-term occurrence of dementia

Mean values (± SD) for WMH volumes are shown in Figure 5.3B and Table 2. Results of the Cox proportional hazard models for WMH volumes at baseline are shown in Table 2. Cox proportional hazard Model 1 was adjusted for age, sex, cognitive status at baseline, and intracranial volume. Higher total WMH volume (HR 1.68, 95% CI 1.54 to 1.87; p <0.001), higher periventricular/confluent WMH volume (HR 1.71, 95% CI 1.55 to 1.89; p <0.001), and higher deep WMH volume (HR 1.17, 95% CI 1.08 to 1.27; p <0.001) were significantly associated with an increased long-term dementia risk. Additional adjustments for cardiovascular risk factors, infarcts, and coronary artery disease (Models 2 and 3) did not affect the association of WMH volumes and long-term dementia risk. This shows that the associations are independent of cardiovascular risk factors, the occurrence of coronary artery disease, or presence of brain infarcts at baseline.

In secondary analyses of deep WMH volume per lobe, we found that frontal and parietal lobe deep WMH volumes were significantly associated with long-term dementia risk (Table S.5.8.4). Higher deep WMH volumes in the occipital lobe were associated with a lower long-term risk for dementia (Table S.5.8.4).

## 5.4.3 Sensitivity analyses

The results of the volume-weighted WMH shape approach (Table S.5.8.5) were comparable to the original analyses, confirming the robustness of our WMH shape analysis method. The associations of WMH markers with long-term dementia risk were not affected by participants with mild/moderate oversegmentation (n = 62) (Table S.5.8.6) or presence of subcortical infarcts/lacunes (n = 266) (Table S.5.8.7) and there was minor but not significant attenuation due to potential non-linear age-related effects in the development of dementia (Table S.5.8.8) and presence of neurodegenerative brain changes (Table S.5.8.9).

## 5.5 DISCUSSION

We showed that a more irregular shape of periventricular/confluent WMHs was associated with an increased long-term dementia risk in community-dwelling older adults. No associations were found between the shape of deep WMHs and long-term dementia risk. Higher total, periventricular/confluent, and deep WMH volume was associated with an increased long-term dementia risk.

This is the first study investigating the association between WMH shape and long-term dementia risk. Previous studies already suggested that WMH shape could facilitate a more detailed characterization of WMHs,[13, 22, 18] as it can help to more accurately quantify the heterogeneity of WMH related to underlying pathological changes. Distinct WMH shape patterns were previously shown to be associated with increased long-term risk of stroke and mortality.[13] Moreover, a more complex WMH shape was related to physical frailty in a previous study[25] and may also indicate a predisposition for postoperative delirium.[26] In the current study, we showed that distinct WMH shape patterns are related to long-term dementia risk. The current findings strengthen the hypothesis that differences in long-term disease outcome can be predicted by MRI-based WMH shape markers.

WMH shape may be a suitable additional marker next to WMH volume to describe WMH changes, as the heterogeneous nature of WMH that has been demonstrated in histopathological studies cannot be fully described by WMH volume alone.[7, 10] Variations in WMH shape patterns are likely to reflect the heterogeneous nature of the pathologies underlying WMHs. As SVD affects the vasculature of the brain, hypoperfusion is a key pathological contributor to white matter damage.[27] Periventricular/confluent WMHs are located centrally in the brain within a deep watershed area that is vulnerable to hypoperfusion, as this area is supplied by long perforating arterial branches.[7] Disruption of the complex structure of the microvascular network surrounding the lateral ventricles may be reflected in distinct WMH shape patterns.

In previous studies where periventricular WMH and deep WMH burden and volume were analyzed in community-dwelling older adults, periventricular WMH volumes and burden were frequently associated with long-term dementia risk and cognitive decline,[28-30] but not with deep WMH.[28-30] In our study, we indeed showed an association between periventricular WMH volume and long-term dementia occurrence, and additionally showed an association with deep WMH volume. Furthermore, as WMH volume increases, periventricular WMHs can merge with deep WMHs to form confluent WMHs. This will result in a relatively lower deep WMH volume and may

5

explain why we found a lower deep WMH volume in the occipital lobe in participants who developed dementia at follow-up.

Based on the current and previous findings,[13, 22, 18] there is evidence that WMH shape has additional diagnostic value compared to WMH volume alone. WMH shape could be used as a non-invasive independent marker next to other markers of SVD for identification of patients at risk for dementia. Identified patients at risk could undergo lifestyle changes in order to limit progression of SVD and cognitive decline.[3, 5] Specific WMH patterns could also aid as surrogate markers for future drug trails aimed at treatment or prevention of SVD.[4]

A strength of the current study is the large sample size based on the general population, which gives the study significant external validity. Moreover, the long follow-up period and the use of automated image processing techniques, in combination with visual quality checks, are other strengths. A limitation of the study could be the use of a 1.5 Tesla MRI scanner, which was a common field strength for clinical scanners at the time of the baseline scans. Even though lower-field-strength scans with a lower resolution could have resulted in a less accurate WMH shape estimation, we reported significant associations with long-term dementia.

In conclusion, we demonstrated that WMH shape is a promising marker in addition to WMH volume in relation to dementia risk. A more irregular shape of periventricular/confluent WMHs and higher WMH volumes were associated with long-term increased dementia risk in community-dwelling older adults. These findings suggest that WMH shape markers may in the future be useful in determining patient prognosis and may aid in patient selection for future preventive treatments.

## 5.6 ACKNOWLEDGMENTS

## 5.7 REFERENCES

1.   Wardlaw JM, Smith C, Dichgans M. Small vessel disease: mechanisms and clinical implications. Lancet Neurol. 2019;18:684-696

2.   van Veluw SJ, Arfanakis K, Schneider JA. Neuropathology of vascular brain health: insights from ex vivo magnetic resonance imaging– histopathology studies in cerebral small vessel disease. Stroke. 2022;53:404-415.

3.   Dichgans M, Zietemann V. Prevention of vascular cognitive impair- ment. Stroke. 2012;43:3137-3146.

4.   Bath PM, Wardlaw JM. Pharmacological treatment and prevention of cerebral small vessel disease: a review of potential interventions. Int J Stroke. 2015;10:469-478.

5.   Mok V, Kim JS. Prevention and management of cerebral small vessel disease. J Stroke. 2015;17:111-122.

6.   Wardlaw JM, Smith EE, Biessels GJ, et al. Neuroimaging standards for research into small vessel disease and its contribution to ageing and neurodegeneration. Lancet Neurol. 2013;12:822-838.

7.   Alber J, Alladi S, Bae H, et al. White matter hyperintensities in vascular contributions to cognitive impairment and dementia (VCID): knowledge gaps and opportunities. Alzheimer's. Dement Transl Res Clin Interv. 2019;5:107-117.

8.   Prins ND, Scheltens P. White matter hyperintensities, cognitive impairment and dementia: an update. Nat Rev Neurol. 2015;11:157- 165.

9.   Mortamais M, Artero S, Ritchie K. Cerebral white matter hyperintensities in the prediction of cognitive decline and incident dementia. Int Rev Psychiatry. 2013;25:686-698.

10.  Gouw AA, Seewann A, Van Der Flier WM, et al. Heterogeneity of small vessel disease: a systematic review of MRI and histopathology correlations. J Neurol Neurosurg Psychiatry. 2011;82:126-135.

11.  Kim KW, MacFall JR, Payne ME. Classification of white matter lesions on magnetic resonance imaging in elderly persons. Biol Psychiatry. 2008;64:273-280.

12.  Fazekas F, Kleinert R, Offenbacher H, et al. Pathologic correlates of incidental MRI white matter signal hyperintensities. Neurology. 1993;43:1683-1689.

13.  Ghaznawi R, Geerlings MI, Jaarsma-Coes M, Hendrikse J, de BresserJ. Group on behalf of the U-SS. Association of white matter hyperintensity markers on MRI and long-term risk of mortality and ischemic stroke. Neurology. 2021;96:e2172-e2183.

14.  Harris TB, Launer LJ, Eiriksdottir G, et al. Age, gene/environment susceptibility-reykjavik study: multidisciplinary applied phenomics. Am J Epidemiol. 2007;165:1076-1087.

15.  Saczynski JS, Sigurdsson S, Jonsdottir MK, et al. Cerebral infarcts and cognitive performance: importance of location and number of infarcts. Stroke. 2009;40:677-682.

16.  Morris JN, Hawes C, Fries BE, et al. Designing the National Res- ident Assessment Instrument for Nursing Homes. Gerontologist. 1990;30:293-307.

17.  Sveinbjornsdottir S, Sigurdsson S, Aspelund T, et al. Cerebral microbleeds in the population based AGES-Reykjavik study: prevalence and location. J Neurol Neurosurg Psychiatry. 2008;79:1002-1006.

18.  Ghaznawi R, Geerlings MI, Jaarsma-Coes MG, et al. The association between lacunes and white matter hyperintensity features on MRI: the SMART-MR study. J Cereb Blood Flow Metab. 2019;39:2486-2496.

19.  Klein S, Staring M, Murphy K, Viergever MA, Pluim JPW. Elastix: a toolbox for intensity-based medical image registration. IEEE TransMed Imaging. 2010;29:196-205.

20.  Schmidt P. Bayesian Inference for Structured Additive Regression Models for Large-Scale Problems with Applications to Medical Imaging. Maximilians-Universität München; 2017.

5

21. Kempton MJ, Underwood TSA, Brunton S, et al. Acomprehensive testing protocol for MRI neuroanatomical segmentation techniques: evaluation of a novel lateral ventricle segmentation method. Neuroimage. 2011;58:1051-1059.

22. De Bresser J, Kuijf HJ, Zaanen K, et al. White matter hyperintensity shape and location feature analysis on brain MRI; proof of principle study in patients with diabetes. Sci Rep. 2018;8:1-10.

23. Sigurdsson S, Aspelund T, Forsberg L, et al. Brain tissue volumes in the general population of the elderly The AGES-Reykjavik Study. Neuroimage. 2012;59:3862-3870.

24. Zijdenbos AP, Forghani R, Evans AC. Automatic "pipeline" analysis of 3-D MRI data for clinical trials: application to multiple sclerosis. IEEE Trans Med Imaging. 2002;21:1280-1291.

25. Kant IMJ, Mutsaerts HJMM, van Montfort SJT, et al. The association between frailty and MRI features of cerebral small vessel disease. Sci Rep. 2019;9:1-9.

26. Kant IMJ, de Bresser J, van Montfort SJT, et al. Preoperative brain MRI features and occurrence of postoperative delirium. J Psychosom Res. 2021;140:110301.

27. Love S, Miners JS. White matter hypoperfusion and damage in dementia: post-mortem assessment. Brain Pathol. 2015;25:99-107.

28. Godin O, Tzourio C, Rouaud O, et al. Joint effect of white matter lesions and hippocampal volumes on severity of cognitive decline: the 3C-Dijon MRI Study. J Alzheimer's Dis. 2010;20:453- 463.

29. Silbert LC, Howieson DB, Dodge H, Kaye JA. Cognitive impairment risk white matter hyperintensity progression matters. Neurology. 2009;73:120-125.

30. Prins ND, Van Dijk EJ, Den Heijer T, et al. Cerebral small-vessel dis- ease and decline in information processing speed, executive function and memory. Brain. 2005;128:2034-2041.

# 5.8 SUPPLEMENTARY MATERIAL

**S.5.8.1.** Definition of the WMH shape markers.

| WMH type | Shape marker | Description | Formula |
|---|---|---|---|
| Periventricular/ Confluent WMH | Convexity (C) | Convexity and Solidity show how concave or convex a shape is. A maximally convex shape has a convexity and solidity value of 1. Values decrease with a more concave, complex shape. | $C = \dfrac{\text{Convex Hull Area}}{\text{Area}}$ |
| Periventricular/ Confluent WMH | Solidity (S) | | $S = \dfrac{\text{Volume}}{\text{Convex Hull Volume}}$ |
| Periventricular/ Confluent WMH | Concavity Index (CI) | Concavity index—a measure of roughness—describes how dense, irregular or elongated and curved a lesion is. Higher CI values indicate a more complex WMH shape. | $CI = \sqrt{(2-C)^2 + (1-S)^2}$ |
| Periventricular/ Confluent WMH Deep WMH | Fractal Dimension (FD) | The Minkowski-Bouligand dimension (box counting dimension) is a measure of textural roughness. Higher FD values suggest a more complex WMH shape. | $FD = \lim\limits_{r \to 1} \dfrac{\log(n_r)}{\log\left(\frac{1}{r}\right)}$  <br><br> n = number of boxes <br> r = box size |
| Deep WMH | Eccentricity (E) | Eccentricity describes the deviation from a circle. The eccentricity of a circle is 1 and the eccentricity of a line is 0. | $E = \dfrac{\text{Minor Axis}}{\text{Major Axis}}$ <br><br> Major axis: largest diameter in 3D space. <br> Minor axis: smallest diameter orthogonal to the major axis. |

5
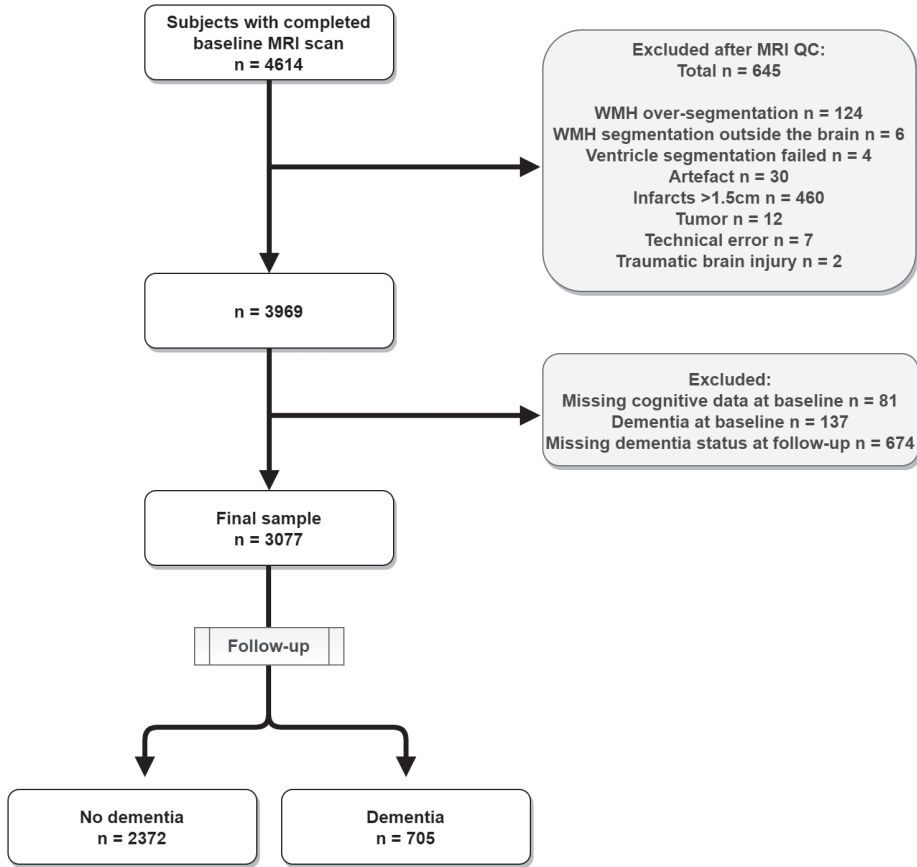
**Figure S.5.8.1. Exclusion scheme of this study.** QC: quality control.

**S.5.8.2.** Area under the curve based on ROC curves per WMH marker. The WMH markers were used as a test variable and dementia occurrence as a state variable.

| | Area under the curve (95% CI) |
|---|---|
| **Periventricular/confluent WMH shape** | |
| Solidity | 0.58 (0.56−0.60) |
| Convexity | 0.66 (0.63−0.68) |
| Concavity Index | 0.68 (0.66−0.70) |
| Fractal dimension | 0.67 (0.64−0.69) |
| **Deep WMH shape** | |
| Eccentricity | 0.51 (0.48−0.53) |
| Fractal dimension | 0.49 (0.47−0.51) |
| **WMH Volumes** | |
| Total WMH volume | 0.70 (0.67−0.72) |
| Periventricular/confluent WMH volume | 0.70 (0.68−0.72) |
| Deep WMH volume | 0.57 (0.55−0.60) |

5

**S.5.8.3.** Secondary analyses in which model 1 was additionally adjusted for total WMH volume.

| | Model 1<br>HR (95% CI) |
|---|---|
| **Periventricular/confluent WMH shape** | |
| Solidity | 1.28 (1.12−1.47)*** |
| Convexity | 1.08 (0.96−1.20) |
| Concavity Index | 1.16 (1.04−1.29)** |
| Fractal Dimension | 1.11 (0.98−1.26) |
| **Deep WMH shape** | |
| Eccentricity | 1.05 (0.97−1.15) |
| Fractal dimension | 1.00 (0.92−1.08) |

A hazard ratio below 1 means that higher values decrease the risk of developing dementia. A hazard ratio above 1 means that higher values increase the risk of developing dementia. Model 1: controlled for age, sex, cognitive status at baseline, and total WMH volume (as percentage of intracranial volume). **p=0.01 ***p<0.001.

**S.5.8.4.** Secondary analyses of WMH volumes per lobe and long-term dementia risk.

| | | No dementia at follow-up (mean ± SD) | Dementia at follow-up (mean ± SD) | Model 1 HR (95% CI) |
|---|---|---|---|---|
| **Frontal lobe** | | | | |
| | Deep volume (ml) | 0.87 ± 1.03 | 1.13 ± 1.02 | 1.25 (1.14−1.36)*** |
| | PV/C volume (ml) | 5.11 ± 6.73 | 10.27 ± 11.01 | 1.58 (1.45−1.73)*** |
| **Parietal lobe** | | | | |
| | Deep volume (ml) | 0.22 ± 0.30 | 0.29 ± 0.32 | 1.21 (1.12−1.31)*** |
| | PV/C volume (ml) | 3.22 ± 4.26 | 6.23 ± 6.36 | 1.56 (1.41−1.73)*** |
| **Occipital lobe** | | | | |
| | Deep volume (ml) | 0.26 ± 0.39 | 0.16 ± 0.33 | 0.90 (0.83−0.98)* |
| | PV/C volume (ml) | 1.87 ± 1.75 | 3.04 ± 2.23 | 1.73 (1.51−1.98)*** |
| **Temporal lobe** | | | | |
| | Deep volume (ml) | 0.05 ± 0.09 | 0.07 ± 0.13 | 1.03 (0.96−1.11) |
| | PV/C volume (ml) | 2.72 ± 2.29 | 4.09 ± 2.80 | 1.51 (1.36−1.68)*** |

A hazard ratio below 1 means that higher values decrease the risk of developing dementia. A hazard ratio above 1 means that higher values increase the risk of developing dementia. As WMH volumes increase, confluent WMH can merge with deep WMH. This will in turn lower the deep WMH volumes and may explain why lower deep WMH volumes were found in the occipital lobe in participants who developed dementia at follow-up. Model 1: controlled for age, sex, cognitive status at baseline and intracranial volume. * p<0.05; ** p<0.01; ***p<0.001.

**S.5.8.5.** Sensitivity analyses in which the primary analyses were performed with volume-weighted WMH shape marker estimation.

| | No dementia at follow-up (mean ± SD) | Dementia at follow-up (mean ± SD) | Model 1 HR (95% CI) | Model 2 HR (95% CI) | Model 3 HR (95% CI) |
|---|---|---|---|---|---|
| **Periventricular/confluent WMH shape** | | | | | |
| Solidity | 0.23 ± 0.13 | 0.18 ± 0.08 | 1.44 (1.26–1.63)*** | 1.42 (1.25–1.62)*** | 1.43 (1.25–1.62)*** |
| Convexity | 1.02 ± 0.18 | 0.92 ± 0.20 | 1.38 (1.28–1.49)*** | 1.39 (1.29–1.50)*** | 1.38 (1.28–1.50)*** |
| Concavity Index | 1.26 ± 0.16 | 1.37 ± 0.17 | 1.44 (1.34–1.56)*** | 1.45 (1.34–1.57)*** | 1.45 (1.34–1.57)*** |
| Fractal Dimension | 1.67 ± 0.12 | 1.74 ± 0.12 | 1.34 (1.24–1.45)*** | 1.34 (1.24–1.45)*** | 1.33 (1.23–1.44)*** |
| **Deep WMH shape** | | | | | |
| Eccentricity | 0.35 ± 0.10 | 0.36 ± 0.08 | 0.95 (0.88–1.03) | 0.96 (0.88–1.03) | 0.96 (0.89–1.04) |
| Fractal dimension | 1.76 ± 0.13 | 1.76 ± 0.12 | 1.02 (0.94–1.10) | 1.01 (0.94–1.10) | 1.01 (0.93–1.09) |
| **WMH Volume** | | | | | |
| Total WMH Volume | 16.95 ± 15.31 | 28.89 ± 21.80 | 1.68 (1.53–1.85)*** | 1.70 (1.54–1.87)*** | 1.70 (1.54–1.87)*** |
| Periventricular/confluent WMH Volume | 15.47 ± 14.92 | 27.13 ± 21.55 | 1.71 (1.55–1.89)*** | 1.73 (1.56–1.91)*** | 1.72 (1.56–1.91)*** |
| Deep WMH Volume | 1.48 ± 1.36 | 1.75 ± 1.36 | 1.16 (1.07–1.26)*** | 1.17 (1.07–1.27)*** | 1.16 (1.07–1.27)*** |

To control for (small) lesion volume, the WMH shape markers were weighted based on their individual volumes. Shape parameters were calculated for each individual lesion and then multiplied with their volume percentage of the total lesion volume per type. The sum of the volume-weighted shape parameters was used in the cox regression models. A hazard ratio below 1 means that higher values decrease the risk of developing dementia. A hazard ratio above 1 means that higher values increase the risk of developing dementia. Model 1: controlled for age, sex, cognitive status at baseline. Model 2: controlled for age, sex, cognitive status at baseline, BMI, diabetes, hypertension, cholesterol level, smoking status. Model 3: controlled for age, sex, cognitive status at baseline, BMI, diabetes, hypertension, cholesterol level, smoking status, infarcts, coronary artery disease. WMH volumes are additionally controlled for intracranial volume. HR: hazard ratio; CI: confidence interval; WMH: white matter hyperintensities; BMI: body mass index. ***p<0.001

5

**S.5.8.6.** Sensitivity analyses excluding over-segmentation. Mean ± SD of WMH shape markers and WMH volumes including the model 1 cox regression.

| | No dementia at follow-up (mean ± SD) n=2330 | Dementia at follow-up (mean ± SD) n=685 | Hazard ratio (95% CI) |
|---|---|---|---|
| **Periventricular/confluent WMH shape** | | | |
| Solidity | 0.20 ± 0.12 | 0.16 ± 0.07 | 1.32 (1.16–1.51) *** |
| Convexity | 1.03 ± 0.17 | 0.93 ± 0.19 | 1.38 (1.28–1.50) *** |
| Concavity Index | 1.27 ± 0.15 | 1.37 ± 0.16 | 1.44 (1.33–1.56) *** |
| Fractal dimension | 1.70 ± 0.16 | 1.79 ± 0.31 | 1.43 (1.31–1.57) *** |
| **Deep WMH shape** | | | |
| Eccentricity | 0.39 ± 0.08 | 0.39 ± 0.06 | 0.98 (0.90–1.06) |
| Fractal dimension | 1.70 ± 0.14 | 1.69 ± 0.12 | 1.04 (0.96–1.13) |
| **WMH Volumes** | | | |
| Total WMH volume | 16.64 ± 14.96 | 28.38 ± 21.45 | 1.69 (1.53–1.86) *** |
| Periventricular/confluent WMH volume | 15.18 ± 14.60 | 26.66 ± 21.23 | 1.72 (1.55–1.90) *** |
| Deep WMH volume | 1.46 ± 1.35 | 1.71 ± 1.32 | 1.16 (1.07–1.26) ** |

The cox-regression results were not affected by participants with mild/moderate over-segmentation (n=62). In order to test this the participants with mild/moderate over-segmentation were excluded and model 1 (adjusted for age, sex, and cognitive status at baseline) was run on the remaining participants. WMH volumes were additionally controlled for intracranial volume. A hazard ratio below 1 means that higher values decrease the risk of developing dementia. A hazard ratio above 1 means that higher values increase the risk of developing dementia. $**p<0.01$ $***p<0.001$

**S.5.8.7.** Sensitivity analyses excluding participants with subcortical infarcts/lacunes. Mean ± SD of WMH shape markers and WMH volumes including the model 1 cox regression.

| | No dementia at follow-up (mean ± SD) n=2186 | Dementia at follow-up (mean ± SD) n=625 | Hazard ratio (95% CI) |
|---|---|---|---|
| **Periventricular/ Confluent WMH shape** | | | |
| Solidity | 0.20 ± 0.12 | 0.16 ± 0.07 | 1.34 (1.17−1.53) *** |
| Convexity | 1.04 ± 0.17 | 0.94 ± 0.19 | 1.40 (1.30−1.53) *** |
| Concavity Index | 1.26 ± 0.15 | 1.36 ± 0.16 | 1.46 (1.34−1.58) *** |
| Fractal dimension | 1.70 ± 0.16 | 1.78 ± 0.13 | 1.42 (1.29−1.56) *** |
| **Deep WMH shape** | | | |
| Eccentricity | 0.39 ± 0.08 | 0.38 ± 0.07 | 1.00 (0.92−1.09) |
| Fractal dimension | 1.69 ± 0.14 | 1.69 ± 0.12 | 1.01 (0.93−1.10) |
| **WMH volumes** | | | |
| Total WMH volume | 16.14 ± 14.54 | 26.62 ± 19.46 | 1.66 (1.49−1.84) *** |
| Periventricular/confluent WMH volume | 14.69 ± 14.15 | 24.88 ± 19.14 | 1.68 (1.51−1.87) *** |
| Deep WMH volume | 1.46 ± 1.35 | 1.74 ± 1.36 | 1.18 (1.08−1.28) *** |

The cox-regression results were not affected by participants with subcortical infarcts/lacunes. 266 participants with subcortical infarcts/lacunes were excluded and model 1 (adjusted for age, sex, and cognitive status at baseline) was performed on the remaining participants. WMH volumes were additionally controlled for intracranial volume. A hazard ratio below 1 means that higher values decrease the risk of developing dementia. A hazard ratio above 1 means that higher values increase the risk of developing dementia. ***p<0.001

5

**S.5.8.8.** Sensitivity analyses in which the primary analyses were rerun on an age and sex matched subset (n=1338).

| | No dementia at follow-up (mean ± SD) | Dementia at follow-up (mean ± SD) | Model 1 HR (95% CI) | Model 2 HR (95% CI) | Model 3 HR (95% CI) |
|---|---|---|---|---|---|
| **Periventricular/confluent WMH shape** | | | | | |
| Solidity | 0.17 ± 0.10 | 0.16 ± 0.07 | 1.24 (1.08–1.41)** | 1.22 (1.07–1.40)** | 1.23 (1.07–1.40)** |
| Convexity | 0.99 ± 0.19 | 0.93 ± 0.20 | (1.20–1.40)*** | 1.29(1.20–1.40)*** | 1.29 (1.19–1.40)*** |
| Concavity Index | 1.32 ± 0.16 | 1.37 ± 0.16 | 1.33 (1.23–1.44)*** | 1.33 (1.23–1.44)*** | 1.33 (1.23–1.44)*** |
| Fractal Dimension | 1.74 ± 0.15 | 1.79 ± 0.13 | 1.33 (1.22–1.46)*** | 1.33 (1.22–1.46)*** | 1.33 (1.21–1.45)*** |
| **Deep WMH shape** | | | | | |
| Eccentricity | 0.39 ± 0.07 | 0.39 ± 0.06 | 1.00 (0.92–1.08) | 1.01 (0.93–1.09) | 1.01 (0.93–1.09) |
| Fractal dimension | 1.67 ± 0.13 | 1.69 ± 0.12 | 1.03 (0.94–1.12) | 1.02 (0.94–1.11) | 1.02 (0.93–1.11) |
| **WMH volumes** | | | | | |
| Total WMH volume | 21.13 ± 17.73 | 28.46 ± 21.63 | 1.49 (1.36–1.64)*** | 1.51 (1.37–1.66)*** | 1.51 (1.36–1.66)*** |
| Periventricular/confluent WMH volume | 19.60 ± 17.49 | 26.73 ± 21.37 | 1.52 (1.37–1.67)*** | 1.53 (1.38–1.69)*** | 1.53 (1.38–1.69)*** |
| Deep WMH volume | 1.53 ± 1.26 | 1.73 ± 1.35 | 1.10 (1.02–1.19)* | 1.10 (1.02–1.19)* | 1.10 (1.02–1.19)* |

Age and sex matching was performed using case-control matching in SPSS, in order to test for a potential non-linear effect of age on dementia occurrence. A hazard ratio below 1 means that higher values decrease the risk of developing dementia. A hazard ratio above 1 means that higher values increase the risk of developing dementia. Model 1: controlled for age, sex, cognitive status at baseline. Model 2: controlled for age, sex, cognitive status at baseline, BMI, diabetes, hypertension, cholesterol level, smoking status. Model 3: controlled for age, sex, cognitive status at baseline, BMI, diabetes, hypertension, cholesterol level, smoking status, infarcts, coronary artery disease. Analyses in WMH volumes are additionally controlled for total intracranial volume. HR: hazard ratio; CI: confidence interval; WMH: white matter hyperintensities; BMI: body mass index. *p<0.05 **p<0.01 ***p<0.001.

**S.5.8.9.** Sensitivity analyses to test the influence of neurodegenerative brain changes on model 1.

| | Model 1<br>HR (95% CI) |
|---|---|
| **Periventricular/confluent WMH shape** | |
| Solidity | 1.38 (1.21–1.57*** |
| Convexity | (1.25–1.46)*** |
| Concavity Index | 1.41 (1.31–1.52)*** |
| Fractal Dimension | 1.41 (1.29–1.54)*** |
| **Deep WMH shape** | |
| Eccentricity | 0.98 (0.90–1.06) |
| Fractal dimension | 1.04 (0.96–1.13) |
| **WMH volumes** | |
| Total WMH volume | 1.60 (1.45–1.76)*** |
| Periventricular/confluent WMH volume | 1.63 (1.47–1.80)*** |
| Deep WMH volume | 1.14 (1.00–1.24)** |

These additional analyses were performed to test the influence of neurodegenerative brain changes on the found associations. For WMH shape a hazard ratio below 1 means that higher values decrease the risk of developing dementia. A hazard ratio above 1 means that higher values increase the risk of developing dementia. Model 1: controlled for age, sex, cognitive status at baseline, and hippocampal volumes (ml). For WMH volumes the analyses were additionally controlled for intracranial volume. **p<0.01 ***p<0.001

5

CHAPTER

6

# IDENTIFICATION OF DISTINCT BRAIN MRI PHENOTYPES AND THEIR ASSOCIATION WITH LONG-TERM DEMENTIA RISK IN COMMUNITY-DWELLING OLDER ADULTS

Jasmin Annica Keller, Sigurdur Sigurdsson, Barbara Schmitz Abecassis, Ilse M.J. Kant, Mark A. Van Buchem, Lenore J. Launer, Matthias Van Osch, Vilmundur Gudnason, Jeroen De Bresser.

# 6.1 ABSTRACT

Individual brain MRI markers only show at best a modest association with long-term occurrence of dementia. Therefore, it is challenging to accurately identify individuals at increased risk for dementia. We aimed to identify different brain MRI phenotypes by hierarchical clustering analysis based on combined neurovascular and neurodegenerative brain MRI markers and to determine the long-term dementia risk within the brain MRI phenotype subgroups.

Hierarchical clustering analysis based on 32 combined neurovascular and neurodegenerative brain MRI markers in community-dwelling individuals of the Age-Gene/Environment Susceptibility Reykjavik Study was applied to identify brain MRI phenotypes. A Cox proportional hazards regression model was used to determine the long-term risk for dementia per subgroup.

We included 3056 participants and identified 15 subgroups with distinct brain MRI phenotypes. The phenotypes ranged from limited burden, mostly irregular white matter hyperintensity (WMH) shape and cerebral atrophy, mostly irregularly WMHs and microbleeds, mostly cortical infarcts and atrophy, mostly irregularly shaped WMH and cerebral atrophy to multi-burden subgroups. Each subgroup showed different long-term risks for dementia (min−max range hazard ratios (HRs) 1.01−6.18; mean time to follow-up 9.9 ± 2.6 years); especially the brain MRI phenotype with mainly WMHs and atrophy showed a large increased risk (HR 6.18, 95% CI 3.37−11.32).

Distinct brain MRI phenotypes can be identified in community-dwelling older adults. Our results indicate that distinct brain MRI phenotypes are related to varying long-term risks of developing dementia. Brain MRI phenotypes may in the future assist in an improved understanding of the structural correlates of dementia predisposition.

## 6.2 INTRODUCTION

Most older adults have brain changes on MRI, such as cerebral atrophy or manifestations of cerebral small vessel disease (SVD).[1] These brain MRI markers mostly represent late resulting damage of different underlying pathologies and are therefore largely unspecific. This makes differentiation of underlying pathology based on brain MRI challenging.[1] Moreover, some brain abnormalities detected on MRI are regarded as related to normal ageing. It is currently unknown if specific brain MRI phenotypes represent an increased risk for dementia. The ability to determine an individual's risk for dementia based on MRI may in the future be useful to determine patient prognosis and may aid in patient selection for future treatment studies. Common brain MRI markers of neurovascular and neurodegenerative diseases are white matter hyperintensities (WMHs), lacunes, microbleeds, enlarged perivascular spaces, and cerebral atrophy. These brain MRI markers have been studied previously and are associated with the occurrence of dementia.[2-6] However, individual brain MRI markers only show at best a modest association with long-term occurrence of dementia.[4] It, therefore, remains challenging to identify individuals who are at increased risk to develop dementia.[2] Because of heterogenous etiology and mixed pathologies, methods combining different brain MRI markers into one model may likely aid in a more detailed characterization of, potential prognostically relevant, so-called brain MRI phenotypes. In a previous study within our group (in a different cohort), we aimed to detect an increased stroke and mortality risk in patients with manifest arterial disease and analyzed brain MRI markers in a combined way using a hierarchical clustering approach, resulting in the identification of different brain MRI phenotypes.[7] In that study, distinct brain MRI phenotypes were detected that were associated with a different risk of future stroke and mortality. These brain MRI phenotypes can aid to identify the structural correlates of predisposition to different disease outcome. The association of distinct brain MRI phenotypes with long-term dementia risk remains unknown. We therefore aimed to identify different brain MRI phenotypes in community-dwelling individuals by combined hierarchical clustering analysis based on neurovascular and neurodegenerative brain MRI markers. Within each of these brain MRI phenotype subgroups, we determined the long-term dementia risk.

## 6.3 METHODS

### 6.3.1 Participants and study design

The data set used for the current analysis was acquired as part of the population based Age-Gene/Environment Susceptibility (AGES) Reykjavik Study.[8] The cohort study was originally established in 1967 to prospectively study cardiovascular disease

in a random sample from the general population in Iceland. Participants were born between 1907 and 1935 and were living in Reykjavik in 1967. Remaining participants of the cohort were randomly selected for a follow-up and underwent a baseline brain MRI scan between 2002 and 2006.

Baseline diagnosis of dementia was assessed in a 3-step process, as described previously.[9] In short, participants underwent the Mini-Mental State Examination and the Digit Symbol Substitution Test. Participants were administered a second battery of diagnostic tests based on positive results in the previous tests and possibly a third stage, which included neurologic tests and a proxy interview.[9] Based on these tests, participants were considered to have normal cognition, mild cognitive impairment, or dementia at baseline. Dementia diagnosis based on the Diagnostic and Statistical Manual, Fourth Edition, guidelines was made in a consensus meeting with a geriatrician, neurologist, neuropsychologist, and neuroradiologist.

Education level and smoking status were collected using questionnaires. The highest completed education level (primary school, secondary school, college, and university) was entered. Participants who never smoked were categorized as non-smokers, participants who smoked regularly and at least 100 cigarettes or 20 cigars in a lifetime were categorized as former smokers, and participants who currently smoke were categorized as current smokers. Height (in centimeters) and weight (in kilograms) were measured and used to calculate body mass index. Hypertension was based on self-report, use of antihypertensive medication, or based on the measurements of systolic blood pressure >140 mm Hg and/or diastolic blood pressure >90 mm Hg. A standard mercury sphygmomanometer was used to measure systolic and diastolic blood pressure; the mean of 2 measurements was calculated. Diabetes mellitus was based on self-report of diabetes, use of antidiabetic medication, or fasting blood glucose level >7.0 mmol/L. Coronary artery disease was based on self-report plus the use of nitrates or evidence of a myocardial infarction on electrocardiogram.

Participants were followed from the date of the baseline MRI scan until diagnosis of dementia, loss to follow-up, or end of follow-up. Loss to follow-up means that the participants died or could not be contacted. Tracking for dementia diagnosis was done through vital statistics and hospital records and by the nursing home and home-based resident assessment instrument. The dementia follow-up of the AGES Reykjavik Study was concluded in 2015 (end of follow-up). The inclusion and exclusion of participants from the AGES Reykjavik Study for the current study is illustrated in Figure 6.1. For example, participants who were demented at baseline were excluded.
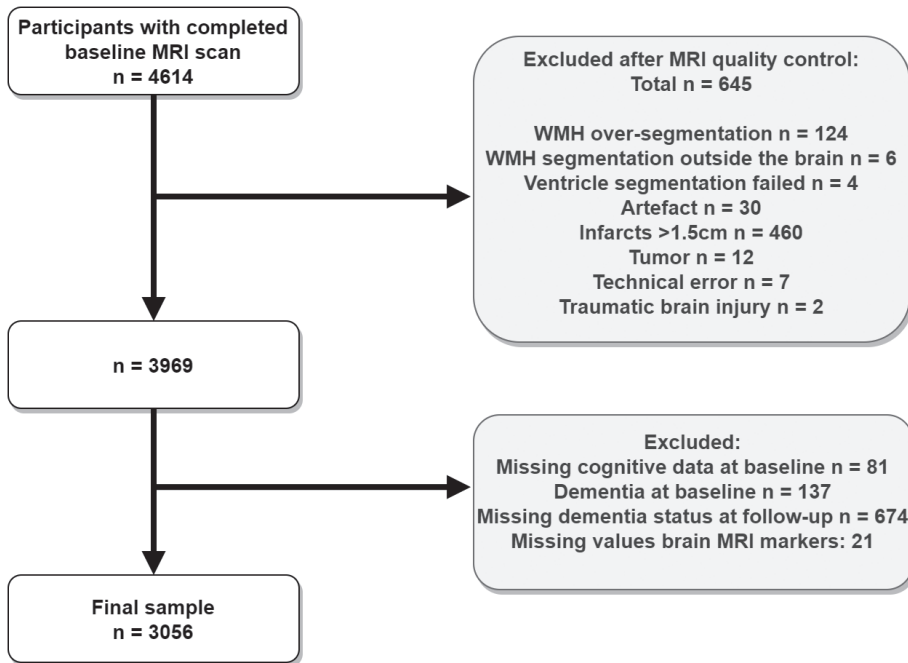
**Figure 6.1 Flowchart Illustrating the Inclusion and Exclusion of Participants.**

## 6.3.2 Standard protocol approvals, registrations, and patient consents

The study was approved by the Icelandic National Bioethics Committee, VSN:00-063, and the institutional review board responsible for the National Institute on Aging research; all participants signed for informed consent.

## 6.3.3 MRI Scanning protocol

A baseline brain MRI scan was acquired on a 1.5 T Signa TwinSpeed system (General Electric Medical Systems, Waukesha, WI). The MRI protocol included a fluid-attenuated inversion recovery (FLAIR) sequence (repetition time = 8000 milliseconds; time to echo = 100 milliseconds; inversion time = 2000 milliseconds; field of view = 220 mm; voxel size = $0.86 \times 0.86 \times 3.00$ mm$^3$; interleaved slices) and a T1-weighted sequence (repetition time = 21 milliseconds; time to echo = 8 milliseconds; field of view = 240 mm; slice thickness = 1.5 mm; voxel size = $0.94 \times 0.94 \times 1.50$ mm$^3$).[11] A T2*-weighted gradient echo-type echo planar sequence (time to echo = 50 milliseconds; repetition time = 3050 milliseconds; flip angle = 90°; field of view = 220 mm; matrix = 256 × 256) and a proton density/T2-weighted fast-spin echo sequence (time to first echo = 22 milliseconds; time to second echo = 90 milliseconds; repetition time = 3220 milliseconds; echo train length = 8; flip angle = 90°; field of view = 220 mm; matrix = 256 × 256) were also part of the MRI protocol.

## 6.3.4 Brain MRI markers

The brain MRI markers included to determine the brain MRI phenotypes were brain tissue volumes for the estimation of brain atrophy, WMH volumes, WMH shape markers, brain infarcts, microbleeds, and enlarged perivascular spaces. Gray matter, white matter, CSF, and WMH were segmented automatically with a modified algorithm based on the Montreal Neurological Institute pipeline.[12] Intracranial volume was calculated by adding gray matter, white matter, CSF, and WMH volumes.[13] Brain parenchymal fraction, white matter fraction, gray matter fraction, and lateral ventricle fraction were calculated by expressing the volumes as a fraction of intracranial volume.

Volumes of periventricular/confluent, deep, and total WMH were determined automatically using an in-house developed pipeline.[14] Moreover, volumes of deep and periventricular WMH per lobe were calculated using a mask to delineate the lobes. WMH shape markers (fractal dimension, solidity, convexity, concavity index, and eccentricity[15]) were calculated, as previously described.[14] A description of the shape markers, as well as their corresponding formulas, can be found in supplementary table S.6.8.1. and supplementary figure S.6.8.1. links.lww.com/WNL/D459). Brain infarcts (subcortical, cerebellar, and cortical infarcts), microbleeds, and enlarged perivascular spaces were visually scored.[9] Microbleeds were first scored by neuroradiologists and then by trained radiographers.[11] Infarcts were defined as parenchymal defects with a signal intensity that is isointense to that of CSF on all MRI sequences (i.e., FLAIR, T2-weighted, proton density-weighted).[9] Cortical infarcts were defined as infarcts involving or limited to the cortical gray matter and surrounded by a high signal intensity area on FLAIR images. Subcortical infarcts were categorized as such when they do not extend into the cortex and are surrounded by a high signal intensity area on FLAIR images of ≥4 mm in diameter.

Parenchymal defects in the subcortical area without a rim or area of high signal intensity on FLAIR images and without evidence of hemosiderin on the T2*-weighted scan were scored as enlarged perivascular spaces. Enlarged perivascular spaces were excluded from the definition of subcortical infarcts. Enlarged perivascular spaces were documented separately in the whole brain and in the basal ganglia. Cerebellar infarcts were scored without any size criteria. Infarcts covering 2 of the mentioned areas were attributed to the location in which the largest measured diameter was located (in millimeters).[9]

## 6.3.5 Statistical analysis

### 6.3.5.1 Identification of subgroups with different brain MRI phenotypes

All brain MRI markers were normalized as z-scores (after multiplication by 100 and natural log transformation when not normally distributed). Variables that were not normally distributed were WMH volumes, solidity, number of WMH, and lateral ventricle volume fraction. Binary variables (presence of microbleeds, infarcts, and enlarged perivascular spaces) were used as −2 and 2 to approximate the z-score distributions of continuous variables. Hierarchical clustering was performed by applying Ward's method in R version 4.1.0 (R Core Team, 2021) and packages factoextra,[16] cluster,[17] and dendextend[18] on 32 brain MRI markers. Hierarchical clustering groups participants together based on similarities in brain MRI markers. The approach starts with every participant as a separate cluster and then repeatedly merging of the 2 closest clusters, subsequently updating the distance matrix. Thus, each cluster is the result of the merge of 2 subclusters, resulting in a hierarchical tree (dendrogram, Figure 6.2). At each level of the dendrogram, clusters are joined and the number of clusters therefore decreases. This is repeated until only 1 cluster, representing the total group of participants, remains. An optimal number of clusters need to be determined for further analysis. In an optimally clustered data set, the clusters have a high within-cluster cohesion, while having a high separation between different clusters. The optimal dendrogram cutoff, that is, the optimal number of clusters, was determined using the Dunn index (supplementary figure S.6.8.2., links. lww.com/WNL/D459) and the heatmap (Figure 6.2). The Dunn index is the ratio of the smallest distance between observations in different clusters over the largest between cluster distance and should be maximal. After this procedure, a number of subgroups remained, representing the subgroups with different brain MRI phenotypes.

Brain MRI markers and cardiovascular risk factors were compared between subgroups with chi-squared test for binary variables and 1-way analysis of variances for continuous variables by using SPSS version 25 (Chicago, IL). For these analyses, WMH volumes, number of WMH, solidity, ventricle volume fraction, and time to follow-up were log transformed due to a non-normal distribution. A p value <0.05 was considered statistically significant.

### 6.3.5.2 Sensitivity analysis

To assess the robustness of the hierarchical clustering model, we reran the analysis with 2 random subsets of this dataset.

### *6.3.5.3 Long-term outcome assessment*

A Cox proportional hazard model was used to estimate the risk of future dementia occurrence within the brain MRI phenotype subgroups (adjusted for age, sex, and cognitive status at baseline (mild cognitive impairment or normal cognition). The reference subgroup was chosen based on having the fewest brain abnormalities. SPSS version 25 was used for statistical testing.

**Table 6.1.** Baseline characteristics of the total study sample.

| | Community-dwelling individuals (n = 3056) |
|---|---|
| **Age** (years) | 75.6 ± 5.2 |
| **Time to follow-up** (years) | 9.9 ± 2.6 |
| **Female sex** | 1884 (62%) |
| **Mild cognitive impairment** | 257 (8%) |
| **BMI** (kg/m$^2$) | 26.97 ± 4.19 |
| **Hypertension** | 2380 (78%) |
| **Type 2 diabetes** | 277 (9%) |
| **Cholesterol** (mmol/L) | 5.71 ± 1.14 |
| **Smoking status** | |
| Never | 1397 (46%) |
| Former | 1334 (44%) |
| Current | 324 (11%) |
| **Coronary artery disease** | 497 (16%) |

Data are shown as means ± SD or percentages of individuals per subgroup. BMI, body mass index; SD, standard deviation.

## 6.3.6 Data availability

The AGES I-II data set cannot be made publicly available because the informed consent signed by the participants prohibits data sharing on an individual level, as outlined by the study approval by the Icelandic National Bioethics Committee. Requests for these data may be sent to the AGES Reykjavik Study Executive Committee, contact: Ms. Camilla Kritjansdottir, Camilla@hjarta.is.
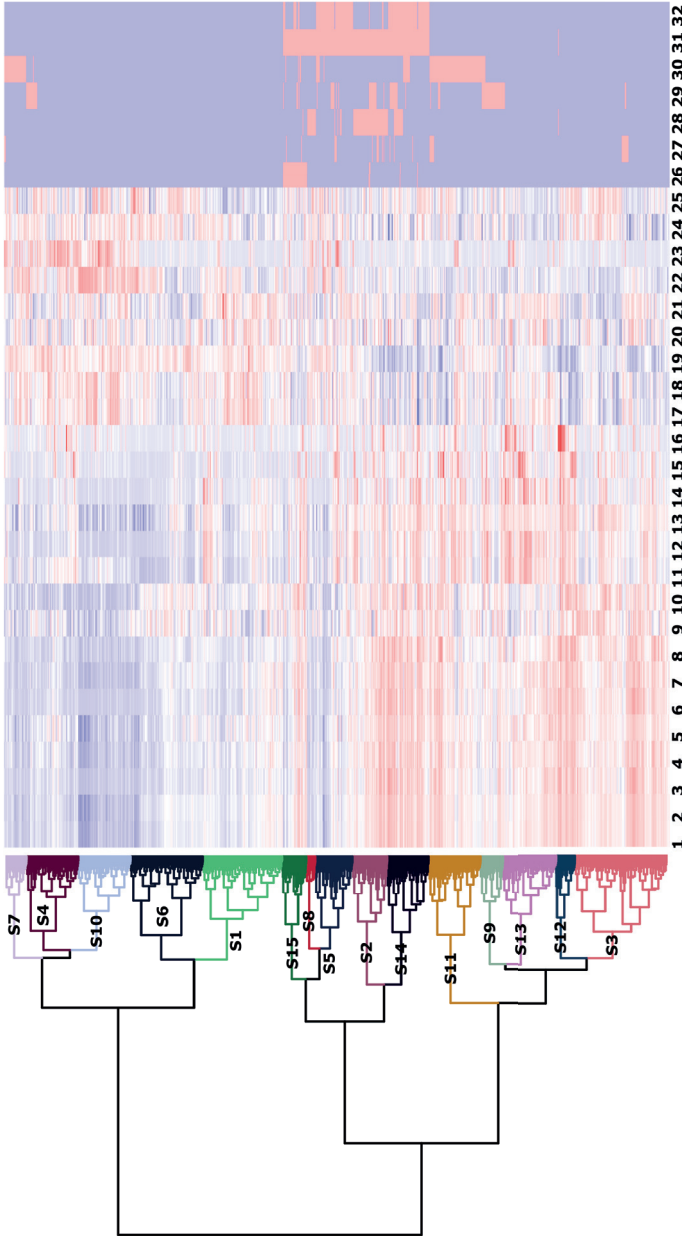
**Figure 6.2 Heatmap and Dendrogram: Results of the Hierarchical Clustering Analysis**
Red indicates high values, and blue indicates low values. Every line represents a participant, and every column represents a MRI marker. 1: total WMH volume; 2: PV/C WMH volume; 3: PV/C WMH volume frontal lobe; 4: other PV/C WMH volume; 5: PV/C WMH fractal dimension; 6: PV/C WMH volume parietal lobe; 7: PV/CWMH volume temporal lobe; 8: PV/C WMH concavity index; 9: % lateral ventricle volume; 10: PV/C WMH volume occipital lobe; 11: deep WMH volume frontal lobe; 12: deep WMH volume temporal lobe; 13: number of deep WMH; 14: deep WMH volume parietal lobe; 15: other deep WMH volume; 16: deep WMH volume temporal lobe; 17:%total brain volume; 18: % gray matter volume; 19: PV/C convexity; 20: % white matter volume; 21: deep WMH eccentricity; 22: deep WMH fractal dimension; 23: PV/C solidity; 24: deep WMH occipital lobe; 25: number of PV/C; 26: enlarged perivascular spaces in and around basal ganglia; 27: microbleeds; 28: cortical infarcts; 29: subcortical infarcts; 30: enlarged perivascular spaces in the white matter; 31: infarcts (whole brain); 32: cerebellar infarcts. Other PV/C WMH volume or other deep WMH volume were defined as Lesions or parts of lesions that were outside of the brain lobe masks, for example the brain stem and within the internal capsule. PV/C = periventricular/confluent; S = subgroup; WMH = white matter hyperintensity.

6

## 6.4 RESULTS

The total sample included 3056 community-dwelling older adults. The average time to follow-up for dementia outcome (yes/ no) was 9.9 ± 2.6 years (min−max range 0.6−13.4 years). The baseline characteristics of the total sample are presented in Table 6.1. A hierarchical clustering model was applied on brain MRI markers (WMH volumes, brain volumes, WMH shape markers, infarcts, enlarged perivascular spaces, microbleeds). The optimal cut-off of the hierarchical clustering model was determined to be at 15 subgroups (Figure 6.2), based on the Dunn index (supplementary figure S.6.8.2., links.lww.com/WNL/D459) and the heatmap (Figure 6.2). The sizes of the subgroups ranged from 42 to 425 participants. As a sensitivity analysis to test the robustness of the clustering method, we reran the model on 2 random subsets (subset 1: n = 2,311 and subset 2: n = 2,250). On average, 68% of participants remained in the same cluster compared with the main analysis. Baseline characteristics of the study sample per subgroup are shown in Table 2. The subgroups differed significantly in age (min−max range of mean age 71.6−78.8 years), sex (min−max range of mean sex distribution 37%−81% females), cognitive status at baseline (min−max range of mean prevalence 3%−15%), hypertension (min−max range of mean prevalence 64%−90%), type 2 diabetes mellitus (min−max range of mean prevalence 4%−15%), cholesterol levels (min−max range of mean 5.20−5.97 mmol/L), coronary artery disease (min−max range of mean prevalence 7%−30%), and time to follow-up (min−max range of mean time to follow-up 8.2−10.9 years; Table 6.2).

Brain MRI markers per subgroup are presented in Table 6.3. All brain MRI markers differed significantly between subgroups, as could be expected as the subgroups were based on the hierarchical clustering result. The main MRI markers per subgroup are illustrated in a simplified and summarized manner in Figure 6.3. The brain MRI phenotypes of the subgroups ranged from limited burden (subgroup 10), mostly irregular WMH shape and cerebral atrophy (subgroup 12), mostly irregularly shaped WMH and microbleeds (subgroup 9), mostly cortical infarcts and atrophy (subgroup 15), mostly irregularly shaped WMH and cerebral atrophy (subgroup 3) to multi-burden subgroups (subgroup 2, subgroup 14). A complete and detailed description of the main MRI markers of each subgroup can be found in S.6.8.1 supplementary results (links.lww.com/WNL/D459).

Subgroup 10 was determined to have the least amount of brain abnormalities and was used as the reference subgroup in the survival analysis (Figure 6.4). Dementia cases at follow-up ranged from 6% to 46% per subgroup. Compared with the reference subgroup, most other subgroups (except subgroup 4, subgroup 7, and subgroup 8) showed a higher long-term risk for dementia. The range of statistically

significant hazard ratios (HRs) across the subgroups varied between 1.01 and 6.18. The subgroup with relatively severe WMH and atrophy (subgroup 12) showed the largest long-term risk for dementia (HR 6.18, 95% CI 3.37–11.32) compared with the reference subgroup (subgroup 10). The multi-burden subgroups (subgroup 2: HR 3.68, 2.06–6.61; subgroup 14: HR 3.48, 1.96–6.16), the subgroup with mostly irregularly shaped WMH and cerebral atrophy (subgroup 3: HR 3.33, 1.94–5.73), the subgroup with mostly irregularly shaped WMH and microbleeds (subgroup 9: HR 2.99, 1.60–5.56), and the subgroup with mostly cortical infarcts and atrophy (subgroup 15: HR 3.16, 1.70–5.86) also showed a relatively high long-term risk for dementia.

| | WMH volumes | WMH shape | Cerebellar infarcts | Cortical infarcts | Subcortical infarcts | Atrophy | Microbleeds | Enlarged PVS |
|---|---|---|---|---|---|---|---|---|
| S1 | | | | | | | | |
| S2 | | | | | | | | |
| S3 | | | | | | | | |
| S4 | | | | | | | | |
| S5 | | | | | | | | |
| S6 | | | | | | | | |
| S7 | | | | | | | | |
| S8 | | | | | | | | |
| S9 | | | | | | | | |
| S10 | | | | | | | | |
| S11 | | | | | | | | |
| S12 | | | | | | | | |
| S13 | | | | | | | | |
| S14 | | | | | | | | |
| S15 | | | | | | | | |

**Figure 6.3. Symbolic illustration of the brain MRI markers per subgroup.** Small circles indicate low WMH volumes or low amount of cerebral atrophy. Big circles indicate high WMH volumes or cerebral atrophy. WMH shape is illustrated with symbols with three varying degrees of shape irregularity (regular, moderate, and irregular). Pie charts indicate percentages of participants with infarcts, enlarged PVS or microbleeds. S: subgroup; WMH: white matter hyperintensities; enlarged PVS: enlarged perivascular spaces in and around the basal ganglia.

6

**Table 6.2.** Baseline characteristics of the study sample per subgroup. S: subgroup; BMI: body mass index.

| | S1 N=368 | S2 N=161 | S3 N=425 | S4 N=239 | S5 N=171 | S6 N=333 | S7 N=98 |
|---|---|---|---|---|---|---|---|
| **Age** (years) | 74.4 ± 4.7 | 77.5 ± 5.3 | 77.8 ± 4.9 | 73.4 ± 4.1 | 75.6 ± 5.1 | 74.3 ± 4.8 | 74.2 ± 4.8 |
| **Time to dementia follow-up** (years) | 10.33 ± 2.02 | 8.89 ± 2.80 | 9.27 ± 2.93 | 10.89 ± 1.83 | 9.94 ± 2.33 | 10.36 ± 2.25 | 10.41 ± 2.33 |
| **Female sex** | 73% | 52% | 50% | 74% | 65% | 54% | 70% |
| **Mild cognitive impairment** | 7% | 11% | 12% | 3% | 9% | 5% | 3% |
| **BMI** (kg/m2) | 26.74 ± 4.29 | 27.35 ± 4.29 | 27.02 ± 4.47 | 27.18 ± 4.07 | 26.85 ± 4.11 | 26.53 ± 4.13 | 26.99 ± 4.07 |
| **Hypertension** | 75% | 88% | 81% | 76% | 80% | 70% | 68% |
| **Type 2 diabetes** | 6% | 14% | 10% | 6% | 10% | 6% | 9% |
| **Cholesterol** (mmol/L) | 5.82 ± 1.10 | 5.44 ± 1.08 | 5.67 ± 1.15 | 5.91 ± 1.16 | 5.55 ± 1.20 | 5.77 ± 1.04 | 5.75 ± 1.10 |
| **Smoking status** | | | | | | | |
|     Never | 49% | 35% | 45% | 47% | 44% | 44% | 54% |
|     Former | 41% | 53% | 47% | 42% | 44% | 44% | 38% |
|     Current | 9% | 11% | 8% | 10% | 12% | 12% | 8% |
| **Coronary artery disease** | 10% | 24% | 16% | 14% | 19% | 10% | 10% |

Data are shown as means ± SD or percentages of individuals per subgroup. Baseline characteristics and cardiovascular risk factors were compared between subgroups with chi-square test for binary variables, and one-way ANOVAs for continuous variables. S, subgroup; BMI, body mass index; SD, standard deviation.

| S8 N=42 | S9 N=105 | S10 N=241 | S11 N=240 | S12 N=87 | S13 N=245 | S14 N=190 | S15 N=111 | P value |
|---|---|---|---|---|---|---|---|---|
| 72.7 ± 3.2 | 76.8 ± 4.8 | 71.6 ± 3.4 | 76.5 ± 5.0 | 78.2 ± 4.9 | 75.6 ± 5.0 | 78.8 ± 5.3 | 77.3 ± 5.1 | <0.001 |
| 10.53 ± 1.66 | 9.43 ± 2.68 | 10.70 ± 1.54 | 9.54 ± 2.89 | 8.18 ± 3.10 | 10.28 ± 2.50 | 8.78 ± 2.85 | 9.14 ± 2.77 | <0.001 |
| 62% | 54% | 81% | 61% | 37% | 79% | 45% | 43% | <0.001 |
| 5% | 12% | 5% | 9% | 11% | 8% | 15% | 15% | <0.001 |
| 27.18 ± 4.28 | 25.91 ± 3.52 | 27.18 ± 3.99 | 26.90 ± 4.19 | 28.41 ± 4.52 | 27.29 ± 4.55 | 27.12 ± 3.51 | 26.72 ± 3.93 | 0.021 |
| 79% | 84% | 64% | 83% | 90% | 82% | 88% | 82% | <0.001 |
| 17% | 10% | 4% | 9% | 11% | 11% | 15% | 15% | <0.001 |
| 5.63 ± 0.87 | 5.69 ± 1.22 | 5.97 ± 1.07 | 5.76 ± 1.23 | 5.52 ± 1.08 | 5.75 ± 1.14 | 5.48 ± 1.22 | 5.20 ± 1.12 | 0.023 |
| 36% | 45% | 54% | 49% | 38% | 43% | 44% | 44% | 0.034 |
| 45% | 44% | 39% | 40% | 47% | 42% | 46% | 45% | 0.295 |
| 19% | 11% | 7% | 11% | 15% | 15% | 10% | 11% | 0.214 |
| 7% | 21% | 7% | 21% | 23% | 18% | 29% | 30% | <0.001 |

6

**Table 6.3.** Between-group differences of brain MRI markers.

| | S1<br>N=368 | S2<br>N=161 | S3<br>N=425 | S4<br>N=239 | S5<br>N=171 | S6<br>N=333 | S7<br>N=98 |
|---|---|---|---|---|---|---|---|
| **Total WMH volume** | 11.87 ± 4.69 | 35.85± 22.86 | 29.93 ± 16.76 | 7.50 ± 3.33 | 11.76 ± 7.66 | 8.02 ± 3.72 | 5.77 ± 2.25 |
| **PV/C WMH volume** | 10.68 ± 4.59 | 33.76 ± 22.83 | 28.51 ± 16.81 | 6.05 ± 3.10 | 10.28 ± 7.04 | 7.57 ± 3.60 | 4.83 ± 2.14 |
| **Deep WMH volume** | 1.18 ± 0.94 | 2.09 ± 1.52 | 1.42 ± 0.91 | 1.45 ± 0.85 | 1.49 ± 1.69 | 0.45 ± 0.39 | 0.94 ± 0.81 |
| **Number of PV/C** | 14.69 ± 5.70 | 14.86± 5.03 | 14.96 ± 5.51 | 14.90 ± 5.89 | 14.71 ± 5.07 | 15.27 ± 6.19 | 15.53 ± 6.06 |
| **Number of deep WMH** | 25.40 ± 15.29 | 44.69 ± 29.64 | 41.26 ± 25.69 | 21.23 ± 13.84 | 28.89 ± 26.73 | 16.39 ± 13.72 | 15.06 ± 10.83 |
| **PV/C solidity** | 0.18 ± 0.07 | 0.15 ± 0.05 | 0.13 ± 0.05 | 0.23 ± 0.11 | 0.21 ± 0.13 | 0.20 ± 0.11 | 0.25 ± 0.11 |
| **PV/C convexity** | 1.11 ± 0.12 | 0.87 ± 0.18 | 0.89 ± 0.14 | 1.13 ± 0.13 | 1.08 ± 0.14 | 1.13 ± 0.12 | 1.13 ± 0.11 |
| **PV/C concavity index** | 1.22 ± 0.07 | 1.42 ± 0.14 | 1.41 ± 0.11 | 1.17 ± 0.07 | 1.22 ± 0.11 | 1.19 ± 0.08 | 1.15 ± 0.07 |
| **PV/C fractal dimension** | 1.69 ± 0.09 | 1.84 ± 0.11 | 1.82 ± 0.08 | 1.65 ± 0.11 | 1.67 ± 0.14 | 1.62 ± 0.11 | 1.58 ± 0.12 |
| **Deep WMH eccentricity** | 0.56 ± 0.06 | 0.61 ± 0.06 | 0.63 ± 0.06 | 0.61 ± 0.07 | 0.62 ± 0.08 | 0.65 ± 0.08 | 0.62 ± 0.08 |
| **Deep WMH fractal dimension** | 1.79 ± 1.79 | 1.69 ± 0.12 | 1.65 ± 0.12 | 1.71 ± 0.13 | 1.69 ± 0.13 | 1.59 ± 0.12 | 1.69 ± 0.15 |
| **% lateral ventricle volume** | 2.61 ± 0.97 | 3.23 ± 1.09 | 3.60 ± 1.15 | 2.18 ± 0.72 | 2.63 ± 1.08 | 2.82 ± 0.93 | 2.19 ± 0.72 |
| **% total brain volume** | 74.52 ± 3.02 | 71.48 ± 3.59 | 70.80 ± 3.02 | 74.27 ± 2.45 | 72.91 ± 3.07 | 72.25 ± 2.82 | 73.44 ± 3.62 |
| **% grey matter volume** | 46.84 ± 2.60 | 44.50 ± 2.96 | 43.97 ± 2.62 | 47.28 ± 2.04 | 45.95 ± 2.70 | 45.41 ± 2.43 | 46.49 ± 3.09 |
| **% white matter volume** | 27.68 ± 1.49 | 26.98 ± 1.93 | 26.83 ± 1.35 | 26.98 ± 1.55 | 26.96 ± 1.47 | 26.84 ± 1.49 | 26.95 ± 1.54 |
| **PVS (basal ganglia)** | 0% | 9% | 8% | 0% | 5% | 0% | 4% |
| **PVS** | 0% | 0% | 0% | 3% | 10% | 0% | 100% |
| **Microbleeds** | 0% | 14% | 1% | 16% | 12% | 0% | 0% |
| **Subcortical infarcts** | 0% | 100% | 0% | 0% | 8% | 0% | 0% |
| **Cerebellar infarcts** | 0% | 5% | 0% | 0% | 98% | 0% | 0% |
| **Cortical infarcts** | 0% | 4% | 0% | 0% | 1% | 0% | 0% |
| **Infarcts** | 0% | 100% | 0% | 0% | 100% | 0% | 0% |

Data shown as mean ±SD or percentages of individuals per subgroup. Brain MRI markers were compared between subgroups with chi-square Test for binary variables, and one-way ANOVAs for continuous variables. The data for WMH volumes per lobe are shown in supplementary table S.6.8.2. S, subgroup; WMH, white matter hyperintensity; PV/C periventricular/confluent WMH; PVS, enlarged perivascular spaces; SD, standard deviation.

| S8 N=42 | S9 N=105 | S10 N=241 | S11 N=240 | S12 N=87 | S13 N=245 | S14 N=190 | S15 N=111 | P value |
|---|---|---|---|---|---|---|---|---|
| 6.07 ± 2.66 | 22.90 ± 12.89 | 3.20 ± 1.44 | 25.93 ± 15.89 | 50.32 ± 20.71 | 24.56 ± 9.63 | 41.11 ± 21.16 | 22.85 ± 16.85 | <0.001 |
| 5.18 ± 2.65 | 21.05 ± 12.86 | 2.37 ± 1.29 | 23.93 ± 15.72 | 46.99 ± 20.77 | 21.43 ± 9.71 | 39.19 ± 21.46 | 21.29 ± 16.60 | <0.001 |
| 0.89 ± 0.75 | 1.85 ± 1.41 | 0.83 ± 0.51 | 2.00 ± 1.27 | 3.33 ± 1.51 | 3.13 ± 1.81 | 1.91 ± 1.36 | 1.57 ± 1.35 | <0.001 |
| 15.36 ± 5.94 | 14.78 ± 5.57 | 16.00 ± 5.98 | 14.93 ± 6.08 | 15.62 ± 6.12 | 15.23 ± 5.94 | 14.78 ± 5.46 | 14.57 ± 5.41 | <0.001 |
| 14.67± 10.29 | 41.90 ± 22.40 | 8.20 ± 5.11 | 46.33 ± 26.79 | 86.90 ± 40.35 | 45.49 ± 16.62 | 46.88 ± 28.29 | 34.59 ± 23.67 | <0.001 |
| 0.25 ± 0.12 | 0.13 ± 0.05 | 0.39 ± 0.16 | 0.14 ± 0.05 | 0.03 ± 0.15 | 0.14 ± 0.04 | 0.14 ± 0.05 | 0.17 ± 0.07 | <0.001 |
| 1.15 ± 0.11 | 0.97 ± 0.16 | 1.12 ± 0.11 | 0.92 ± 0.19 | 0.67 ± 0.13 | 0.97 ± 0.14 | 0.81 ± 0.16 | 1.00 ± 0.17 | <0.001 |
| 1.15 ± 0.06 | 1.35 ± 0.12 | 1.09 ± 0.06 | 1.38 ± 0.15 | 1.59 ± 0.11 | 1.34 ± 0.10 | 1.47 ± 0.13 | 1.31 ± 0.14 | <0.001 |
| 1.58 ± 0.11 | 1.78 ± 0.10 | 1.48 ± 0.14 | 1.80 ± 0.11 | 1.92 ± 0.07 | 1.81 ± 0.09 | 1.87 ± 0.09 | 1.74 ± 0.12 | <0.001 |
| 0.60 ± 0.10 | 0.61 ± 0.07 | 0.64 ± 0.08 | 0.61 ± 0.06 | 0.66 ± 0.05 | 0.58 ± 0.05 | 0.63 ± 0.06 | 0.62 ± 0.06 | <0.001 |
| 1.68 ± 0.12 | 1.68 ± 0.13 | 1.72 ± 0.13 | 1.69 ± 0.13 | 1.60 ± 0.11 | 1.77 ± 0.08 | 1.66 ± 0.12 | 1.70 ± 0.12 | <0.001 |
| 2.21 ± 0.91 | 3.09 ± 1.21 | 1.85 ± 0.64 | 2.92 ± 1.06 | 3.43 ± 0.98 | 2.50 ± 0.82 | 3.64 ± 1.21 | 3.08 ± 1.07 | <0.001 |
| 74.93 ± 3.16 | 72.02 ± 3.56 | 75.73 ± 3.07 | 71.94 ± 3.60 | 68.76 ± 4.15 | 74.55 ± 2.93 | 70.69 ± 4.01 | 71.75 ± 3.09 | <0.001 |
| 47.86 ± 2.32 | 45.06 ± 2.85 | 48.20 ± 2.58 | 44.96 ± 2.93 | 42.71 ± 3.40 | 46.76 ± 2.41 | 43.72 ± 3.38 | 44.45 ± 2.83 | <0.001 |
| 27.07 ± 1.35 | 26.96 ± 1.74 | 27.53 ± 1.48 | 26.98 ± 1.70 | 26.05 ± 2.03 | 27.79 ± 1.63 | 26.97 ± 1.85 | 27.30 ± 1.59 | <0.001 |
| 0% | 0% | 0% | 8% | 2% | 0% | 6% | 8% | <0.001 |
| 0% | 17% | 0% | 99% | 2% | 0% | 17% | 16% | <0.001 |
| 5% | 66% | 0% | 2% | 1% | 0% | 9% | 7% | <0.001 |
| 100% | 0% | 0% | 0% | 3% | 0% | 22% | 5% | <0.001 |
| 0% | 0% | 0% | 0% | 0% | 0% | 99% | 29% | <0.001 |
| 0% | 0% | 0% | 0% | 0% | 0% | 4% | 100% | <0.001 |
| 100% | 0% | 0% | 0% | 3% | 0% | 100% | 100% | <0.001 |

6

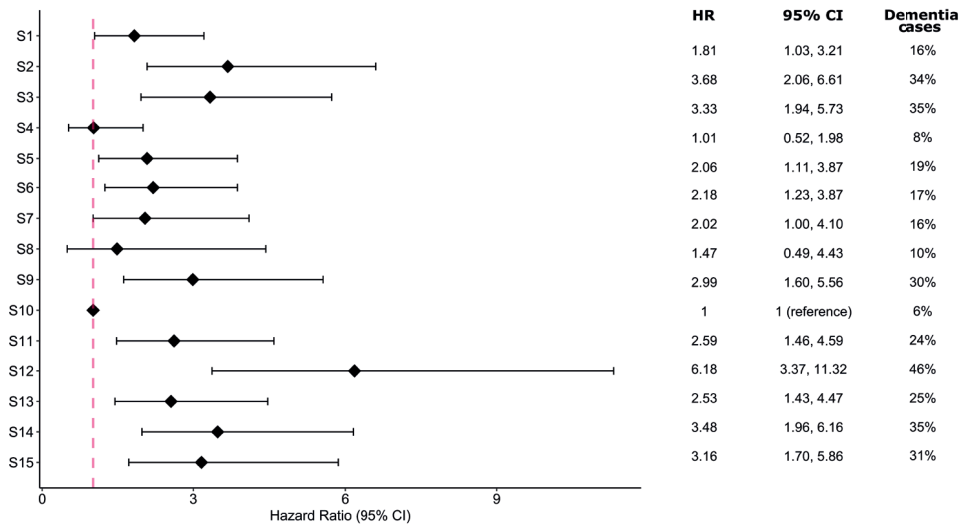| | HR | 95% CI | Dementia cases |
|---|---|---|---|
| S1 | 1.81 | 1.03, 3.21 | 16% |
| S2 | 3.68 | 2.06, 6.61 | 34% |
| S3 | 3.33 | 1.94, 5.73 | 35% |
| S4 | 1.01 | 0.52, 1.98 | 8% |
| S5 | 2.06 | 1.11, 3.87 | 19% |
| S6 | 2.18 | 1.23, 3.87 | 17% |
| S7 | 2.02 | 1.00, 4.10 | 16% |
| S8 | 1.47 | 0.49, 4.43 | 10% |
| S9 | 2.99 | 1.60, 5.56 | 30% |
| S10 | 1 | 1 (reference) | 6% |
| S11 | 2.59 | 1.46, 4.59 | 24% |
| S12 | 6.18 | 3.37, 11.32 | 46% |
| S13 | 2.53 | 1.43, 4.47 | 25% |
| S14 | 3.48 | 1.96, 6.16 | 35% |
| S15 | 3.16 | 1.70, 5.86 | 31% |

**Figure 6.4. Hazard ratios per subgroup based on the Cox regression analysis.** Controlled for age, sex, and cognitive status at baseline. Subgroup 10 was used as the reference subgroup in the model, as it was the subgroup with the lowest amount of brain abnormalities. S: subgroup; HR: hazard ratio; CI: confidence interval.

## 6.5 DISCUSSION

We showed that distinct brain MRI phenotypes can be identified in community-dwelling older adults. Some of the 15 distinct subgroups that were identified showed a different long-term dementia risk, with an increased risk, especially in individuals in the multi-burden brain pathology subgroups, and in the subgroup with relatively severe WMH and atrophy. Most subgroups showed a significantly increased risk for dementia compared with the reference subgroup that showed the least abnormalities on brain MRI.

The exact underlying structural correlates of the early predisposition to dementia remain largely unknown. Many validated and commonly used brain MRI markers are nonspecific to pathology and disease and commonly occur with ageing.[19] Nevertheless, previous studies frequently focused on single or small groups of MRI markers and their relationship with neurovascular or neurodegenerative diseases.[20-23] A combined analysis of brain MRI markers could improve our understanding of the pathophysiology of and early predisposition for dementia, as different brain diseases usually lead to patterns of different brain abnormalities.[24] In other fields of research, combined analysis to identify phenotypes has previously been performed. Examples are the identification of asthma phenotypes[25,26] and subphenotypes of chronic

obstructive pulmonary disease.[27,28] Moreover, it is frequently used in the field of genetics to identify genotypes, for example, to identify differences in DNA methylation and gene expression in breast cancer.[29]

There are some previous studies on combined analysis of brain MRI markers or data-driven approaches in the field of dementia research. In a previous study, using an unsupervised deep learning approach on a large diverse data set of T1-weighted brain MRI scans showed that the difference between predicted brain age and chronological age is associated with the presence of different diseases (e.g., schizophrenia, and Alzheimer disease (AD)).[30] In another study, a semi-supervised deep-clustering method identified 4 neurodegenerative brain MRI patterns based on atrophy regions of interests on T1 scans in a data set including cognitively healthy individuals and patients with cognitive impairment and dementia.[31] Another study identified 3 brain MRI patterns (neurodegeneration, white matter disease, and typical brain ageing) on T1-weighted scans using a machine learning–based method that can be used to identify individual brain health.[32] These previous studies used (semi) supervised deep learning approaches, which is a different approach compared with our unsupervised machine learning approach. There are also some previous studies that have used a more similar approach compared with ours, albeit in different patient populations. For example, a previous study has applied hierarchical clustering to identify patterns of markers (including brain MRI markers, blood values, and CSF markers) related to the conversion from mild cognitive impairment to AD.[33] Here, 4 subgroups were identified with a different risk for conversion to AD.33 The subgroup with the highest risk showed the most severe biomarker profile, for example, the highest WMH volumes, the lowest CSF amyloid beta, the highest CSF tau, and the lowest entorhinal cortical thickness.[33] Another previous study showed that midlife white matter textural properties were associated with future dementia risk.[34] A more heterogeneous normal appearing white matter intensity profile was associated with a higher WMH burden in the future, and a more heterogeneous intensity of normal appearing white matter was related to increased dementia risk. Another study found 2 distinct subgroups of mild cognitive impairment based on radiomics similarity networks.[35] Significant differences between the 2 mild cognitive impairment subgroups were found, among others, in the regional radiomics similarity networks of the hippocampus, temporal lobe, parahippocampal gyrus, and amygdala, as well as in the gray matter volume and cortical thickness. Furthermore, the 2 subgroups were significantly different from each other in clinical measures and the number of participants progressing to dementia within 3 years.[35] Our study is the first to apply an unsupervised machine learning approach in a large group of community-dwelling individuals to assess the association of brain MRI phenotypes and long-term

6

dementia risk. The large sample size of community-dwelling individuals in our study aids the generalizability of our results. Our study is further strengthened by the long follow-up time to the assessment of occurrence of dementia. Because of our study design, in the future, our method could help in assessing an individuals increased dementia risk at an early stage to determine patient prognosis in clinical practice and may aid in patient selection for future treatment studies.

A hierarchical clustering model allows combining of a spectrum of brain MRI markers and to find patterns in these data. We have previously applied the hierarchical clustering method in different data sets with different MRI markers to identify MRI phenotypes of the brain related to future stroke and mortality in patients with manifest arterial disease,[7] as well as related to increased postoperative delirium risk in preoperative patients.[36] To the best of our knowledge, this study assessed brain MRI phenotypes in relation to long-term dementia risk in community-dwelling older adults. Our results identified 15 distinct subgroups of individuals with different distributions of brain MRI markers of neurodegenerative and neurovascular disease. The multi-burden group with the highest long-term risk for dementia (subgroup 12) does show markers of SVD, such as high WMH volumes and an irregular WMH shape, but includes only few individuals with brain infarcts. In addition, subgroup 12 showed the most severe cerebral atrophy, which may suggest that this subgroup has more underlying neurodegenerative pathology. Subgroup 2 has, similar to subgroup 12, high WMH volumes and an irregular WMH shape but also includes a high number of participants with subcortical, cerebellar, and cortical infarcts. Atrophy is less prominent in subgroup 2 compared with subgroup 12. Subgroup 15 may include mostly patients with large vessel disease, as WMH volumes and shape are only moderately abnormal, while all participants in this group have cortical infarcts. We showed that different brain MRI phenotypes, characterized by a distinct combination of brain MRI markers, predispose to occurrence of dementia and are related to different long-term dementia risks.

Strengths of our study include the use of multiple brain MRI markers in one framework, a large sample size, and a long follow-up period for dementia outcome. Furthermore, we mostly included markers that can be (semi) automatically detected on brain MRI scans (e.g., WMH volumes and brain atrophy) and the inclusion of novel brain MRI markers (such as WMH shape). An automated, unsupervised approach to identify groups was applied that allowed us to identify novel patterns of brain MRI markers. Limitations of this study might be the somewhat subjective cut-offs within the model, such as the dendrogram cut-off. However, to increase objectivity, we used the Dunn index and the heatmap to determine the cut-off for the number of

subgroups. Another limitation could be that the model is dependent on the selection of brain MRI markers that were included in the model. We therefore chose to include etiologically and prognostically relevant and validated brain MRI markers of which many can be quantified automatically. Moreover, the hierarchical clustering results could also be influenced by the choice of linkage method (e.g., Ward's, centroid), which is used to delineate the subgroups. We have chosen to use Ward's criteria as a linkage method because it generates subgroups with minimal within subgroup variance and to maximize the between-subgroup variance, which we deemed as most suitable for this data set and type of analysis. Another general limitation of the clustering method could be that in our sensitivity analyses, we showed that there is some dependency of the clustering results based on the number and selection of participants. For future research the Subtype and Stage Inference (SuStaIn) method, an unsupervised machine learning technique that identifies population subgroups with common patterns of disease progression could be an interesting approach.[37] SuStaIn could provide additional insights since it combines traditional clustering with disease progression modeling, but the effect of this approach on reproducibility is also of interest. Another limitation of this study could be that most neuroimaging research 1.5T MRI scanners are nowadays replaced with a 3T MRI system, which was not yet the case at the time of the data collection for our study. Nevertheless, we did successfully identify distinct brain MRI phenotypes based on our data set.

In conclusion, distinct brain MRI phenotypes are related to varying long-term risks of developing dementia. Brain MRI phenotypes may assist in an improved understanding of the structural correlates of dementia predisposition. These findings may aid in the future to determine patient prognosis and for patient selection for future treatment studies.

## 6.6 ACKNOWLEDGEMENTS

6

# 6.7 REFERENCES

1.    Duering M, Biessels GJ, Brodtmann A, et al. Neuroimaging standards for research into small vessel disease—advances since 2013. Lancet Neurol. 2023;22(7):602-618. doi: 10.1016/S1474-4422(23)00131-X

2.    Alber J, Alladi S, Bae H, et al. White matter hyperintensities in vascular contributions to cognitive impairment and dementia (VCID): knowledge gaps and opportunities. Alzheimers Dement (NY). 2019;5:107-117. doi:10.1016/j.trci.2019.02.001

3.    Benveniste H, Nedergaard M. Cerebral small vessel disease: a glymphopathy? Curr Opin Neurobiol. 2022;72:15-21. doi:10.1016/J.CONB.2021.07.006

4.    Bos D, Wolters FJ, Darweesh SKL, et al. Cerebral small vessel disease and the risk of dementia: a systematic review and meta-analysis of population-based evidence. Alzheimers Dement. 2018;14(11):1482-1492. doi:10.1016/j.jalz.2018.04.007

5.    De Guio F, DueringM, Fazekas F, et al. Brain atrophy in cerebral small vessel diseases: extent, consequences, technical limitations and perspectives: the HARNESS initiative. J Cereb Blood Flow Metab. 2020;40(2):231-245. doi:10.1177/0271678X19888967

6.    Ding J, Sigurðsson S, Jonsson PV, et al. Space and location of cerebral microbleeds, cognitive decline, and dementia in the community. Neurology. 2017;88(22):2089-2097. doi:10.1212/WNL.0000000000003983

7.    Jaarsma-Coes MG, Ghaznawi R, Hendrikse J, et al; Second Manifestations of ARTerial disease SMART Study group. MRI phenotypes of the brain are related to future stroke and mortality in patients with manifest arterial disease: the SMART-MR study. J Cereb Blood Flow Metab. 2020;40(2):354-364. doi:10.1177/0271678X18818918

8.    Harris TB, Launer LJ, Eiriksdottir G, et al. Age, gene/environment susceptibility Reykjavik study: multidisciplinary applied phenomics. Am J Epidemiol. 2007;165(9):1076-1087. doi:10.1093/aje/kwk115

9.    Saczynski JS, Sigurdsson S, Jonsdottir MK, et al. Cerebral infarcts and cognitive performance: importance of location and number of infarcts. Stroke. 2009;40(3): 677-682. doi:10.1161/STROKEAHA.108.530212

10.   Morris JN, Hawes C, Fries BE, et al. Designing the national resident assessment instrument for nursing homes. Gerontologist. 1990;30(3):293-307. doi:10.1093/GERONT/30.3.293

11.   Sveinbjornsdottir S, Sigurdsson S, Aspelund T, et al. Cerebral microbleeds in the population based AGES-Reykjavik study: prevalence and location. J Neurol Neurosurg Psychiatry. 2008;79(9):1002-1006. doi:10.1136/JNNP.2007.121913

12.   Zijdenbos AP, Forghani R, Evans AC. Automatic "pipeline" analysis of 3-D MRI data for clinical trials: application to multiple sclerosis. IEEE Trans Med Imaging. 2002;21(10):1280-1291. doi:10.1109/TMI.2002.806283

13.   Sigurdsson S, Aspelund T, Forsberg L, et al. Brain tissue volumes in the general population of the elderly: the AGES-Reykjavik Study. Neuroimage. 2012;59(4):3862-3870. doi:10.1016/j.neuroimage.2011.11.024

14.   Keller JA, Sigurdsson S, Klaassen K, et al. White matter hyperintensity shape is associated with long-term dementia risk. Alzheimers Dement. 2023;19(12):5632-5641. doi:10.1002/ALZ.13345

15.   Ghaznawi R, Geerlings MI, Jaarsma-Coes MG, et al. The association between lacunes and white matter hyperintensity features on MRI: the SMART-MR study. J Cereb Blood Flow Metab. 2019;39(12):2486-2496. doi:10.1177/0271678X18800463

16.   Kassambara A. FactoExtra: extract and visualize the results of multivariate data analyses for R, version 1.0.7. 2020.

17.   Maechler M, Rousseeuw P, Struyf A, et al. Package "cluster": R package version 2.1.2.2021.

18. Galili T. dendextend: an R package for visualizing, adjusting and comparing trees of hierarchical clustering. Bioinformatics. 2015;31(22):3718-3720. doi:10.1093/bioinformatics/btv428

19. Pantoni L. Cerebral small vessel disease: from pathogenesis and clinical characteristics to therapeutic challenges. Lancet Neurol. 2010;9(7):689-701. doi:10.1016/S1474-4422(10)70104-6

20. Apostolova LG, Mosconi L, Thompson PM, et al. Subregional hippocampal atrophy predicts Alzheimer's dementia in the cognitively normal. Neurobiol Aging. 2010;31(7):1077-1088. doi:10.1016/J.NEUROBIOLAGING.2008.08.008

21. Debette S, Beiser A, Decarli C, et al. Association of MRI markers of vascular brain injury with incident stroke, mild cognitive impairment, dementia, and mortality: the Framingham Offspring Study. Stroke. 2010;41(4):600-606. doi:10.1161/STROKEAHA.109.570044

22. Godin O, Tzourio C, Rouaud O, et al. Joint effect of white matter lesions and hippocampal volumes on severity of cognitive decline: the 3C-Dijon MRI study. J Alzheimers Dis. 2010;20(2):453-463. doi:10.3233/JAD-2010-1389

23. van Rooden S, Goos JDC, van Opstal AM, et al. Increased number of microinfarcts in Alzheimer disease at 7-T MR imaging. Radiology. 2014;270(1):205-211. doi:10.1148/radiol.13130743

24. Habes M, Grothe MJ, Tunc B, McMillan C, Wolk DA, Davatzikos C. Disentangling heterogeneity in Alzheimer's disease and related dementias using data-driven methods. Biol Psychiatry. 2020;88(1):70-82. doi:10.1016/J.BIOPSYCH.2020.01.016

25. Haldar P, Pavord ID, Shaw DE, et al. Cluster analysis and clinical asthma phenotypes. Am J Respir Crit Care Med. 2008;178(3):218-224. doi:10.1164/RCCM.200711-1754OC

26. Moore WC, Meyers DA, Wenzel SE, et al; National Heart, Lung, and Blood Institute's Severe Asthma Research Program. Identification of asthma phenotypes using cluster analysis in the Severe Asthma Research Program. Am J Respir Crit Care Med. 2010;181(4):315-323. doi:10.1164/RCCM.200906-0896OC

27. Burgel PR, Paillasseur JL, Caillaud D, et al; Initiatives BPCO Scientific Committee. Clinical COPD phenotypes: a novel approach using principal component and cluster analyses. Eur Respir J. 2010;36(3):531-539. doi:10.1183/09031936.00175109

28. Fens N, Van Rossum AGJ, Zanen P, et al. Subphenotypes of mild-to-moderate COPD by factor and cluster analysis of pulmonary function, CT imaging and breathomics in a population-based survey. COPD. 2013;10(3):277-285. doi:10.3109/15412555.2012.744388

29. Lin IH, Chen DT, Chang YF, et al. Hierarchical clustering of breast cancer methylomes revealed differentially methylated and expressed breast cancer genes. PLoS One. 2015;10(2):e0118453. doi:10.1371/JOURNAL.PONE.0118453

30. Bashyam VM, Erus G, Doshi J, et al. MRI signatures of brain age and disease over the lifespan based on a deep brain network and 14 468 individuals worldwide. Brain. 2020;143(7):2312-2324. doi:10.1093/BRAIN/AWAA160

31. Yang Z, Nasrallah IM, Shou H, et al; iSTAGING Consortium; Baltimore Longitudinal Study of Aging BLSA; Alzheimer's Disease Neuroimaging Initiative ADNI. A deep learning framework identifies dimensional representations of Alzheimer's Disease from brain structure. Nat Commun. 2021;12:7065. doi: 10.1038/s41467-021-26703-z

32. Habes M, Pomponio R, Shou H, et al; iSTAGING consortium, the Preclinical AD consortium, the ADNI, and the CARDIA studies. The Brain Chart of Aging: machine-learning analytics reveals links between brain aging, white matter disease, amyloid burden, and cognition in the iSTAGING consortium of 10,216 harmonizedMRscans. Alzheimers Dement. 2021;17(1):89-102. doi:10.1002/ALZ.12178

33. Nettiksimmons J, DeCarli C, Landau S, Beckett L; Alzheimer's Disease Neuroimaging Initiative. Biological heterogeneity in ADNI amnestic mild cognitive impairment. Alzheimers Dement. 2014;10(5):511-521.e1. doi:10.1016/J.JALZ.2013.09.003

6

**34.** Dounavi ME, Low A, Muniz-Terrera G, et al. Fluid-attenuated inversion recovery magnetic resonance imaging textural features as sensitive markers of white matter damage in midlife adults. Brain Commun. 2022;4(3):fcac116. doi:10.1093/BRAINCOMMS/FCAC116

**35.** Zhao K, Zheng Q, Dyrba M, et al; Alzheimer's Disease Neuroimaging Initiative. Regional radiomics similarity networks reveal distinct subtypes and abnormality patterns in mild cognitive impairment. Adv Sci. 2022;9(12):e2104538. doi:10.1002/ADVS.202104538

**36.** Kant IMJ, Slooter AJC, Jaarsma-Coes M, et al; BioCog consortium. Preoperative MRI brain phenotypes are related to postoperative delirium in older individuals. Neurobiol Aging. 2021;101:247-255. doi:10.1016/J.NEUROBIOLAGING.2021.01.033

**37.** Young AL, Marinescu RV, Oxtoby NP, et al; Genetic FTD Initiative GENFI; Alzheimer's Disease Neuroimaging Initiative ADNI. Uncovering the heterogeneity and temporal complexity of neurodegenerative diseases with Subtype and Stage Inference. Nat Commun. 2018;9(1):4273. doi:10.1038/S41467-018-05892-0

# 6.8 SUPPLEMENTARY MATERIAL

**Table S.6.8.1.** Definition of the WMH shape markers.

| Shape marker | WMH type | Description | Formula |
|---|---|---|---|
| Solidity (S) | Periventricular/Confluent WMH | Solidity and Convexity show how concave or convex a shape is. A maximally convex shape has a convexity and solidity value of 1. Values decrease with a more concave, complex shape. A convex hull is the smallest convex envelop of a shape. | $S = \dfrac{\text{Volume}}{\text{Convex Hull Volume}}$ |
| Convexity (C) | Periventricular/Confluent WMH | | $C = \dfrac{\text{Convex Hull Area}}{\text{Area}}$ |
| Concavity Index (CI) | Periventricular/Confluent WMH | Concavity index—a measure of roughness—describes how dense, irregular or elongated and curved a lesion is. Higher CI values indicate a more complex WMH shape. | $CI = \sqrt{(2 - C)^2 + (1 - S)^2}$ |
| Fractal Dimension (FD) | Periventricular/Confluent and deep WMH | The Minkowski-Bouligand dimension (box counting dimension) is a measure of textural roughness. Higher FD values suggest a more complex WMH shape. | $FD = \lim\limits_{r \to 1} \dfrac{\log(n_r)}{\log\left(\frac{1}{r}\right)}$ <br> $n$ = number of boxes <br> $r$ = box size |
| Eccentricity (E) | Deep WMH | Eccentricity describes the deviation from a circle. The eccentricity of a circle is 0 and the eccentricity of a line is 1. | $E = \dfrac{\text{Major Axis}}{\text{Minor Axis}}$ <br> Major axis: largest diameter in 3D space. Minor axis: smallest diameter orthogonal to the major axis. |

Lower convexity and solidity and a higher concavity index and fractal dimension indicate a more irregularly shaped WMH. A higher eccentricity corresponds to a more elongated lesion, while a lower eccentricity corresponds to a rounder lesion. Averages were calculated per participant for each shape marker. A more irregular shape of a WMH type was defined by taking the separate markers and their directionality into account to assess the main shape. This was only done for interpretation and description of the findings.

6

convex     concave
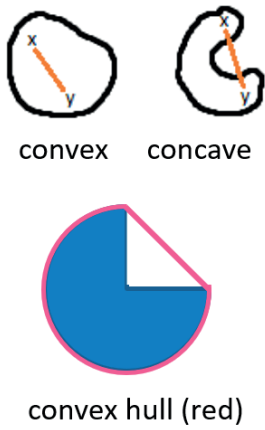


convex hull (red)

**Figure S.6.8.1. Simplified illustrations of the concepts of convexity and convex hull.** A shape is convex if you can connect any two points (e.g. x and y) within the shape, while the connecting line (orange) is also always within the shape. If this is not possible the shape is concave. A convex hull (red) is the smallest convex set that contains the shape (blue).



**Figure S.6.8.2. The Dunn index is shown on the y-axis, and on the x-axis the number of clusters/subgroups is shown.** The Dunn index should be maximized for an optimal number of groups. The red line indicates 15 groups, which is the number of groups used in the analysis. ks, number of clusters; DI, Dunn index.

6

**Table S.6.8.2.** Between-group differences of WMH volumes per lobe.

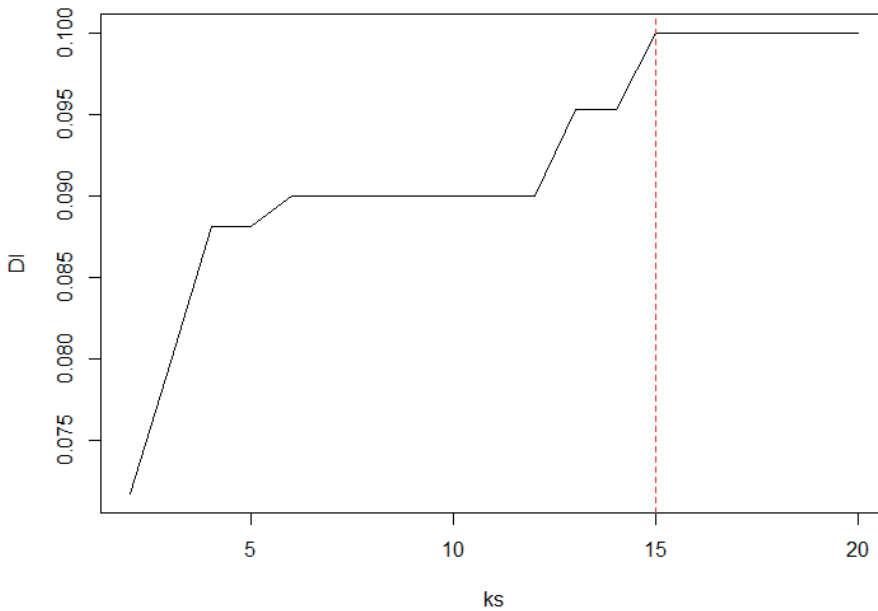| | S1<br>N=368 | S2<br>N=161 | S3<br>N=425 | S4<br>N=239 | S5<br>N=171 | S6<br>N=333 | S7<br>N=98 |
|---|---|---|---|---|---|---|---|
| **PV/C WMH volume frontal lobe** | 2.84 ± 1.66 | 12.89 ± 12.26 | 10.33 ± 9.30 | 1.86 ± 1.34 | 3.16 ± 3.24 | 1.74 ± 1.07 | 1.23 ± 0.75 |
| **PV/C WMH volume parietal lobe** | 1.78 ± 1.63 | 8.06 ± 6.48 | 6.75 ± 5.42 | 0.78 ± 0.93 | 1.76 ± 2.06 | 0.98 ± 0.89 | 0.44 ± 0.45 |
| **PV/C WMH volume temporal lobe** | 2.16 ± 1.15 | 5.10 ± 2.74 | 4.44 ± 2.23 | 1.17 ± 0.69 | 1.89 ± 1.34 | 1.54 ± 0.87 | 0.98 ± 0.53 |
| **PV/C WMH volume occipital lobe** | 1.68 ± 1.01 | 3.35 ± 2.41 | 3.25 ± 1.73 | 0.55 ± 0.59 | 1.42 ± 1.26 | 1.71 ± 1.03 | 0.85 ± 0.76 |
| **Other PV/C WMH volume** | 2.23 ± 0.75 | 4.36 ± 2.02 | 3.74 ± 1.41 | 1.69 ± 0.66 | 2.04 ± 0.98 | 1.60 ± 0.65 | 1.33 ± 0.55 |
| **Deep WMH volume frontal lobe** | 0.79 ± 0.72 | 1.44 ± 1.20 | 0.98 ± 0.71 | 0.46 ± 0.50 | 0.79 ± 1.09 | 0.24 ± 0.28 | 0.27 ± 0.36 |
| **Deep WMH volume parietal lobe** | 0.21 ± 0.25 | 0.33 ± 0.34 | 0.22 ± 0.19 | 0.11 ± 0.13 | 0.21 ± 0.34 | 0.07 ± 0.09 | 0.07 ± 0.13 |
| **Deep WMH volume temporal lobe** | 0.03 ± 0.05 | 0.07 ± 0.09 | 0.04 ± 0.05 | 0.06 ± 0.09 | 0.05 ± 0.08 | 0.02 ± 0.03 | 0.03 ± 0.05 |
| **Deep WMH occipital lobe** | 0.10 ± 0.17 | 0.11 ± 0.20 | 0.09 ± 0.18 | 0.74 ± 0.47 | 0.37 ± 0.52 | 0.09 ± 0.14 | 0.52 ± 0.60 |
| **Other deep WMH volume** | 0.05 ± 0.06 | 0.13 ± 0.12 | 0.09 ± 0.10 | 0.08 ± 0.09 | 0.08 ± 0.10 | 0.03 ± 0.04 | 0.04 ± 0.06 |

Data are shown as means ± SD. Brain MRI markers were compared between subgroups with one-way ANOVAs. S, subgroup; WMH, white matter hyperintensity; PV/C periventricular/confluent WMH; SD, standard deviation. Other PV/C WMH volume or other deep WMH volume are defined as lesions or parts of lesions that outside of the brain lobe masks, towards the brain stem, and internal capsule.

| S8 N=42 | S9 N=105 | S10 N=241 | S11 N=240 | S12 N=87 | S13 N=245 | S14 N=190 | S15 N=111 | P value |
|---|---|---|---|---|---|---|---|---|
| 1.35 ± 0.81 | 6.99 ± 6.30 | 0.71 ± 0.46 | 8.35 ± 7.36 | 18.00 ± 11.01 | 7.28 ± 5.08 | 15.71 ± 12.19 | 6.91 ± 7.89 | <0.000 |
| 0.66 ± 0.78 | 4.55 ± 3.84 | 0.16 ± 0.23 | ± 5.15 | 10.91 ± 6.03 | 4.80 ± 3.27 | 9.50 ± 6.50 | 4.79 ± 5.31 | <0.000 |
| 1.11 ± 0.68 | 3.61 ± 2.04 | 0.46 ± 0.35 | 3.93 ± 2.26 | 7.15 ± 3.13 | 4.03 ± 1.85 | 5.66 ± 2.68 | 3.66 ± 2.33 | <0.000 |
| 0.75 ± 0.65 | 2.62 ± 1.58 | 0.21 ± 0.32 | 2.69 ± 1.77 | 5.54 ± 3.14 | 1.83 ± 1.07 | 3.80 ± 2.31 | 2.87 ± 2.02 | <0.000 |
| 1.31 ± 0.58 | 3.28 ± 1.38 | 0.84 ± 0.43 | 3.61 ± 1.58 | 5.39 ± 1.69 | 3.49 ± 1.04 | 4.53 ± 1.65 | 3.05 ± 1.58 | <0.000 |
| 0.27 ± 0.36 | 1.27 ± 1.05 | 0.10 ± 0.14 | 1.36 ± 0.96 | 2.11 ± 1.11 | 2.14 ± 1.43 | 1.30 ± 1.05 | 1.03 ± 1.14 | <0.000 |
| 0.07 ± 0.08 | 0.32 ± 0.32 | 0.03 ± 0.04 | 0.31 ± 0.26 | 0.60 ± 0.50 | 0.56 ± 0.47 | 0.34 ± 0.33 | 0.26 ± 0.24 | <0.000 |
| 0.04 ± 0.05 | 0.06 ± 0.09 | 0.03 ± 0.04 | 0.07 ± 0.09 | 0.29 ± 0.29 | 0.11 ± 0.14 | 0.07 ± 0.09 | 0.04 ± 0.06 | <0.000 |
| 0.47 ± 0.44 | 0.09 ± 0.15 | 0.64 ± 0.48 | 0.13 ± 0.23 | 0.11 ± 0.11 | 0.18 ± 0.34 | 0.09 ± 0.12 | 0.17 ± 0.27 | <0.000 |
| 0.05 ± 0.07 | 0.11 ± 0.11 | 0.04 ± 0.05 | 0.14 ± 0.14 | 0.22 ± 0.14 | 0.14 ± 0.14 | 0.12 ± 0.11 | 0.07 ± 0.09 | <0.000 |

6

## S.6.8.1 Supplementary results

Our model resulted in 15 distinct subgroups with unique combinations of brain MRI markers. Below is a more detailed description of the brain MRI markers and the most important characteristics per subgroup. Subjective and relative cut-off points where used for the below used description of the subgroups. For continuous variables the subgroups were split into three thirds, with the highest, moderate and lowest values. WMH shape was considered as regular/moderate/irregular looking at all shape markers together and assessing the main shape. A low solidity, low convexity, high concavity index, and high fractal dimension indicate a more irregular shape. A high eccentricity indicates a rounder shape, while a low eccentricity indicates a more elongated shape. Total WMH volumes were used to describe relatively low/moderate/high WMH volumes. WMH below ~20 ml were considered relatively low volumes, between ~20 ml and ~30 ml relatively moderate volumes and above ~30 ml as relatively high volumes. Total brain volumes above ~74% of intracranial volume were considered as relatively low atrophy, between ~72 and ~74% of intracranial volume as relatively moderate atrophy and below ~72% of intracranial volume as relatively severe atrophy.

Subgroup 1 has relatively low WMH volumes, no infarcts, microbleeds or enlarged PVS, a moderately irregular WMH shape and relatively low atrophy.

Subgroup 2 has relatively high WMH volumes, a high prevalence of subcortical infarcts (100%), some cortical, and cerebellar infarcts, an irregular WMH shape, some enlarged PVS (in and around the basal ganglia) and microbleeds, and relatively severe cerebral atrophy.

Subgroup 3 has relatively high WMH volumes, some enlarged PVS (in and around the basal ganglia), an irregular WMH shape, and relatively severe cerebral atrophy.

Subgroup 4 has relatively low WMH volumes, no infarcts, almost no enlarged PVS, a relatively regular WMH shape, some microbleeds, and relatively low cerebral atrophy.

Subgroup 5 has relatively low WMH volumes, cerebellar infarcts (98%), some enlarged PVS (in and around the basal ganglia, and white matter) and microbleeds, a moderately irregular WMH shape, and moderate cerebral atrophy.

Subgroup 6 has relatively low WMH volumes, a moderately irregular WMH shape, no infarcts, no enlarged PVS or microbleeds, and moderate cerebral atrophy.

Subgroup 7 has relatively low WMH volumes, no infarcts, a relatively regular WMH shape, enlarged PVS (in the white matter 100%), no microbleeds, and moderate cerebral atrophy.

Subgroup 8 has relatively low WMH volumes, a relatively regular WMH shape, enlarged PVS (mostly in and around the basal ganglia, and some in the white matter), a high prevalence of subcortical infarcts (100%) and a relatively low amount of cerebral atrophy.

Subgroup 9 has moderately high WMH volumes, a relatively irregular WMH shape, the most microbleeds (66%), no infarcts, some enlarged PVS (in the white matter), and moderate cerebral atrophy.

Subgroup 10 has the lowest WMH volumes, no infarcts or enlarged PVS, the most regular WMH shape, and the lowest amount of cerebral atrophy (the highest brain volumes). Furthermore, this subgroup has the lowest number of participants with hypertension (64%), type 2 diabetes (4%), and includes the most female participants (81%).

Subgroup 11 has moderately high WMH volumes, a relatively irregular WMH shape, no infarcts, some microbleeds, enlarged PVS (mostly in the white matter, 99%; basal ganglia: 8%), and moderate cerebral atrophy.

Subgroup 12 has the highest WMH volumes, some subcortical infarcts, some PVS (in and around the basal ganglia, and whole brain), the most irregular WMH shape, and the most severe cerebral atrophy. Moreover, this subgroup has the highest deep WMH volumes in the temporal lobe ($0.29 \pm 0.29$ ml) and the highest percentage of participants with hypertension (90%).

Subgroup 13 has moderately high WMH volumes, no infarcts or enlarged PVS, a relatively irregular WMH shape, and a relatively low amount of cerebral atrophy.

Subgroup 14 has relatively high WMH volumes and a relatively irregular WMH shape, some enlarged PVS (in and around the basal ganglia, and in the white matter), some subcortical infarcts, a large amount of cerebellar infarcts (99%), some cortical infarcts, and a relatively high amount of cerebral atrophy.

Subgroup 15 has moderately high WMH volumes, a moderately irregular WMH shape, some cerebellar infarcts (29%), a large amount of cortical infarcts (100%), some subcortical infarcts, a relatively high amount of cerebral atrophy, some microbleeds, and some enlarged PVS (in and around the basal ganglia, and in the white matter).

6

CHAPTER

7

# STUDY PROTOCOL OF THE WHIMAS: IDENTIFICATION OF NOVEL 7T MRI WHITE MATTER HYPERINTENSITY SHAPE AND BRAIN CLEARANCE MARKERS FOR CEREBRAL SMALL VESSEL DISEASE

Jasmin Annica Kuhn-Keller, Ingmar Eiling, Lydiane Hirschler, Lena Václavů, Marie-Noëlle Witjes-Ané, Marjolein Wijngaarden, Martijn Nagtegaal, Ece Ercan, Nathaly Rius Ottenheim, Marjan van der Elst, Evelien Sohl, Mark A. van Buchem, Simon Mooijaart, Matthias J.P. van Osch, Jeroen de Bresser.

# 7.1 ABSTRACT

Sporadic cerebral small vessel disease (SVD) has heterogeneous underlying pathology and current SVD MRI markers do not accurately capture this heterogeneity. Novel ultra-high field (7T) brain MRI markers provide a window of opportunity to study early changes and potential determinants of SVD. White matter hyperintensity (WMH) shape is a relatively novel MRI marker of SVD and has shown prognostic potential. However, the exact microstructural changes within or surrounding WMHs or potential causes related to WMH shape variations are unknown. Furthermore, impaired brain clearance via the recently discovered brain glymphatic system may be another early change or potential cause of SVD. In the WHIMAS (white matter hyperintensity shape and glymphatics study) we aim to study the link between WMH and especially their shape with brain clearance and other MRI markers on ultra-high field (7T) brain MRI and show if these markers are associated with cognitive functioning in older adults with memory complaints.

The WHIMAS is a cross-sectional study that will be conducted at the Leiden University Medical Center (LUMC). Fifty outpatients from the memory/geriatric clinic, aged 65 years or older will be recruited for a 3T and a 7T MRI scan, as well as a standardised neuropsychological test battery (domains: memory, executive function, visuoconstruction, and processing speed). We will assess WMH shape markers (solidity, convexity, concavity index, fractal dimension, and eccentricity) and brain clearance markers (CSF-BOLD-coupling, CSF-mobility) and study their relation to other MRI markers and cognitive functioning.

We aim to understand variations in WMH shape and find their relation to cerebral SVD and markers of brain clearance and cognitive functioning. These markers early in the disease process of SVD are extremely important as they may represent a basis for future patient selection for lifestyle interventions or for treatment trials aimed at prevention of dementia.

## 7.2 STRENGTHS AND LIMITATIONS OF THIS STUDY

- In depth study of the link between white matter hyperintensities and especially their shape with brain clearance and other MRI markers on ultra-high field (7T) brain MRI in a memory clinic population.
- Advanced and novel imaging techniques will be used both at 3T and ultra-high field (7T) MRI combined with novel advanced image processing techniques.
- In depth study of the relation between white matter hyperintensity shape and glymphatics markers and cognitive functioning.
- This observational study serves to steer future investigations and could be extended into a longitudinal study.
- The studied markers early in the disease process of cerebral small vessel disease are extremely important as they may represent a basis for future patient selection for lifestyle interventions or for treatment trials aimed at prevention of dementia.

## 7.3 INTRODUCTION

Dementia is often characterized by a combination of neurovascular and neurodegenerative disease processes and mixed pathologies are common.[1] The most common mixed pathology is Alzheimer's dementia (AD) and cerebral small vessel disease (SVD).[2,3] SVD contributes to the clinical phenotype of dementia in around 45% of dementia cases.[2–4] There are two main types SVD in an ageing population. One is SVD due to arteriolosclerosis, often related to hypertension.[5] The other one is cerebral amyloid angiopathy, characterized by progressive amyloid accumulation in the vessel walls.[5] Current SVD markers, such as white matter hyperintensities of presumed vascular origin (WMH), are unspecific and they fail to accurately capture the heterogeneity of SVD pathology. Therefore, novel brain MRI markers are needed to identify early changes and potential determinants of SVD. These markers are extremely important early in the disease process of SVD as they may represent a basis for future patient selection for lifestyle interventions or as outcome markers for treatment trials (such as currently being developed for cerebral amyloid angiopathy[6] aimed at prevention of dementia.

WMH are the key brain MRI manifestation of cerebral SVD.[7] Around 92% of all individuals over 60 years of age have WMHs[8–10] and a higher WMH burden is a risk factor for occurrence of stroke and dementia.[10] Especially the volume of WMH has been extensively studied, but this is a generic and non-specific marker that only has modest prognostic value.[11] Although there is considerable variation in the shape of WMH, this marker has received only little attention.[12] Recent studies have shown that normal appearing white matter around WMH that will progress on follow-up

MRI scans, already showed changes in structural integrity and hemodynamics at baseline.[13,14] Furthermore, WMH typically localize at vascular endzones and progress along more proximal parts of the perforating arteries.[15] How the perforating arteries are affected depends on the underlying pathological changes, such as large vessel atheromas at the origin of perforating arteries, small vessel atheromas or micro-embolisms.[16,17] These pathological changes may lead to hypoperfusion, defective cerebrovascular reactivity, and blood-brain barrier dysfunction,[11] which in turn may be related to increase of WMH and thus also changes in their shape.[12,17] Previous studies have also indicated that WMH shape may provide a better indication of underlying pathophysiological mechanisms than WMH volume alone and may harbor strong prognostically relevant information.[12,18–20]

SVD is a heterogeneous disease with many possible underlying causes. An important factor leading to brain changes in SVD might be impaired clearance of waste products, which has been linked to aging and dementia pathology.[7] The process of brain clearance is postulated to be partly driven by the glymphatic system, where cerebrospinal fluid (CSF) and interstitial fluid 'flush' brain tissue and transport waste products out of the brain via perivascular spaces. Some first studies have shown that in cerebral amyloid angiopathy and Alzheimer's dementia glymphatic function might be impaired.[21] Currently, brain clearance related processes can only be studied invasively in humans, for example by contrast-enhanced MRI following intrathecal injection.[22] This limitation made it difficult to implement research related to glymphatic dysfunction into clinical study protocols. However, recently developed novel ultra-high field (7T) brain MRI markers provide a window of opportunity to study the human glymphatic system in a non-invasive way.

In the WHIMAS (white matter hyperintensity shape and glymphatics study) we aim to study the link between WMH, and especially their shape, with brain clearance and other MRI markers on high field (3T) and ultra-high field (7T) brain MRI. Furthermore, we aim to study the relation between WMH shape and glymphatics markers and cognitive functioning. Studying these imaging markers in SVD is important because at an early stage cerebral SVD is a target for preventive treatment that may postpone or even prevent the occurrence of dementia and stroke. Our study contributes to the first steps in this research into early detection of dementia. We specifically strive for early detection of the potentially treatable/modifiable part of the dementia pathology, namely SVD. Previous studies have already shown that early lifestyle interventions in populations at risk can slow the pathophysiological processes of cerebral SVD.[23–25] However, it is currently impossible to non-invasively identify individuals who have an increased risk of dementia at an early stage of the disease and who may benefit most

from available lifestyle interventions or from future preventive treatment. We aim to pave the way for personalized medicine approaches by finding brain MRI biomarkers that can identify these individuals at risk.

## 7.4 METHODS

### 7.4.1 Study design

This study is an observational cross-sectional study that will be conducted at the Leiden University Medical Center (LUMC). The study (NL78641.058.21) was approved by the Medical Ethics Committee Leiden Den Haag Delft (reg. P21.114) and is registered on ClinicalTrials.gov (ID-number: NCT06010511). The patient and funding organization Alzheimer Nederland has funded part of this research and is involved in the conduct and in the dissemination plans of our study. The study involves a whole-day visit at the LUMC for each participant and includes the following procedures: a 3T brain MRI scan of 60 minutes, a 7T brain MRI scan of 60 minutes, a neuropsychological assessment, and questionnaires on demographics and vascular risk factors. An overview of the study procedures can be found in figure 7.1. Objectives of the study include the following: 1) To study the association of a more complex WMH shape with anatomical, hemodynamic, and white matter integrity abnormalities on MRI; 2) To study the association between WMH shape and cognition/other cerebral SVD markers; 3) To study the association of novel MRI markers of brain clearance with cerebral SVD markers and cognition.

7

| Inclusion | Study assessments | 3T MRI | 7T MRI |
|---|---|---|---|
| 50 participants from memory/geriatric clinic ≥65 years of age | Demographic information:<br>▪ Age<br>▪ Sex<br>▪ Education level | ▪ 3D T1<br>▪ 3D FLAIR<br>▪ T2<br>▪ SWI<br>▪ DWI<br>▪ CSF-BOLD<br>▪ Q-flow<br>▪ MR-fingerprinting<br>▪ Inhomogeneous magnetic transfer<br>▪ Flow-territory mapping | ▪ 3D T1<br>▪ 3D FLAIR<br>▪ 3D T2<br>▪ T2*<br>▪ CSF-Stream<br>▪ Phase contrast |
| Exclusion criteria:<br>▪ Claustrophobia<br>▪ Contraindications for MRI<br>▪ Regular use of benzodiazepines<br>▪ Initiated treatment with antidepressants less than 6 weeks prior to inclusion<br>▪ Not being able to provide written informed consent<br>▪ Individuals who have been declared mentally incapacitated<br>▪ Other severe neurological disease outside of the dementia spectrum<br>▪ Cognitive impairment due to known other neurological disease<br>▪ Previous brain surgery | Clinical information:<br>▪ Sleep habits<br>▪ Height and weight<br>▪ Medical history<br>▪ Psychiatric comorbidity<br>▪ Medication<br>▪ Blood values<br>▪ Cardiovascular risk factor questionnaire: hypertension, diabetes, arrythmia, alcohol consumption, smoking, physical activity, and medical history<br><br>Neuropsychological assessment:<br>▪ Mini-mental state examination<br>▪ Clock drawing<br>▪ 15-Word Verbal Learning Test<br>▪ Visual Association Test<br>▪ Stroop Color Word Test<br>▪ Trail Making Test A&B<br>▪ Letter Digit Substitution Test<br>▪ Animal fluency test<br>▪ Hospital anxiety and depression scale<br>▪ Informant Questionnaire on Cognitive Decline in the Elderly | | |

**Figure 7.1. Overview of the study procedures.**
3D T1: T1-weighted MRI scan; 3D FLAIR: 3D fluid-attenuated inversion recovery SWI: susceptibility-weighted scan; DWI: diffusion weighted scan; CSF: cerebrospinal fluid selective-T2prep-REadout with Acceleration and Mobility encoding

## 7.4.2 Population

We will prospectively include 50 outpatients over 65 years of age with memory complaints from the memory/geriatric clinic at one of their first visits, at the Leiden University Medical Center or the Alrijne hospital in Leiden. All participants give written informed consent prior to any study procedures. The current study involves 3T and 7T MRI and newly developed sequences and markers, especially for brain clearance, which have not been applied in patient populations before. Therefore, we performed the sample size calculation based on the WMH shape analysis. To provide a frame of reference we performed a sample size calculation using data from a previous manuscript.[26] The linear regression performed on hypertension and convexity, corrected for age and sex, was performed with data of 71 non-demented older adults. The same WMH shape analysis pipeline was used in the previous study as we aim to use in the current study. Using the data from this significant results, the sample size calculation performed in G*Power[27] showed a result of 79 participants. As the data used in the calculation was obtained from community-dwelling individuals, we expect higher effect sizes in our study consisting of a memory clinic population.

In this population, the prevalence and severity of SVD and thus WMH will be higher, justifying our assumption of increased power. At the same time we do not want to risk an underpowered study. For example, in a case-control study comparing type 2 diabetes patients with healthy controls an average effect size of 0.37 for a more complex WMH shape was found.[12] To illustrate this we have calculated the sample size with two different effect sizes that are higher than the one used in the initial calculation (0.2 and 0.3), but still lower than 0.37 (as found by De Bresser et al., 2018). These calculations resulted in a sample size of 42 or 29 participants. Therefore, a number of 50 participants should give the necessary statistical power to overcome biological and clinical variation.

In order to be eligible to participate in the current study, a participant must meet all of the following criteria; participants receive care in the outpatient memory clinic or the geriatric clinic of the LUMC or the memory clinic of the Alrijne hospital in Leiden. Inclusion can be done if the participant is over 65 years of age and eligible for MRI. Moreover, the participant has to be native-level in the Dutch language.

A potential participant who meets any of the following criteria will be excluded from participation in this study:
 • Claustrophobia
 • Contraindications for MRI such as metal implants and pacemaker
 • Regular use of benzodiazepines
 • Initiated treatment with antidepressants less than 6 weeks prior to inclusion
 • Not being able to provide written informed consent (assessed by the treating physician)
 • Individuals who have been declared mentally incapacitated
 • Other severe neurological disease outside of the dementia spectrum
 • Cognitive impairment due to known other neurological disease
 • Previous brain surgery

## 7.4.3 Clinical data

We will collect basic demographic information including age, sex and education level. Information about medical history, psychiatric comorbidity, medication, and current blood values are extracted from the clinical file of the participant. Furthermore, a cardiovascular risk factor questionnaire is used to gather information about hypertension, diabetes, arrythmia, alcohol consumption, smoking, physical activity, and medical history. Another questionnaire includes questions about sleep

habits, using an adapted version of the Pittsburg Sleep Quality Index.[28] The sleep questionnaire is included, because of the influence of sleep on the glymphatic system.

The following tests are included in the neuropsychiatric assessment:
- Mini-mental state examination[29]
- Clock drawing[30]
- 15-Word Verbal Learning Test (immediate and delayed)[31]
- Visual Association Test[32]
- Stroop Color Word Test, 40 item version[33]
- Trail Making Test A&B[34,35]
- Letter Digit Substitution Test[36]
- Animal fluency test[37]
- Hospital anxiety and depression scale[38]
- Informant Questionnaire on Cognitive Decline in the Elderly[39]

## 7.4.4 MRI scans

All MRI scans are performed at the LUMC using a 3T Philips Ingenia Elition and a 7T Philips Achieva MRI scanner (Philips Healthcare). The MRI scan protocols are shown in table 7.1.

Conventional (3T) brain MRI scans will be used to determine global and functional markers of cerebral SVD, like WMH volume and presence of lacunes, microbleeds and superficial siderosis (on a 3D T1-weighted (3D T1), 3D fluid-attenuated inversion recovery (3D FLAIR), susceptibility-weighted imaging (SWI), and a diffusion weighted imaging (DWI) scan), hemodynamics (flow territory mapping;[40]). Furthermore, white matter structural integrity will be measured with a MR fingerprinting sequence[41] and an inhomogeneous magnetization transfer (ihMT) scan[42]. An fMRI scan technique will be used to measure CSF fluctuations in the 4th ventricle as a measure of brain clearance[43].

Ultra-high field (7T) brain MRI scans will be used to determine WMH shape (solidity, convexity, concavity index, fractal dimension, and eccentricity) and other markers of cerebral SVD in or surrounding the WMH, like enlarged perivascular spaces, (cortical) microinfarcts and microbleeds (on a T1-, T2-, FLAIR, and a T2*-weighted scan). Examples of WMH segmentations and the shape markers are shown in figures 7.2 and 7.3. Moreover, a recently implemented MRI technique called CSF-STREAM (CSF-selective-T2prepared REadout with Acceleration and Mobility encoding) will be used to measure CSF-mobility in perivascular spaces, as a proxy of glymphatic activity[44]. An example of measurements obtained with this technique can be seen in figure 7.4.

Heart rate and respiratory signal will be measured during the scans (3T and 7T MRI) with standard vendor-supplied equipment, namely a respiratory belt and pulse oximeter.
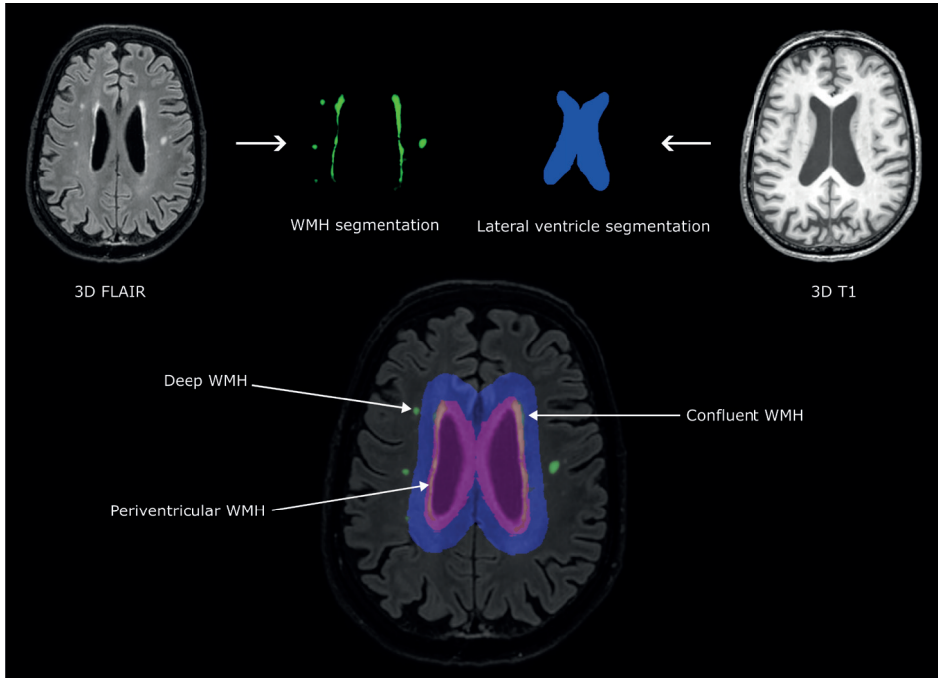


**Figure 7.2. Overview of the MRI image processing pipeline for WMH shape.** WMHs are automatically segmented from FLAIR MRI scans. T1-weighted scans are used to segment the lateral ventricles. The lateral ventricle masks are inflated and used to delineate between periventricular/confluent WMH. Then, the WMH shape markers are calculated on individual lesions.

7

**Table 7.1** MRI scan protocols on the 3T and 7T MRI scanner.

| | Purpose | Contrast parameters | Resolution (acquisition) | Resolution (reconstruction) | Field of View | Acquisition time (min) | Additional information |
|---|---|---|---|---|---|---|---|
| **3T MRI** | | | | | | | |
| 3D T1 | Anatomical information | TR/TE = 9.9/4.6 ms | 1 mm isotropic | 1 mm isotropic | 256 mm | 4:20 | Flip angle = 8° |
| 3D FLAIR | WMH, lacunes | TR/TI = 4800/1650 ms TE = 346 ms | $0.98 \times 0.98 \times 1.00$ mm³ | $0.92 \times 0.92 \times 0.5$ mm³ | 220 mm | 4:48 | Refocusing angle = 40° |
| T2 | Perivascular spaces | TR = 4490 ms; TE = 80 ms | $0.40 \times 0.50 \times 3.00$ mm³ | $0.22 \times 0.22 \times 3.00$ mm³ | 230 mm | 2:15 | Flip angle = 90° |
| SWI | Iron, microbleeds, superficial siderosis | TR = 31 ms; TE = 7.20 ms | $0.60 \times 0.60 \times 2.00$ mm³ | $0.23 \times 0.23 \times 1.00$ mm³ | 220 mm | 2:35 | Flip angle = 17° |
| DWI | Acute or recent ischemic lesions | TR = 3206 ms; TE = 67 ms; | $1.96 \times 2.44 \times 5.00$ mm³ | $0.86 \times 0.86 \times 5.00$ mm³ | 220 mm | 0:38 | b-value = 1000 |
| CSF_BOLD | CSF-BOLD coupling | TR = 370 ms; TE = 25 ms | $2.88 \times 2.88 \times 5.00$ mm³ | $2.40 \times 2.40 \times 5.00$ mm³ | 230 mm | 5:07 | Flip angle = 40° |
| Q-flow | Large vessel flow | TR/TE = 15/7.2 ms; | $0.45 \times 0.45 \times 4.00$ mm³ | $0.45 \times 0.45 \times 4.00$ mm³ | 230 mm | 1.02 | Venc =80 cm/s |
| MR-fingerprinting | White matter structural integrity; Myelin-water imaging | TR/TE = 15/3.0 ms | $1.00 \times 1.00 \times 4.00$ mm³ | $1.00 \times 1.00 \times 4.00$ mm³ | 240 mm | 5:00 | Flip angle range: 10.0° - 60.0° |
| Inhomogeneous magnetic transfer | White matter structural integrity | TR/TE = 90/1.31 ms | $2.29 \times 2.29 \times 5.00$ mm³ | $1.72 \times 1.72 \times 5.00$ mm³ | 220 mm | 7:17 | Flip angle = 7° |
| Flow territory mapping | Perfusion scan | TR/TE = 4550/16 ms | $2.50 \times 2.56 \times 5.00$ mm³ | $1.88 \times 1.88 \times 5.00$ mm³ | 240 mm | 4:56 | |

**7T MRI**

| | Purpose | Contrast parameters | Resolution (acquisition) | Resolution (reconstruction) | Field of View | Acquisition time (min) | Additional information |
|---|---|---|---|---|---|---|---|
| 3DT1 | Anatomical information | TR/TE = 4.2/1.9 ms | $0.90 \times 0.90 \times 0.90$ mm$^3$ | $0.85 \times 0.85 \times 0.90$ mm$^3$ | 246x 246x174 mm | 2:22 | Flip angle: 7° |
| 3D FLAIR | WMH, lacunes | TR/TI = 8000/2200 ms TE = 252 ms | $0.70 \times 0.70 \times 1.40$ mm$^3$ | $0.68 \times 0.68 \times 0.70$ mm$^3$ | 240x209x180 mm | 5:12 | Flip angle:90° |
| 3D TSE (T2) | Perivascular spaces, arteries | TR = 3000 ms TE = 283 ms | $0.75 \times 0.75 \times 0.75$ mm$^3$ | $0.65 \times 0.65 \times 0.75$ mm$^3$ | 250x250x190 mm | 4:06 | Flip angle=100° |
| T2* Duyn | Iron, microbleeds, superficial siderosis, veins | TR/TE = 1830/25 ms | $0.24 \times 0.24 \times 1.00$ mm$^3$ | $0.23 \times 0.23 \times 1.00$ mm$^3$ | 240x180x101 mm | 10:32 | Flip angle 60° |
| CSF-STREAM | CSF mobility in the perivascular spaces | TR = 3430 ms TE = 497 ms | $0.45 \times 0.45 \times 0.45$ mm$^3$ | $0.45 \times 0.45 \times 0.45$ mm$^3$ | 250x250x190 mm | 21:57 | Flip angle 90° degrees |
| 2x Phase contrast | CSF flow in/out of the cranium | TR/TE = 6.7/3.6 ms | $1.72 \times 1.72 \times 10.0$ mm$^3$ | $0.63 \times 0.63 \times 10.0$ mm$^3$ | 110x110 | 2x2:08 | Venc 10 cm/s and venc 80 cm/s Flip angle 4° |

7

# WMH shape markers



Solidity

$$\text{Solidity} = \frac{\text{Volume}}{\text{Convex Hull Volume}}$$

Convexity

$$\text{Convexity} = \frac{\text{Convex Hull Area}}{\text{Area}}$$

Concavity index

$$\text{Concavity index} = \sqrt{(2 - C)^2 + (1 - S)^2}$$

Fractal dimension

$$\text{Fractal Dimension} = \lim_{r \to 1} \frac{\log(n_r)}{\log\left(\frac{1}{r}\right)}$$

Eccentricity

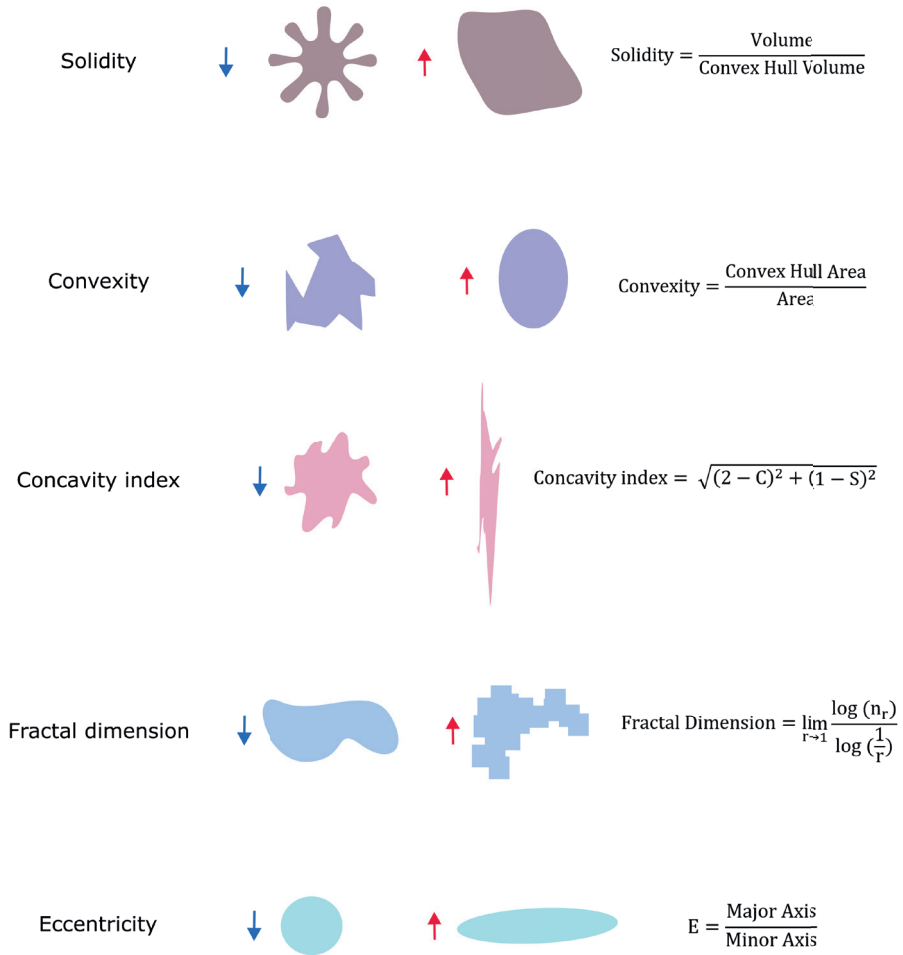$$E = \frac{\text{Major Axis}}{\text{Minor Axis}}$$

**Figure 7.3. Examples of shapes with high or low values of different shape markers**. Solidity, convexity, concavity index, and fractal dimension are calculated for periventricular/confluent WMH. Eccentricity and fractal dimension are the shape markers that are calculated for deep WMH.
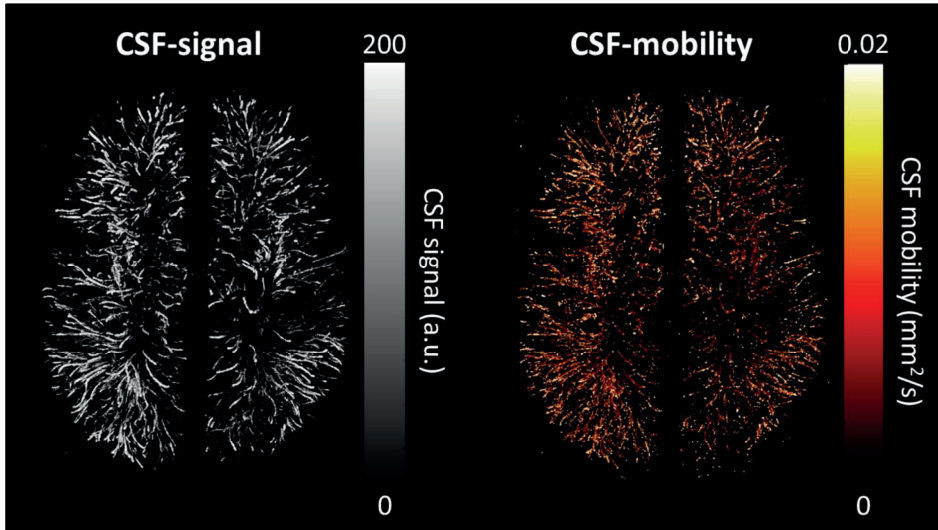
**Figure 7.4. Examples of images obtained with the CSF-STREAM sequence as a measure of glymphatic activity.** An image of the CSF-signal is shown on the left, and on the right is an example of a CSF-mobility map.

## 7.4.5 Statistics

Linear and logistic regression analyses will be performed to investigate the association between WMH shape and brain clearance/other MRI markers/cognitive functioning. Potentially confounding demographic variables, such as age, sex, level of education and vascular risk factors will be included as covariates for subsequent analyses. The distributions of the variables will be tested for normality. If applicable, appropriate nonparametric test will be used of variables will be log transformed. For the main analyses the significance will be set at $p < 0.05$.

## 7.5 DISCUSSION

SVD in an ageing population has heterogeneous underlying pathology which current MRI markers do not accurately capture. Novel 7T brain MRI markers provide a window of opportunity to study early structural changes and potential determinants of SVD. WMH shape is a relatively novel MRI marker and earlier studies have shown prognostic potential.[18,19] However, the exact microstructural changes within or surrounding WMHs or potential determinants related to WMH shape variations remain unknown. Furthermore, impaired brain clearance via the recently discovered brain glymphatic system may be another early change or potential cause of SVD.[45] In the WHIMAS study we aim to study the link between WMH and especially their shape with brain clearance and other MRI markers on high field (3T) and ultra-high

field (7T) brain MRI. Furthermore, we aim to study the relation between WMH shape and glymphatics markers and cognitive functioning.

The WHIMAS study will generate data that can be used to postulate underlying mechanisms related to WMH shape variations as we will study the association between a more complex WMH shape and advanced structural and functional markers of cerebral SVD. We expect to gain a better understanding of the structural correlates of WMH shape variation using and combining the advanced measurements at 7T MRI. WMH shape has previously been related to an increased long-term dementia risk[18] and increased long-term stroke- and mortality risk.[19] In our study we expect that a more irregular shape of WMH will be related to disease severity (captured by other SVD markers) and cognition (memory, executive function, visuoconstruction, and processing speed). Moreover, we expect to capture WMH shape and other structures that may influence shape (such as veins) better at 7T MRI due to an increased spatial resolution. This will allow a more precise investigation of WMH shape in relation to other SVD markers and structural changes.

Animal studies suggest that dysfunction of the glymphatic system plays a major role in the initiation and progression of not only neurodegenerative pathologies, but also SVD.[45] Novel non-invasive markers of brain clearance that we will use in our study will allow us to study brain clearance in vivo in a non-invasive way. In our study we expect to find an association between CSF mobility and disease severity. Moreover, the BOLD-CSF coupling has been found to be reduced in patients with Alzheimer's disease[46] and cerebral amyloid angiopathy.[47] Therefore, in our study we expect that the CSF-BOLD coupling will be reduced in our patient population, and will show an association with disease severity.

Biomarkers early in the disease process of cerebral SVD are extremely important as they may represent a basis for future patient selection for lifestyle interventions and as outcome markers of treatment trials aimed at prevention or treatment of dementia. The results of our study will contribute as a body of evidence for novel brain MRI markers that could hopefully serve as early biomarkers for SVD.

Strengths of our study include the specific patient population and the use of advanced ultra-high field 7T MRI state of the art imaging techniques in combination with advanced image processing techniques largely developed within our research group. The current study serves to steer future investigations and could be extended into a longitudinal study.

In conclusion, in the WHIMAS study we aim to find brain MRI changes that represent early determinants or changes of cerebral SVD. These markers early in the disease process of SVD are extremely important as they may represent a basis for future patient selection for lifestyle interventions or for treatment trials aimed at prevention of dementia.

## 7.6 ACKNOWLEDGEMENTS

7

## 7.7 REFERENCES

1. Jellinger KA, Attems J. Challenges of multimorbidity of the aging brain: a critical update. J Neural Transm. 2015;122:505–21.

2. Kovacs GG, Milenkovic I, Wöhrer A, et al. Non-Alzheimer neurodegenerative pathologies and their combinations are more frequent than commonly believed in the elderly brain: A community-based autopsy series. Acta Neuropathol. 2013;126:365–84.

3. Gorelick PB, Scuteri A, Black SE, et al. Vascular contributions to cognitive impairment and dementia: A statement for healthcare professionals from the American Heart Association/ American Stroke Association. Stroke. 2011;42:2672–713.

4. Brundel M, Heringa SM, De Bresser J, et al. High Prevalence of Cerebral Microbleeds at 7Tesla MRI in Patients with Early Alzheimer's Disease. Journal of Alzheimer's Disease. 2012;31:259–63.

5. Pantoni L. Cerebral small vessel disease: from pathogenesis and clinical characteristics to therapeutic challenges. Lancet Neurol. 2010;9:689–701.

6. Voigt S, Koemans EA, Rasing I, et al. Minocycline for sporadic and hereditary cerebral amyloid angiopathy (BATMAN): study protocol for a placebo-controlled randomized double-blind trial. Trials. 2023;24:1–6.

7. Wardlaw JM, Smith C, Dichgans M. Mechanisms of sporadic cerebral small vessel disease: Insights from neuroimaging. Lancet Neurol. 2013;12:483–97.

8. Bos D, Wolters FJ, Darweesh SKL, et al. Cerebral small vessel disease and the risk of dementia: A systematic review and meta-analysis of population-based evidence. Alzheimer's and Dementia. 2018;14:1482–92.

9. de Leeuw F -E., de Groot JC, Oudkerk M, et al. Hypertension and cerebral white matter lesions in a prospective cohort study. Brain. 2002;125:765–72.

10. Debette S, Markus HS. The clinical importance of white matter hyperintensities on brain magnetic resonance imaging: systematic review and meta-analysis. BMJ. 2010;341:288.

11. Alber J, Alladi S, Bae H, et al. White matter hyperintensities in vascular contributions to cognitive impairment and dementia (VCID): Knowledge gaps and opportunities. Alzheimer's & Dementia: Translational Research & Clinical Interventions. 2019;5:107–17.

12. De Bresser J, Kuijf HJ, Zaanen K, et al. White matter hyperintensity shape and location feature analysis on brain MRI; Proof of principle study in patients with diabetes. Sci Rep. 2018;8:1–10.

13. Promjunyakul NO, Dodge HH, Lahna D, et al. Baseline NAWM structural integrity and CBF predict periventricular WMH expansion over time. Neurology. 2018;90:e2107–18.

14. Maillard P, Fletcher E, Lockhart SN, et al. White matter hyperintensities and their penumbra lie along a continuum of injury in the aging brain. Stroke. 2014;45:1721–6.

15. Duering M, Csanadi E, Gesierich B, et al. Incident lacunes preferentially localize to the edge of white matter hyperintensities: insights into the pathophysiology of cerebral small vessel disease. Brain. 2013;136:2717–26.

16. Wardlaw JM, Smith C, Dichgans M. Small vessel disease: mechanisms and clinical implications. Lancet Neurol. 2019;18:684–96.

17. Gouw AA, Seewann A, Van Der Flier WM, et al. Heterogeneity of small vessel disease: A systematic review of MRI and histopathology correlations. J Neurol Neurosurg Psychiatry. 2011;82:126–35.

18. Keller JA, Sigurdsson S, Klaassen K, et al. White matter hyperintensity shape is associated with long-term dementia risk. Alzheimer's and Dementia. 2023;19:5632–5641.

19. Ghaznawi R, Geerlings MI, Jaarsma-Coes M, et al. Association of White Matter Hyperintensity Markers on MRI and Long-term Risk of Mortality and Ischemic Stroke. Neurology. 2021;96:e2172–83.

20. Ghaznawi R, Geerlings MI, Jaarsma-Coes MG, et al. The association between lacunes and white matter hyperintensity features on MRI: The SMART-MR study. Journal of Cerebral Blood Flow and Metabolism. 2019;39:2486–96.

21. Peng W, Achariyar TM, Li B, et al. Suppression of glymphatic fluid transport in a mouse model of Alzheimer's disease. Neurobiol Dis. 2016;93:215–25.

22. Ringstad G, Valnes LM, Dale AM, et al. Brain-wide glymphatic enhancement and clearance in humans assessed with MRI. JCI Insight. 2018;3:e121537.

23. Bath PM, Wardlaw JM. Pharmacological treatment and prevention of cerebral small vessel disease: a review of potential interventions. Int J Stroke. 2015;10:469–78.

24. Dichgans M, Zietemann V. Prevention of vascular cognitive impairment. Stroke. 2012;43:3137–46.

25. Mok V, Kim JS. Prevention and Management of Cerebral Small Vessel Disease. J Stroke. 2015;17:111–22.

26. Keller JA, Kant IMJ, Slooter AJC, et al. Different cardiovascular risk factors are related to distinct white matter hyperintensity MRI phenotypes in older adults. Neuroimage Clin. 2022;35. doi: 10.1016/j.nicl.2022.103131

27. Faul F, Erdfelder E, Lang AG, et al. G*Power 3: A flexible statistical power analysis program for the social, behavioral, and biomedical sciences. Behav Res Methods. 2007;39:175–91.

28. Buysse DJ, Reynolds CF, Monk TH, et al. The Pittsburgh sleep quality index: A new instrument for psychiatric practice and research. Psychiatry Res. 1989;28:193–213.

29. Folstein MF, Folstein SE, McHugh PR. 'Mini-mental state'. A practical method for grading the cognitive state of patients for the clinician. J Psychiatr Res. 1975;12:189–98.

30. Royall DR, Cordes JA, Polk M. CLOX: an executive clock drawing task. J Neurol Neurosurg Psychiatry. 1998;64:588–94.

31. Brand N, Jolles J. Learning and retrieval rate of words presented auditorily and visually. J Gen Psychol. 1985;112:201–10.

32. Lindeboom J, Schmand B, Tulner L, et al. Visual association test to detect early dementia of the Alzheimer type. J Neurol Neurosurg Psychiatry. 2002;73:126–33.

33. Stroop, J. R. (1935). Studies of Interference in Serial Verbal Reactions. Journal of Experimental Psychology, 18, 643-662.

34. Reitan RM. The relation of the trail making test to organic brain damage. J Consult Psychol. 1955;19:393–4.

35. Tombaugh TN. Trail Making Test A and B: normative data stratified by age and education. Arch Clin Neuropsychol. 2004;19:203–14.

36. Van Der Elst W, Van Boxtel M, Van Breukelen G, et al. The Letter Digit Substitution Test: normative data for 1,858 healthy participants aged 24-81 from the Maastricht Aging Study (MAAS): influence of age, education, and sex. J Clin Exp Neuropsychol. 2006;28:998–1009.

37. Van Der Elst W, Van Boxtel MPJ, Van Breukelen GJP, et al. Normative data for the Animal, Profession and Letter M Naming verbal fluency tests for Dutch speaking participants and the effects of age, education, and sex. J Int Neuropsychol Soc. 2006;12:80–9.

38. Zigmond AS, Snaith RP. The Hospital Anxiety and Depression Scale. Acta Psychiatr Scand. 1983;67:361–70.

39. Jorm AF, Jacomb PA. The Informant Questionnaire on Cognitive Decline in the Elderly (IQCODE): socio-demographic correlates, reliability, validity and some norms. Psychol Med. 1989;19:1015–22.

40. Gevers S, Bokkers RP, Hendrikse J, et al. Robustness and Reproducibility of Flow Territories Defined by Planning-Free Vessel-Encoded Pseudocontinuous Arterial Spin-Labeling. American Journal of Neuroradiology. 2012;33:E21–5.

7

**41.** Jiang Y, Ma D, Seiberlich N, et al. MR fingerprinting using fast imaging with steady state precession (FISP) with spiral readout. Magn Reson Med. 2015;74:1621–31.

**42.** Ercan E, Varma G, Mädler B, et al. Microstructural correlates of 3D steady-state inhomogeneous magnetization transfer (ihMT) in the human brain white matter assessed by myelin water imaging and diffusion tensor imaging. Magn Reson Med. 2018;80:2402–14.

**43.** Fultz NE, Bonmassar G, Setsompop K, et al. Coupled electrophysiological, hemodynamic, and cerebrospinal fluid oscillations in human sleep. Science (1979). 2019;366:628–31.

**44.** Hirschler L., Aldea R., Petitclerc L., Ronen I., de Koning P.J.H., van Buchem, M. A., van Osch M.J.P. High resolution T2-prepared MRI enables non-invasive assessment of CSF flow in perivascular spaces of the human brain. In: Proceedings of the 28th Annual Meeting of ISMRM, Montréal, Canada, 2019. Abstract 0746.

**45.** Benvenuto H, Nedergaard M. Cerebral small vessel disease: A glymphopathy? Curr Opin Neurobiol. 2022;72:15–21.

**46.** Han F, Chen J, Belkin-Rosen A, et al. Reduced coupling between cerebrospinal fluid flow and global brain activity is linked to Alzheimer disease-related pathology. PLoS Biol. 2021;19:e3001233.

**47.** Hirschler L., Zanon Zotin, M.C., Lewis, L.D., Horn, M.J., Gurol, M.E, Viswanathan, A., Polimeni, J.R., van Osch, M.J.P., van Veluw, S.J., and Greenberg, S.M. Coupling between low-frequency hemodynamic oscillations and cerebrospinal fluid flow is altered in patients with cerebral amyloid angiopathy. ISMRM conference abstract 2023.

7

CHAPTER

8

# GENERAL DISCUSSION

The overarching aim of this thesis was to exploit the shape of WMHs for better characterization of WMHs to improve the clinical interpretation of WMHs and to investigate related disease outcomes. This thesis was mostly based on non-demented and community-dwelling older individuals. Moreover, a study set up focusing on a memory-clinic population was discussed to get more pathology-focused insights into the formation of WMH. In this chapter the methodology, the relation of the findings to other areas of research, future directions, as well as clinical implications are discussed.

## 8.1 KEY FINDINGS OF THIS THESIS

- Different cardiovascular risk factors were found to be related to a distinct pattern of WMH shape markers in non-demented older adults (**Chapter 2**).
- A more irregular shape of periventricular/confluent WMH was associated with a larger increase in WMH volume, and with occurrence of new subcortical infarcts, new microbleeds, enlargement of perivascular spaces, and new cerebellar infarcts 5.2 years later (**Chapter 3**).
- A more complex shape of periventricular/confluent WMH was found to be related to cognitive decline over 5.2 years (**Chapter 4**).
- A more irregular shape of periventricular/confluent WMH was associated with an increased long-term dementia risk over 10 years (**Chapter 5**).
- Distinct brain MRI phenotypes were identified using hierarchical clustering that are related to varying long-term risks of developing dementia (**Chapter 6**).

## 8.2 WMH SHAPE: ADDED VALUE AND CHALLENGES

Volume is a commonly used quantitative, yet crude marker to assess WMHs. In clinical practice the WMHs of two patients can be similar in volume, but can appear visually very different from each other. These visual differences can be described as differences in the shape of WMHs. The findings of this thesis and previous work justify the use of WMH shape as an additional marker to the more commonly used, but unspecific WMH volume (**Chapters 2-6**,[1–3]).There are, however, a few limitations to consider when applying WMH shape.

With current methods of WMH volumetric quantification, separate measures can be obtained for deep, periventricular, and confluent WMH.[3] However, for WMH shape analysis we have to merge periventricular and confluent WMH into one group, because splitting them would add an artificial edge in the WMHs which in turn could falsify the shape analysis. Early periventricular WMH will, however, represent

a different disease stage or process of ageing compared to the bigger confluent WMH.[4] In more progressed small vessel disease (SVD) cases, not only periventricular/confluent WMH will have merged to one big lesion, but also periventricular/confluent WMH and deep WMH can form confluent WMHs. This will result in a higher volume of confluent WMH and also in a relatively lower volume of periventricular and deep WMH. In more severe SVD cases it is, therefore, difficult to investigate different WMH types and their shape separately.

In this thesis, WMH shape was investigated at baseline. It would also be interesting to investigate how WMH shapes evolve over time. However, it is very challenging to model WMH shape changes over time because of the way WMH naturally progress. Smaller irregular lesions might over time blend with bigger WMH, leading to large shape changes caused by a potentially minor size increase. Such an event of WMH progression might engulf irregular edges of smaller lesions that were identifiable at earlier timepoints. Bigger lesions might therefore look more regular in shape, even if they used to be smaller and more irregular at earlier timepoints. WMH shape irregularity is likely to reflect a progression-prone type of SVD, as **Chapter 3** suggests. This limitation suggests that WMH shape can be best utilized as a marker in the earlier disease stages. This does not diminish the clinical importance of WMH shape assessment, since lifestyle changes and treatments that can be used to modify SVD progression are also more effective at earlier disease stages.[5] Based on the growing body of literature, the question to be raised is not if WMH shape is a marker with added value over WMH volume, but how WMH shape should be considered and interpreted, and if and how they are related to aging or possibly different disease stages.

## 8.3 FUTURE DIRECTIONS

Dementia research is a dynamic field where interdisciplinary work is becoming increasingly important. The fact that a big part of dementia cases are later confirmed to be mixed pathologies, makes it important to investigate neurodegenerative and neurovascular pathologies together and not only as separate disease entities.[6] There may be links between the different pathologies and it remains unclear if one disease enhances the other or how much shared disease processes are part of the reason for mixed pathologies.[6] Moreover, SVD is a highly heterogenous whole-brain disease in itself and its subtypes are currently mostly ill-defined. Not only are new biomarkers needed, but we also need to better understand how existing biomarkers relate to different types of SVD pathology.

8

The WHIMAS study proposed in **Chapter 7** will hopefully help to answer several different questions raised in the field. Preclinical studies suggest that glymphatic system dysfunction is not only an important factor in neurodegenerative diseases, but also in SVD.[7,8] Several novel non-invasive techniques are used in the MRI protocol as measures of glymphatic activity.[9,10] Both a clinical MRI scanner as well as a ultra-high field system (7T MRI) will be used not only for imaging the brain clearance system, but also to improve WMH shape assessment. Ultra-high field MRI allows imaging at a higher spatial resolution, which will allow a better identification of WMH-shape and its structural correlates. Higher spatial resolution and increased sensitivity to e.g. iron deposition will also help improve the quality of other markers of cerebrovascular diseases. In this way, we can explore the added value of 7T MRI in dementia. Novel and advanced MRI techniques can be combined with other techniques or already established SVD markers (such as e.g. WMHs, microbleeds) in order to highlight different features of SVD. Combined, these data can provide important insights into the structural correlates of SVD. Longitudinal data is valuable to track both brain changes and clinical outcomes over time. It would therefore be important to extend the WHIMAS study into a longitudinal study. In our informed consent form we did prepare participants for such an extension.

Smaller studies focused on a specific patient population can gather important insights into SVD markers, such as WMH shape. Specific MRI markers can be identified in such smaller, cross-sectional studies, such as the WHIMAS. Thereafter, larger studies in the general population are needed to validate the findings and to gain more generalizability for the newly developed MRI markers. This will in later research stages aid in translation of results to radiological clinical practice and thus to individual patients.

The field is struggling with a lack of understanding of what WMH consist of and an accurate description of their heterogeneity. Pathology studies are rare, especially those directly linking histopathology to individual lesions visible on MRI. Pathological changes detected in such studies were ischemic damage, demyelination, axonal loss, as well as arteriosclerosis.[11–13] WMH are not only developing in various neurological diseases, such as SVD and multiple sclerosis (neuroinflammatory pathology), but they also appear with ageing. Therefore, their heterogeneity needs to be both accurately captured and understood. MRI is a versatile and elegant method to non-invasively investigate the human brain in health and disease and MRI is sensitive to microstructural changes, resulting in a highly diverse imaging modality. In pure imaging studies, however, one can only speculate about the pathological processes causing or co-existing with abnormalities seen on MRI. Image-guided histology

studies are rare, but can give crucial insights linking findings on MRI images to histological staining in the same areas. Combined WMH shape and histology studies could help to confirm and explain the differences in pathology of SVD subtypes that the findings in **Chapter 3** are pointing towards. A questions to be raised in future studies could be; What are the exact histopathological differences between WMH with a different shape?

## 8.4 POTENTIAL FOR TRANSLATION INTO CLINICAL PRACTICE

Often there is a large gap between techniques that are developed and used in research compared to clinical practice. Many elegant and advanced techniques and applications may never translate into clinical practice. There are several challenges when attempting to move "from bench to bedside". An important question that remains is, therefore, how the novel techniques presented in this thesis can eventually be of benefit to patients. Oftentimes scientific findings obtained in large population-based studies, enable us to understand associations between different pathologies and risk factors on a group level. However, the results found in such studies are usually not easily translatable to an individual patient. One of the reasons for this is that in a research setting different factors are prioritized compared to clinical practice. For instance, disease prognosis is frequently investigated in research, but is a lot less commonly used in dementia patients in daily clinical practice. Since many diseases, such as vascular dementia, are most effectively modifiable at early stages, disease prognosis may shift towards a more important role also in clinical practice in the future.

Clinicians require tools that are easy to use, deliver clear output, and which can help to make the diagnosis more specific and accurate. Some types of SVD, such as cerebral amyloid angiopathy (CAA) and cerebral autosomal dominant arteriopathy with subcortical infarcts and leukoencephalopathy (CADASIL) have a more defined imaging pattern and definition. On the other hand, sporadic types of SVD are highly heterogenous and lack such a clear definition. It is unlikely that a single brain MRI marker will provide enough precision and information to make individual clinical decisions in such heterogenous disease cases. Models with combined SVD markers (e.g. WMH shape, atrophy, microbleeds) will, therefore, become increasingly relevant. Multimodal data can be used to build large prediction models with which we could categorize patients according to their predicted prognosis regarding disease progression. We aimed to perform the first steps into this direction in **Chapter 6**. A next step could be that the software using MRI images could be combined with

8

clinical patient data to create subgroups of patients with specific phenotypes. Such software needs to be validated in bigger populations and with data from different MRI scanners before it can be used in clinical practice. It should be noted that the possible clinical translation described may only be adopted in the future, when more treatment options for selected patients are available as this could lead to a cost-effective approach. Frequent MRI scanning as a population screening tool is unlikely to be feasible due to high costs and logistic constraints. Therefore, general practitioners could make a first assessment of risk factors for dementia and preselect patients for an MRI scan. Software-based brain image analysis results, including WMH shape markers, could subsequently be integrated leading to individualized risk assessment into the radiological report. With all novel data-driven or machine learning methods emerging these days, the question should not be if we should use them, but how.

## 8.5 REFERENCES

1.  Ghaznawi R, Geerlings M, Jaarsma-Coes M, Hendrikse J, de Bresser J. Association of White Matter Hyperintensity Markers on MRI and Long-term Risk of Mortality and Ischemic Stroke. Neurology 2021; : 10.1212/WNL.0000000000011827.

2.  De Bresser J, Kuijf HJ, Zaanen K, Viergever MA, Hendrikse J, Biessels GJ et al. White matter hyperintensity shape and location feature analysis on brain MRI; Proof of principle study in patients with diabetes. Sci Rep 2018; 8: 1–10.

3.  Ghaznawi R, Geerlings MI, Jaarsma-Coes MG, Zwartbol MHT, Kuijf HJ, van der Graaf Y et al. The association between lacunes and white matter hyperintensity features on MRI: The SMART-MR study. Journal of Cerebral Blood Flow and Metabolism 2019; 39: 2486–2496.

4.  Alber J, Alladi S, Bae H, Barton DA, Beckett LA, Bell JM et al. White matter hyperintensities in vascular contributions to cognitive impairment and dementia (VCID): Knowledge gaps and opportunities. Alzheimer's & Dementia: Translational Research & Clinical Interventions 2019; 5: 107–117.

5.  Wardlaw JM, Smith C, Dichgans M. Small vessel disease: mechanisms and clinical implications. Lancet Neurol 2019; 18: 684–696.

6.  Ter Telgte A, Van Leijsen EMC, Wiegertjes K, Klijn CJM, Tuladhar AM, De Leeuw FE. Cerebral small vessel disease: From a focal to a global perspective. Nat Rev Neurol. 2018; 14: 387–398.

7.  Han F, Chen J, Belkin-Rosen A, Gu Y, Luo L, Buxton O et al. The coupling of global brain activity and cerebrospinal fluid inflow is correlated with Alzheimer's disease related pathology. 2020. doi:10.1101/2020.06.04.134726.

8.  Benveniste H, Nedergaard M. Cerebral small vessel disease: A glymphopathy? Curr Opin Neurobiol 2022; 72: 15–21.

9.  Hirschler L., Aldea R., Petitclerc L., Ronen I., de Koning P.J.H., van Buchem, M. A., van Osch M.J.P. High resolution T2-prepared MRI enables non-invasive assessment of CSF flow in perivascular spaces of the human brain. In: Proceedings of the 28th Annual Meeting of ISMRM, Montréal, Canada, 2019. Abstract 0746.

10. Fultz NE, Bonmassar G, Setsompop K, Stickgold RA, Rosen BR, Polimeni JR et al. Coupled electrophysiological, hemodynamic, and cerebrospinal fluid oscillations in human sleep. Science (1979) 2019; 366: 628–631.

11. Fazekas F, Kleinert R, Offenbacher H, Schmidt R, Kleinert G, Payer F et al. Pathologic correlates of incidental MRI white matter signal hyperintensities. Neurology 1993; 43: 1683–1689.

12. Kalaria RN, Kenny RA, Ballard CG, Perry R, Ince P, Polvikoski T. Towards defining the neuropathological substrates of vascular dementia. J Neurol Sci 2004; 226: 75–80.

13. Fernando MS, Simpson JE, Matthews F, Brayne C, Lewis CE, Barber R et al. White matter lesions in an unselected cohort of the elderly: molecular pathology suggests origin from chronic hypoperfusion injury. Stroke 2006; 37: 1391–1398.

**8**

CHAPTER

9

SUMMARY

## 9.1 ENGLISH SUMMARY

### 9.1.1 Background

Cerebral small vessel disease (SVD) is a major contributor to cognitive impairment and dementia. White matter hyperintensities (WMHs) are a key imaging marker of SVD and are visible on brain MRI. In neuroimaging research WMHs were traditionally quantified using their volume. However, this is a rather crude marker that fails to fully capture the heterogeneity of cerebral SVD. When inspecting MRI scans visually, WMHs can appear very different from each other in shape and location, even if their calculated volumes may be roughly the same. However, measures to objectively quantify such differences that may easily be caught by the eye of a neuroradiologist, were lacking. In this thesis, WMH shape is investigated as a novel marker of SVD to improve our understanding of WMHs.

### 9.1.2 Aim

The overarching aim of this thesis was to exploit the shape of WMHs for better characterization of WMH to improve the clinical interpretation of WMHs and to investigate related disease outcomes. This thesis was mostly based on non-demented and community-dwelling older individuals. Moreover, a study set up focusing on a memory-clinic population was discussed to get more pathology-focused insights into the formation of WMH.

### 9.1.3 Summary of results

In **Chapter 2** the association of different cardiovascular risk factors with WMH shape was investigated in older adults of the 'biomarker development for postoperative cognitive impairment in the elderly' (BIOCOG) study. The study included non-demented older adults scheduled for major elective surgery. The association between cardiovascular risk factors and quantitative MRI-based WMH shape and volume markers were examined using linear regression analysis. Presence of hypertension was associated with a more irregular shape of periventricular/confluent WMH, but not with total WMH volume. Presence of diabetes was associated with deep WMH volume. Body mass index or hyperlipidemia showed no association with WMH markers. This study showed that different cardiovascular risk factors seem to be related to a distinct pattern of WMH shape markers in non-demented older adults. These findings may suggest that different underlying cardiovascular pathological mechanisms lead to different WMH MRI phenotypes, which may be valuable for early detection of individuals at risk for stroke and dementia.

Whether WMH shape is related to long-term progression of cerebrovascular disease in community-dwelling older adults was examined in **Chapter 3** in a large population-based longitudinal study (the Age, Gene/Environment Susceptibility (AGES) Reykjavik study). The relationship of baseline WMH shape and WMH volume increase, different types of infarcts, microbleeds and enlarged perivascular spaces at follow-up were studied in this chapter. A more irregular shape of periventricular/confluent WMH at baseline was associated with a larger increase in WMH volume over time, and with occurrence of new subcortical infarcts, new microbleeds, new enlargement of perivascular spaces, and new cerebellar infarcts at the 5.2-year follow-up. Furthermore, less elongated and more irregularly shaped deep WMHs were associated with a larger increase in WMH volume, and new cortical infarcts at follow-up. A less elongated shape of deep WMH was associated with new microbleeds at follow-up. Our findings show that WMH shape may be indicative of the type of cerebrovascular disease progression. This underlines the significance of WMH shape to aid in the prediction of cerebrovascular disease progression.

In **Chapter 4** the focus was on investigating the association between baseline WMH shape and cognitive decline measured in three different domains (memory, executive function, and processing speed) over 5.2 years in community-dwelling older adults in the AGES Reykjavik dataset. A more complex shape of periventricular/confluent WMH was related to cognitive decline in the memory domain, the executive function domain and the processing speed domain over 5.2 years. No associations were found between deep WMH shape and cognitive decline in any of the cognitive domains. These findings show that in community-dwelling older adults, WMH shape patterns may be indicative of cognitive decline in a relatively short time-frame. This supports the evidence of WMH shape being a valuable marker that may be used to predict cognitive outcome related to cerebrovascular disease progression.

In **Chapter 5**, the association of baseline WMH shape and long-term dementia risk after 9.9 ± 2.6 years was assessed in community-dwelling older adults in the AGES Reykjavik study. A more irregular shape of periventricular/confluent WMH, higher periventricular/confluent WMH volume and higher deep WMH volume were associated with an increased long-term dementia risk. WMH shape markers may in the future be useful in determining patient prognosis and may aid in patient selection for future preventive treatments in community-dwelling older adults.

In **Chapter 6** brain MRI phenotypes were obtained using a hierarchical clustering method in community-dwelling older adults in the AGES Reykjavik dataset. In a second step, it was investigated whether these phenotypes were related to long-

9

term (10 years) risk for dementia. In total 3056 participants were included and we identified 15 subgroups with distinct brain MRI phenotypes. The phenotypes ranged from limited burden, mostly irregular WMH shape and cerebral atrophy, mostly irregularly WMHs and microbleeds, mostly cortical infarcts and atrophy, mostly irregularly shaped WMHs and cerebral atrophy to multi-burden subgroups. Each subgroup showed different long-term risks for dementia, with especially the brain MRI phenotype with mainly WMHs and atrophy showing an increased risk for dementia. Our results indicate that distinct brain MRI phenotypes can be identified in community-dwelling older adults and that these subgroups have a varying long-term risk for development of dementia. Brain MRI phenotypes may in the future assist in an improved understanding of the structural correlates of dementia predisposition.

In **Chapter 7** a novel prospective cross-sectional study was presented applying high spatial resolution WMH shape markers and other cutting-edge MRI techniques to further understand processes involved in SVD. The WHIte MAtter hyperintensity Shape and glymphatics (WHIMAS) study is including memory and geriatric clinic outpatients with MRI scanning performed both at 3 Tesla as well as at 7 Tesla MRI. The aim of the WHIMAS study is to understand variations in WMH shape and find their relation to cerebral SVD and markers of brain clearance and cognitive functioning. Such early markers of SVD are extremely important as they may represent a basis for future patient selection for lifestyle interventions or for treatment trials aimed at prevention of dementia.

## 9.2 DUTCH SUMMARY

### 9.2.1 Achtergrond

Cerebrale small vessel disease (SVD; cerebrale ziekte van de kleine bloedvaten) levert een belangrijke bijdrage aan het ontstaan van cognitieve stoornissen en dementie. Hyperintensiteiten van de witte stof (WMH's) zijn een belangrijke marker in de beeldvorming van SVD en kunnen worden gevisualiseerd op een MRI scan van de hersenen. In wetenschappelijk onderzoek worden WMH's traditioneel gekwantificeerd door middel van hun volume. Dit is echter een nogal ruwe marker die er niet in slaagt om de heterogeniteit van cerebrale SVD volledig vast te leggen. Bij visuele beoordeling van MRI-scans kunnen WMH's qua vorm en locatie heel verschillend zijn, zelfs als de berekende volumes ongeveer hetzelfde zijn. Methoden om dergelijke verschillen objectief te kwantificeren ontbraken echter. In dit proefschrift wordt de vorm van WMH onderzocht als een nieuwe marker voor SVD om de kennis over WMH's te verbeteren.

### 9.2.2 Doel

De overkoepelende doelen van dit proefschrift zijn om de vorm van WMH's te gebruiken voor een betere karakterisering van WMH, om de klinische interpretatie van WMH's te verbeteren en om gerelateerde ziekteprocessen te onderzoeken. Dit proefschrift is voornamelijk gebaseerd op data van niet-dementerende en thuiswonende ouderen. Bovendien is er een studie opgezet die zich richt op een geheugenkliniek populatie om meer pathologische inzichten te krijgen gerelateerd aan de vorming van WMH.

### 9.2.3 Samenvatting van de resultaten

In **hoofdstuk 2** werd de associatie van verschillende cardiovasculaire risico-factoren met de vorm van WMH onderzocht bij ouderen die deelnamen aan de 'biomarkerontwikkeling voor postoperatieve cognitieve stoornissen bij ouderen' (BIOCOG) studie. De studie bestaat uit niet-dementerende ouderen die een grote geplande operatie moesten ondergaan. De associatie tussen cardiovasculaire risicofactoren en kwantitatieve MRI-gebaseerde WMH-vorm markers en volumemarkers werd onderzocht met behulp van een lineaire regressieanalyse. Hypertensie was geassocieerd met een meer onregelmatige vorm van periventriculaire/confluerende WMH, maar niet met het totale WMH volume. Diabetes was geassocieerd met het volume van diepe WMH. De body mass index en hyperlipidemie toonde geen verband met WMH markers. Deze studie toonde aan dat verschillende cardiovasculaire risicofactoren verband lijken te hebben met een verschillend patroon van de WMH vorm bij niet-dementerende ouderen. Deze

9

bevindingen kunnen erop duiden dat verschillende onderliggende cardiovasculaire pathologische mechanismen leiden tot verschillende WMH MRI-fenotypes. Dit kan waardevol zijn voor het vroeg opsporen van personen die een verhoogd risico lopen op een beroerte en/of dementie.

Het verband tussen de WMH-vorm en lange termijn progressie van cerebrovasculaire markers bij ouderen, werd onderzocht in **hoofdstuk 3** in een groot longitudinaal populatieonderzoek (de Age, Gene/Environment Susceptibility (AGES) Reykjavik-studie). Het verband tussen de WMH-vorm op baseline en de toename van het WMH-volume, nieuwe infarcten, nieuwe microbloedingen en nieuwe verwijde perivasculaire ruimten bij follow-up werden in dit hoofdstuk bestudeerd. Een meer onregelmatige vorm van periventriculaire/confluerende WMH op baseline ging gepaard met een grotere toename van het WMH-volume na verloop van tijd en met het optreden van nieuwe subcorticale infarcten, nieuwe microbloedingen, nieuwe verwijde perivasculaire ruimten en nieuwe cerebellaire infarcten na 5,2 jaar. Bovendien waren minder langwerpige en meer onregelmatig gevormde diepe WMH's geassocieerd met een grotere toename van het WMH-volume en nieuwe corticale infarcten bij de follow-up. Een minder langwerpige vorm van diepe WMH was geassocieerd met nieuwe microbloedingen bij de follow-up. Onze bevindingen tonen aan dat de vorm van WMH indicatief kan zijn voor het type progressie van cerebrovasculaire ziekten. Dit benadrukt het belang van de WMH-vorm als marker voor het voorspellen van progressie van cerebrovasculaire ziekten.

In **hoofdstuk 4** lag de focus op het onderzoeken van de associatie tussen WMH-vorm op baseline en cognitieve achteruitgang gemeten in drie verschillende domeinen (geheugen, executieve functie en verwerkingssnelheid) over een periode van 5,2 jaar bij ouderen van de AGES Reykjavik studie. Een meer onregelmatige vorm van periventriculaire/confluerende WMH was gerelateerd aan cognitieve achteruitgang in het geheugendomein, het domein van de uitvoerende functies en het domein van de verwerkingssnelheid over een periode van 5,2 jaar. Er werd geen verband gevonden tussen diepe WMH-vorm en cognitieve achteruitgang. Deze bevindingen laten zien dat bij ouderen de patronen van WMH-vorm indicatief kunnen zijn voor cognitieve achteruitgang in een relatief kort tijdsbestek. Dit ondersteunt het bewijs dat de WMH-vorm een waardevolle marker is die kan worden gebruikt om de cognitieve uitkomst gerelateerd aan de progressie van cerebrovasculaire ziekten te voorspellen.

In **hoofdstuk 5** werd de associatie tussen WMH-vorm op baseline en het risico op dementie op lange termijn na 9,9 ± 2,6 jaar onderzocht bij ouderen in de AGES Reykjavik studie. Een meer onregelmatige vorm en groter volume van periventriculaire/

confluerende WMH en een groter volume van diepe WMH zijn geassocieerd met een verhoogd risico op dementie op de lange termijn. WMH-vorm markers kunnen in de toekomst nuttig zijn bij het bepalen van de prognose en kunnen helpen bij de selectie van personen voor toekomstige preventieve behandelingen.

In **hoofdstuk 6** werden MRI-fenotypes van de hersenen verkregen met behulp van een hiërarchische clusteringsmethode op MRI scans van ouderen in de AGES Reykjavik studie. In een tweede stap werd onderzocht of deze fenotypes gerelateerd waren aan het lange termijnrisico (10 jaar) op dementie. In totaal werden 3056 deelnemers geïncludeerd en we identificeerden 15 subgroepen met verschillende MRI-fenotypes van de hersenen. Deze fenotypes varieerden van beperkte afwijkingen, voornamelijk een onregelmatige WMH-vorm en cerebrale atrofie, voornamelijk een onregelmatige WMH-vorm en microbloedingen, voornamelijk corticale infarcten en atrofie, voornamelijk onregelmatig gevormde WMH's en cerebrale atrofie tot subgroepen met multipele afwijkingen. Elke subgroep vertoonde een verschillend lange termijnrisico op het krijgen van dementie, waarbij vooral het MRI-fenotype van de hersenen met voornamelijk WMH's en atrofie een sterk verhoogd risico op dementie liet zien. Onze resultaten laten zien dat verschillende MRI-fenotypes van de hersenen kunnen worden geïdentificeerd bij thuiswonende ouderen en dat deze subgroepen op de lange termijn een verschillend risico hebben op het ontstaan van dementie. MRI-fenotypes van de hersenen kunnen in de toekomst helpen om de structurele afwijkingen van predispositie voor dementie beter te begrijpen.

In **hoofdstuk 7** werd een nieuwe prospectieve cross-sectionele studie gepresenteerd waarbij WMH-vorm markers met hoge spatiële resolutie en andere geavanceerde MRI-technieken zullen worden toegepast om de processen die betrokken zijn bij SVD beter te begrijpen. De WHIte Matter hyperintensity Shape and glymphatics (WHIMAS) studie bestaat uit poliklinische geheugen- en geriatrische patiënten die zowel een 3 Tesla als 7 Tesla MRI-scans van de hersenen ondergaan. Het doel van de WHIMAS-studie is om variaties in de vorm van WMH beter te begrijpen en hun relatie met cerebrale SVD en hersenklaring markers en cognitief functioneren te onderzoeken. Dergelijke vroege markers van SVD zijn uiterst belangrijk omdat deze aan de basis kunnen staan van toekomstige selectie voor leefstijlinterventies of voor behandelstudies gericht op preventie van dementie.

9

## 9.3 GERMAN SUMMARY

### 9.3.1 Hintergrund

Small Vessel Disease (SVD) trägt wesentlich zu kognitiven Beeinträchtigungen und Demenz bei. White matter hyperintensities (WMHs) sind ein wichtiger Marker für SVD und werden Magnetresonanztomografie- (MRT) Bildern des Gehirns sichtbar. In der Neuroimaging-Forschung wurden WMHs traditionell anhand ihres Volumens quantifiziert. Dies ist jedoch ein recht grober Marker, der die Heterogenität der zerebralen SVD nicht vollständig erfassen kann. Bei der visuellen Inspektion von MRT-Scans können sich die WMHs in Form und Position stark voneinander unterscheiden, auch wenn ihre berechneten Volumina ungefähr gleich sind. Allerdings fehlten bisher Maßnahmen zur objektiven Quantifizierung solcher Unterschiede, die einem Neuroradiologen visuell leicht auffallen. In dieser Dissertation wird die Form der WMHs als neuartiger Marker für SVD untersucht, um unser Verständnis der WMHs zu verbessern.

### 9.3.2 Ziel

Das übergeordnete Ziel dieser Dissertation war es, die Form der WMHs für eine bessere Charakterisierung der WMHs zu nutzen, um die klinische Interpretation der WMHs zu verbessern und die damit verbundenen Krankheitsfolgen zu untersuchen. Diese Abhandlung basiert hauptsächlich auf nicht dementen älteren Menschen. Darüber hinaus wurde eine Studie vorgestellt, die sich auf eine Population in einer Gedächtnisklinik konzentriert, um mehr pathologiebezogene Einblicke in die Entstehung von WMH zu erhalten.

### 9.3.3 Zusammenfassung der Ergebnisse

In **Kapitel 2** wurde der Zusammenhang zwischen verschiedenen kardiovaskulären Risikofaktoren und der Form der WMH bei älteren Erwachsenen im Rahmen der „biomarker development for postoperative cognitive impairment in the elderly" (BIOCOG) Studie untersucht. Die Studie umfasste nicht demente ältere Erwachsene, bei denen eine größere elektive Operation geplant war. Der Zusammenhang zwischen kardiovaskulären Risikofaktoren und quantitativen MRT-basierten WMH-Form- und Volumenmarkern wurde mittels linearer Regressionsanalyse untersucht. Bluthochdruck war mit einer unregelmäßigeren Form der periventrikulären/ konfluenten WMH assoziiert, jedoch nicht mit dem Gesamtvolumen der WMH. Diabetes mellitus war mit dem Volumen tiefer WMHs assoziiert. Body-Mass-Index oder Hyperlipidämie zeigten keinen Zusammenhang mit den WMH-Markern. Diese Studie zeigte, dass verschiedene kardiovaskuläre Risikofaktoren bei nicht dementen älteren Erwachsenen mit einem unterschiedlichen Muster von WMH-Formmarkern

verbunden zu sein scheinen. Diese Befunde könnten darauf hindeuten, dass verschiedene zugrunde liegende kardiovaskuläre pathologische Mechanismen zu unterschiedlichen WMH-MRT-Phänotypen führen, die für die Früherkennung wertvoll sein könnten.

In **Kapitel 3** wurde in einer großen populationsbasierten Studie (der Age, Gene/ Environment Susceptibility (AGES) Reykjavik-Studie) untersucht, ob die Form der WMH mit dem langfristigen Fortschreiten von zerebrovaskulären Erkrankungen bei älteren Erwachsenen zusammenhängt. In diesem Kapitel wurde die Beziehung zwischen der Form der WMH zu Beginn der Studie und der Zunahme des WMH-Volumens, verschiedenen Infarkttypen, Mikroblutungen und vergrößerten perivaskulären Räumen bei der Nachuntersuchung untersucht. Eine unregelmäßigere Form der periventrikulären/konfluenten WMH zu Beginn der Studie war mit einer stärkeren Zunahme des WMH-Volumens im Laufe der Zeit sowie mit dem Auftreten neuer subkortikaler Infarkte, neuer Mikroblutungen, neuer Vergrößerungen der perivaskulären Räume und neuer Kleinhirninfarkte bei der Nachuntersuchung nach 5,2 Jahren verbunden. Außerdem waren weniger langgestreckte und unregelmäßig geformte tiefe WMHs mit einer größeren Zunahme des WMH-Volumens und neuen kortikalen Infarkten bei der Nachuntersuchung verbunden. Eine weniger längliche Form der tiefen WMH war mit neuen Mikroblutungen bei der Nachuntersuchung verbunden. Unsere Ergebnisse zeigen, dass die Form der WMH ein Indikator für die Art des Fortschreitens der zerebrovaskulären Erkrankung sein kann. Dies unterstreicht die Bedeutung der WMH-Form für die Vorhersage des Fortschreitens einer zerebrovaskulären Erkrankung.

In **Kapitel 4** lag der Schwerpunkt auf der Untersuchung des Zusammenhangs zwischen der Form der WMH zu Beginn der Studie und dem kognitiven Abbau in drei verschiedenen Bereichen (Gedächtnis, Exekutivfunktion und Verarbeitungsgeschwindigkeit) über 5,2 Jahre bei älteren Erwachsenen im AGES Reykjavik-Datensatz. Eine komplexere Form der periventrikulären/konfluenten WMH stand in Zusammenhang mit dem kognitiven Abbau in den Bereichen Gedächtnis, exekutive Funktionen und Verarbeitungsgeschwindigkeit über 5,2 Jahre. Es wurde kein Zusammenhang zwischen der Form der tiefen WMH und dem kognitiven Abbau in einem der kognitiven Bereiche festgestellt. Diese Ergebnisse zeigen, dass bei älteren Erwachsenen die Form der WMH in einem relativ kurzen Zeitrahmen auf einen kognitiven Abbau hinweisen kann. Dies untermauert die Belege dafür, dass die Form der WMH ein wertvoller Marker ist, der zur Vorhersage der kognitiven Ergebnisse im Zusammenhang mit dem Fortschreiten der zerebrovaskulären Erkrankung verwendet werden kann.

9

In **Kapitel 5** wurde der Zusammenhang zwischen der Ausgangsform der WMH und dem langfristigen Demenzrisiko nach 9,9 ± 2,6 Jahren bei in älteren Erwachsenen in der AGES-Reykjavik-Studie untersucht. Eine unregelmäßigere Form der periventrikulären/konfluenten WMH, ein höheres periventrikuläres/konfluentes WMH-Volumen und ein höheres Volumen tiefer WMHs waren mit einem erhöhten langfristigen Demenzrisiko verbunden. Marker für die WMH-Form könnten in Zukunft bei der Bestimmung der Patientenprognose nützlich sein und bei der Auswahl von Patienten für künftige präventive Behandlungen bei älteren Erwachsenen helfen.

In **Kapitel 6** wurden MRT-Phänotypen des Gehirns mit Hilfe einer hierarchischen Clusteringmethode bei älteren Erwachsenen aus dem AGES-Reykjavik-Datensatz ermittelt. In einem zweiten Schritt wurde untersucht, ob diese Phänotypen mit dem Langzeitrisiko (10 Jahre) für Demenz zusammenhängen. Insgesamt wurden 3056 Teilnehmer einbezogen, und wir identifizierten 15 Untergruppen mit unterschiedlichen MRT-Phänotypen. Die Phänotypen reichten von begrenzter Belastung, meist unregelmäßiger WMH-Form und zerebraler Atrophie, meist unregelmäßigen WMHs und Mikroblutungen, meist kortikalen Infarkten und Atrophie, meist unregelmäßig geformten WMHs und zerebraler Atrophie, bis zu Untergruppen mit Mehrfachbelastung. Jede Untergruppe wies ein unterschiedliches Langzeitrisiko für Demenz auf, wobei vor allem der MRT-Phänotyp mit hauptsächlich WMHs und Atrophie ein erhöhtes Demenzrisiko aufwies. Unsere Ergebnisse deuten darauf hin, dass sich bei älteren Erwachsenen verschiedene MRT-Phänotypen des Gehirns identifizieren lassen und dass diese Untergruppen ein unterschiedliches Langzeitrisiko für die Entwicklung einer Demenz haben. Die MRT-Phänotypen des Gehirns könnten in Zukunft zu einem besseren Verständnis der strukturellen Korrelate der Demenzprädisposition beitragen.

In **Kapitel 7** wurde eine neuartige prospektive Querschnittsstudie vorgestellt, bei der hochauflösende WMH-Form-Marker und andere hochmoderne MRT-Techniken eingesetzt werden, um die an der SVD beteiligten Prozesse besser zu verstehen. Die WHIMAS-Studie (WHIte Matter hyperintensity Shape and glymphatics) umfasst Gedächtnis- und geriatrische Ambulanzpatienten, deren MRT-Scans sowohl mit 3 Tesla, als auch mit 7 Tesla durchgeführt werden. Ziel der WHIMAS-Studie ist es, Unterschiede in der Form der WMH zu verstehen und ihre Beziehung zu zerebralen SVD und Markern des Hirn-Clearance und kognitiven Funktionen zu ermitteln. Solche frühen Marker für SVD sind äußerst wichtig, da sie eine Grundlage für die künftige Auswahl von Patienten für Lebensstilinterventionen oder für Behandlungsversuche zur Vorbeugung von Demenz darstellen könnten.

9

APPENDICES

A

**LIST OF PUBLICATIONS**

**CV**

**ACKNOWLEDGEMENTS**

## LIST OF PUBLICATIONS

**Kuhn-Keller** J. A., Sigurdsson S., Launer L. J., van Buchem M. A., van Osch M. J. P., Gudnason V., de Bresser J. White matter hyperintensity shape is related to long-term progression of cerebrovascular disease in community-dwelling older adults. Journal of Cerebral Blood Flow & Metabolism. 2024;0(0). https://doi.org/10.1177/0271678x241270538

**Keller, J. A.**, Sigurdsson, S., Schmitz Abecassis B., Kant, I.M.J., van Buchem, M. A., Launer, L. J., van Osch, M. J. P., Gudnason, V., & de Bresser, J. H. J. M. White matter hyperintensity shape is associated with long-term dementia risk. Neurology. 2024;102:e209176. https://doi.org/10.1212/WNL.0000000000209176

Abecassis, B. S.-, Dirven, L., Jiang, J., **Keller, J. A.**, Croese, R. J. I., van Dorth, D., Ghaznawi, R., Kant, I. M. J., Taphoorn, M. J. B., van Osch, M. J. P., Koekkoek, J. A. F., & de Bresser, J. MRI phenotypes of glioblastomas early after treatment are suggestive of overall patient survival. Neuro-Oncology Advances. 2023;5,1–11. https://doi.org/10.1093/NOAJNL/VDAD133

**Keller, J. A**., Sigurdsson, S., Klaassen, K., Hirschler, L., van Buchem, M. A., Launer, L. J., van Osch, M. J. P., Gudnason, V., & de Bresser, J. H. J. M. (2023). White matter hyperintensity shape is associated with long-term dementia risk. Alzheimer's and Dementia. 2023,19,5632–5641. https://doi.org/10.1002/ALZ.13345

van Egmond, L. T., Meth, E. M. S., Engström, J., Ilemosoglou, M., **Keller, J. A**., Vogel, H., & Benedict, C. Effects of acute sleep loss on leptin, ghrelin, and adiponectin in adults with healthy weight and obesity: A laboratory study. Obesity. 2023;31,635–641. https://doi.org/10.1002/OBY.23616

**Keller, J. A.**, Kant, I. M. J., Slooter, A. J. C., Van Montfort, S. J. T., Van Buchem, M. A., Van Osch, M. J. P., Hendrikse, J., & de Bresser, J. Different cardiovascular risk factors are related to distinct white matter hyperintensity MRI phenotypes in older adults. NeuroImage: Clinical. 2022;35,103131. https://doi.org/10.1016/j.nicl.2022.103131

van Egmond, L. T., Meth, E. M. S., Bukhari, S., Engström, J., Ilemosoglou, M., **Keller, J. A.**, Zhou, S., Schiöth, H. B., & Benedict, C. How Sleep-Deprived People See and Evaluate Others' Faces: An Experimental Study. Nature and Science of Sleep. 2022;14, 867–876. https://doi.org/10.2147/NSS.S360433

## FIRST-AUTHOR PRESENTATIONS AT INTERNATIONAL CONFERENCES

**Keller, J. A.**, Sigurdsson, S., Schmitz Abecassis, B., Kant, I. M. J., van Buchem, M. A., Launer, L. J., Van Osch, M. J. P., Gudnason, V. and de Bresser, J. H. J. M. (2023), MRI phenotypes of the brain are related to long-term dementia outcome in community-dwelling older adults. Alzheimer's Dementia, 2023;19 (Suppl. 10):e081687. Podium presentation at the Alzheimer's Imaging Consortium 2023 in Amsterdam. (nominated for best oral presentation)

**Keller, J. A**., Sigurdsson, S., Launer, L. J., van Buchem, M. A., Van Osch, M. J. P., Gudnason, V. and de Bresser, J. H. J. M. (2023) White matter hyperintensity shape in relation to long-term small vessel disease progression in community-dwelling older adults Alzheimer's Dementia, 2023;19 (Suppl. 10):e081711. Poster presentation at the Alzheimer's Imaging Consortium 2023 in Amsterdam.

**Keller, J. A**., Sigurdsson, S., Schmitz Abecassis, B., Kant, I. M. J., van Buchem, M. A., Launer, L. J., Van Osch, M. J. P., Gudnason, V. and de Bresser, J. H. J. M. (2023), MRI phenotypes of the brain are related to long-term dementia outcome in community-dwelling older adults. Poster presentation at the Alzheimer's Association International Conference 2023 in Amsterdam.

**Keller, J. A**., Sigurdsson, S., Launer, L. J., van Buchem, M. A., Van Osch, M. J. P., Gudnason, V. and de Bresser, J. H. J. M. (2023) White matter hyperintensity shape in relation to long-term small vessel disease progression in community-dwelling older adults. Poster presentation at the Alzheimer's Association International Conference 2023 in Amsterdam.

**Keller, J. A**., Sigurdsson S., Schmitz Abecassis B., Kant I. M. J., van Buchem M. A., Launer L. J., van Osch M. J. P., Gudnason V., de Bresser J. MRI phenotypes of the brain are related to long-term dementia outcome in community-dwelling older adults. (Poster presentation) Proceedings of the 32nd Annual Meeting of the International Society for Magnetic Resonance in Medicine 2023 in Toronto. Abstract #3319

**Keller, J. A**., Sigurdsson S., Launer L. J., van Buchem M. A., van Osch M. J. P., Gudnason V., de Bresser J. White matter hyperintensity shape in relation to long-term small vessel disease progression incommunity-dwelling older adults. (Poster presentation) Proceedings of the 32nd Annual Meeting of the International Society for Magnetic Resonance in Medicine 2023 in Toronto. Abstract #3517.

A

**Keller, J. A**., Sigurdsson S., Schmitz Abecassis B., Kant I. M. J., van Buchem M. A., Launer L. J., van Osch M. J. P., Gudnason V., de Bresser J. MRI phenotypes of the brain are related to long-term dementia outcome in community-dwelling older adults. Oral presentation at the 15th Annual Meeting of the International Society for Magnetic Resonance in Medicine Benelux Chapter 2023 in Brussels.

**Keller, J. A**., Sigurdsson S., Klaassen K., Scholte E., Hirschler L., van Buchem M. A., Launer L. J., van Osch M. J. P., Gudnason V., de Bresser J. The association between white matter hyperintensity shape and long-term dementia outcome in community-dwelling older adults. (Poster presentation) Proceedings of the 31st Annual Meeting of the International Society for Magnetic Resonance in Medicine 2022 in London. Abstract #1552.

**Keller, J. A**., Sigurdsson S., Klaassen K., Scholte E., Hirschler L., van Buchem M. A., Launer L. J., van Osch M. J. P., Gudnason V., de Bresser J. The association between white matter hyperintensity shape and long-term dementia outcome in community-dwelling older adults. Poster presentation at the 14th Annual Meeting of the International Society for Magnetic Resonance in Medicine Benelux Chapter 2022 in Maastricht.

**Keller J. A**., Kant, I. M. J., Slooter A. J. C., van Montfort S. J. T., van Buchem M. A., van Osch M. J. P., Hendrikse J., de Bresser J. The association between cardiovascular risk factors and white matter hyperintensity MRI phenotypes. Cerebral Circulation - Cognition and Behavior, 2024,6,100111. Oral presentation at the 2021 meeting of The International Society of Vascular Behavioural and Cognitive Disorders (online).

## CURRICULUM VITAE

Jasmin Annica Kuhn, née Keller, was born on May 24th 1995 in Böblingen, Germany. After finishing secondary education in 2014 at Biotechnologisches Gymnasium der Mildred Scheel Schule Böblingen she moved to Stockholm, Sweden. In 2018, she graduated from the Bachelor of Pharmaceutical Science programme at Uppsala University. She continued her education with a Master's programme in Biomedicine at Uppsala University. During this time, Jasmin worked as a research assistant at the Uppsala Sleep Science Lab (Principal Investigator: Dr. Christian Benedict). For her Master thesis internship, Jasmin moved to Nijmegen, the Netherlands to work on a sleep science project at Donders Institute. In June 2020, she started her PhD project on MRI markers for small vessel disease at the C.J. Gorter MRI Center, Leiden University Medical Center, the Netherlands, with Dr. Jeroen de Bresser and Prof. Dr. ir. Matthias van Osch. In May 2024, she got married to her husband Wladimir in Holzgerlingen, Germany. Since June 2024, she works as Regulatory Affairs Manager.

A

## ACKNOWLEDGEMENTS

After four eventful, intense, and certainly educational years it is now time to say thank you. The Gorter-Family has been the perfect place for this PhD journey.

Thijs, thank you for your encouraging and patient supervision. I cannot put into words how grateful I am to have had a professor who was always had an open ear.

Jeroen, thank you for your patience, guidance, and giving me the opportunity to do this PhD project in Leiden.

I am extremely grateful that I was part of the MR-Physiology group: Leonie, Sophie, Merlijn, Thijs[2], Thom, Manon, Lydiane, Emiel, Balazs, Ingmar, Barbara, Danielle, Lena, Martijn, Suzanne, Helena, Maddalena, Eva, Ellen, Sanne, thank you for so many discussions, lunches, journal clubs…

I also want to thank the AGES group for an amazing and fruitful collaboration during these four years. Siggi, Villi, and Lenore, thank you for all your advice and discussions. Siggi, thank you for your patience, I really enjoyed working with you.

Lydiane, you have not only been a great co-worker and mentor, but also a friend. Many of us have enjoyed the most delicious dinners at your place.

Emiel, Lydiane, Mathieu, Javad, Balazs, thank you for dinners, board game nights, drinks, laughter, anything really!

I will certainly never forget the great time I had with our ISMRM 2022 apartment crew, Kirsten, Yiming, Bart, Javad, Donnie, my belly still hurts from laughing.

My roomie Manon, thank you for making ISMRM 2023 (my last!) unforgettable. I hope we get to travel again so we can chat all day and night.

Barbara, I really enjoyed figuring out how to do cluster analysis together! We always found time for great discussions.

Vesna and Ghislaine, we met in our office on 5th floor and I am so happy we stayed friends even though some of us "moved out". Thank you for sharing all the interesting stories, coffee breaks, cutting brains, dinners, pain, cat pictures, and laughter.

Two people that were essential for this thesis are my hardworking interns: Kelly and E., thank you so much! I wish you all the best for your careers, you'll do great.

Kirsten, Yiming, and Chang, you created a home during lockdown, thank you for the amazing dinners we had together. I miss you! Yiming prepared us very well for all the delicious spicy Chinese food at ISMRM.

Valeria, my amazing sister in law, thank you so much for creating this beautiful painting we can now admire on the cover of this thesis.

My parents, Angelika & Michael, thank you for your unconditional support throughout all years of my education. It is most certainly not easy to have your only daughter living abroad for an entire decade.

Wowa, thank you for your incredible patience, care, and (mental) support during this time. I can't wait to see what the future holds for us!

**A**